Helminth infection modulation of Antigen-Induced-Arthritis: Characterizing the effects of *Heligmosomoides polygyrus bakeri* infection on murine knee joint inflammation

by

Ana G. Madrigal

A thesis submitted to the McGill Institute of Parasitology in conformity with the requirements for the degree of Master of Science.

Montreal, QC

October 2022

English Abstract

Rheumatoid arthritis (RA) is the most common chronic inflammatory joint disease and is a leading cause of disability worldwide. RA affects 0.5–1% of the world population, affecting approximately 374,000 Canadians aged 16 years and older. It is estimated that RA costs the Canadian economy more than $6.4 billion annually in medical expenses and indirect costs. However, while the prevalence of RA is increasing, current therapies, such as Disease-modifying antirheumatic drugs (DMARDs), are not optimal with 1 in 3 patients not responding adequately to treatment. Ultimately, we seek to broaden RA treatment options available to patient cohorts unresponsive to conventional treatments.

Helminths have been demonstrated to be immunomodulatory, and limit severity in other models of inflammatory diseases. There are, however, relatively few pre-clinical studies relating helminth infection in mice to inflammatory responses in the joints. With previous studies demonstrating that chronic infection with helminths, such as *Heligmosomoides polygyrus bakeri* (Hpb), results in immunomodulation in mice, we hypothesized that infection with Hpb would limit inflammation in the joints of arthritic mice. With this in mind, we focused on characterizing the effects of Hpb infection on the acute phase of murine antigen-induced-arthritis (AIA). AIA is a well-characterized rodent model of RA. In this model, preimmunized C57BL/6 mice receive an intraarticular injection of Ag and develop T-cell-mediated monoarticular inflammatory arthritis.

We observed—to our knowledge, for the first time—that Hpb infection has the capacity to influence the inflammatory response in the joints of mice induced with AIA 7-8 days post Hpb-infection. With a decrease of neutrophil infiltration (as measured by myeloperoxidase), IFN-γ, TNF, and CXCL-1 in the periarticular tissue, and an increase in mononuclear cells in the knee cavity of Hpb-infected-arthritic mice when compared to our arthritic control group. This may be indicative of a faster resolution of inflammation or the prevention of neutrophil infiltration into the periarticular tissue.

We also observed a clear difference in peripheral blood metabolomes (using an untargeted metabolomic approach) between naïve and naïve-Hpb infected, as well as between our AIA-immunized model groups, PBS-control, Arthritic-control, PBS-Hpb-infected, and Hpb-infected-arthritic mice groups. Further, we identified two putative metabolic targets with the potential for RA treatment (Cytidine and Sphinganine) that are inhibited by *Hpb* infection. This could lead to a further understanding of how Hpb affects metabolism, and in turn, the role these potential effects play in the immune system. This knowledge can also better our understanding of how Hpb affects disease mechanisms, which can ultimately aid in the design of more effective RA treatments.

Primary reader: Dr. Fernando Lopes

Secondary reader: Dr. Elias Georges

French Abstract

La polyarthrite rhumatoïde (PR) est la maladie articulaire inflammatoire chronique la plus courante et l'une des principales causes d'invalidité dans le monde. La PR touche 0,5 à 1 % de la population mondiale, touchant environ 374 000 Canadiens âgés de 16 ans et plus. On estime que la PR coûte à l'économie canadienne plus de 6,4 milliards de dollars annuellement en dépenses médicales et en coûts indirects. Cependant, alors que la prévalence de la PR augmente, les traitements actuels, tels que les médicaments antirhumatismaux modificateurs de la maladie (DMARD), ne sont pas optimaux avec 1 patient sur 3 ne répondant pas de manière adéquate au traitement. Le but de ce projet est d'élargir les options de traitement de la PR disponibles pour les cohortes de patients ne répondant pas aux traitements conventionnels.

Il a été démontré que les helminthes possèdent des capacités d'immunomodulateurs et limitent la gravité des symptômes dans d'autres modèles de maladies inflammatoires. Cependant, il existe relativement peu d'études précliniques établissant un lien entre les infections d'helminthes chez la souris et les réponses inflammatoires dans les articulations. Des études antérieures ont démontré qu'une infection chronique par des helminthes, tels que le Heligmosomoides polygyrus bakeri (Hpb), entraîne une immunomodulation chez la souris. Nous avons émis l'hypothèse qu'une infection de Hpb limiterait l'inflammation dans les articulations des souris arthritiques. Dans cet esprit, nous nous sommes concentrés sur la caractérisation des effets d'une infection par Hpb sur la phase aiguë de l'arthrite induite par l'antigène murin (AIA). L'AIA est un modèle de PR bien caractérisé chez les rongeurs. Ce modèle consiste de souris C57BL/6 pré-immunisées qui reçoivent une injection intra-articulaire d'Ag et développent une arthrite inflammatoire monoarticulaire médiée par les lymphocytes T.

Nous avons observé—à notre connaissance, pour la première fois—qu'une infection par Hpb a la capacité d'influencer la réponse inflammatoire dans les articulations des souris induite par AIA aux 7éme et 8éme jours après l'infection. Une diminution de l'infiltration de neutrophiles (mesurée par la myéloperoxydase), de l'IFN-γ, du TNF et du CXCL-1 dans le tissu périarticulaire, et une augmentation des cellules mononucléaires dans la cavité du genou des souris arthritiques infectées par Hpb par rapport à nos souris arthritiques du groupe de contrôle a été observé. Cela pourrait indiquer une résolution plus rapide de l'inflammation ou/et la prévention de l'infiltration de neutrophiles dans le tissu périarticulaire.

Nous avons également observé une nette différence dans les métabolomes du sang périphérique (en utilisant une approche métabolomique non ciblée) entre les souris naïves et les souris naïves infectés par Hpb, ainsi qu'entre nos groupes modèles immunisés par AIA, PBS-contrôle, Arthritique-contrôle, PBS-Hpb-infecté, et des groupes de souris arthritiques infectées par Hpb. De plus, nous avons identifié deux cibles métaboliques supposés avec un potentiel de traitement de la PR (Cytidine et Sphinganine) qui sont inhibées par une infection de Hpb. Cela pourrait conduire à une meilleure compréhension de comment Hpb affecte le métabolisme et, par conséquent, le rôle que ces effets potentiels jouent dans le système immunitaire. Cette connaissance peut également améliorer notre compréhension de l’effet de Hpb sur les mécanismes de la maladie, ce qui pourrait aider à la conception de traitements plus efficaces contre la PR.

Acknowledgments

First, I would like to thank Dr. Lopes for the opportunity to work in this project. I would also like to thank Nathalia Malacco (Natty) for being my lab "partner in crime" and for being there with me during the long hours of work. It was fun sharing a lab together. I would also like to thank Norma Bautista-Lopez for her mentoring and training in terms of operating any equipment needed for my research, and for encouraging me to apply to various competitions and conferences. I would also like to thank Dr. Petra Rohrbach for taking me in during uncertain circumstances and helping with the finalization of this project. Also, I would like to thank Holly Tousignant for all the help fixing my grammar.

Secondly, thanks to my partner, who has been there for me during both the nice and tough times. I appreciate your support so much. Thanks also to my family for their constant support throughout this process.

Finally, thanks to all "the babies"—Miles, Kitty, Tj, Diego, and Jasper—for the constant cuddles, stress relief and "kitty breaks", which were necessary to complete this project.

Contributions

A special thanks to Dr. Armando Jardim for his aid in processing and running all metabolomics samples and processing all LC-MS/MS analyses.

Table of Contents

1. BACKGROUND 1

1.1 RHEUMATOID ARTHRITIS 1

1.1.1 Diagnosis and Therapies 2

1.1.2 Pathology 3

1.2 INFLAMMATION 5

1.2.1 Neutrophils 6

1.3 ANIMAL MODELS OF ARTHRITIS 10

1.3.1 Antigen Induced Arthritis 11

1.4 HELMINTH REGULATION OF INFLAMMATION 15

1.4.1 Heligmosomoides Polygyrus bakeri 18

1.5 METABOLOMICS 23

1.5.1 Metabolomics in RA 24

1.5.2 Metabolomics and Helminths 26

2. RATIONALE 28

3. STUDY OBJECTIVES 30

4. METHODS 31

4.1 MOUSE COLONY AND HPB LIFE CYCLE SETUP 31

4.1.1 Animals. 31

4.1.2 Infection Protocol. 32

4.2 PRELIMINARY TESTS AND OPTIMIZATION 32

4.2.1 Antigen Induced Arthritis Induction. 33

4.2.2 Kinetic of Antigen Induced Arthritis. 34

4.3 IN VIVO EXPERIMENTS 34

4.3.1 Hpb Modulation of Antigen Induced Arthritis Model. 35

4.4 METABOLOMICS METHODS 38

4.4.1 Model. 38

4.4.2 Metabolite analysis. 39

5. RESULTS 40

5.1 PRELIMINARY RESULTS AND OPTIMIZATION 40

5.1.1 Mice Colony and Hpb life cycle setup. 40

5.1.2 Antigen Induced Arthritis Induction. 40

5.2 STANDARDIZATION AND *IN-VIVO* RESULTS 43

5.2.1 Antigen-Induced Arthritis: peak and resolution. 43

5.2.2 Antigen-Induced Arthritis 24 hours after challenge. 44

5.2.3 Characterization of Hpb infection on AIA 24 hours after challenge. 45

5.3 METABOLOMIC RESULTS 51

5.3.1 Metabolomic profiling of AIA serum 24hrs after challenge. 54

5.3.2 Metabolomic characterization of infected AIA serum 24hrs after challenge. 57

5.3.3. Identified metabolomic compounds. 59

6. DISCUSSION 61

7. CONCLUSION AND FUTURE APPLICATIONS 80

8. APPENDIX 83

10. BIBLIOGRAPHY 91

CV 103

List of Figures

Figure 1) Representation of healthy vs rheumatoid joint 4
Figure 2) Initiation of inflammation 5
Figure 3) Representation of neutrophil frustrated phagocytosis 9
Figure 4) Schematic of intestinal cross-section illustrating the life-cycle of H. polygyrus 18
Figure 5) Representation of immunoregulatory effects of H. polygyrus 20

Figure 6) In-lab Hpb life cycle representation 32
Figure 7) Representation of AIA induction 33
Figure 8) Representation of AIA time course 34
Figure 9) Representation of infection and AIA model 35

Figure 10) H. polygyrus life cycle confirmation 40
Figure 11) Characteristics of knee inflammation of mice with AIA 41
Figure 12) Knee inflammation of mice with AIA in male vs females 42
Figure 13) Kinetics of knee inflammation of mice with AIA 44
Figure 14) Characterization of AIA model at 24hrs 45
Figure 15) Hpb Infection in AIA 47
Figure 16) Spleen cytokine levels of AIA following Hpb infection 48
Figure 17) Knee neutrophil viability in AIA following Hpb infection 48
Figure 18) AIA worm burden 49
Figure 19) mBSA IgG 50
Figure 20) Hpb infection effect on peripheral blood leukocytes 51
Figure 21) Metabolomic characterization of Hpb infection on AIA**.** 53
Figure 22) Different metabolomic profiles in AIA and Hpb+AIA. 53
Figure 23) Statistical analysis of Control group vs AIA group. 55
Figure 24) Enrichment of pathway analysis of AIA 56
Figure 25) Statistical analysis of AIA group vs AIA+Hpb group 57
Figure 26) Enrichment of pathway analysis AIA+Hpb 58
Figure 27) Box and whisker plots of plasma metabolite levels 59
Figure 28) Box and whisker plots of plasma metabolite levels 60

List of Supplementary Figures

Supplementary Figure 1) Statistic analysis of all groups 83
Supplementary Figure 2) Metabolomic characterization of Hpb infection on AIA 84
Supplementary Figure 3) Heatmap of enrichment pathway analysis of Ctl PBS vs AIA 84
Supplementary Figure 4) Heatmap of enrichment pathway analysis of AIA vs Hpb-AIA 85
Supplementary Figure 5) Arthritis and cartilage damage in the knee joint 86
Supplementary Figure 6) CXCL-1-induced neutrophil recruitment in the cremaster muscle 88

Abbreviations

List of abbreviations used in the manuscript along with their full forms:

Hpb	*Heligmosomoides polygyrus bakeri*
AIA	Antigen-induced-arthritis
RA	Rheumatoid arthritis
HES	Helminth Excreted-Secreted products
ACPAs	Anti-citrullinated protein antibodies
GNS	N-acetylglucosamine-6-sulfatase
ROS	Reactive oxygen species
TNF	Tumor necrosis factor
CBC	Complete blood count
CMP	Comprehensive metabolic panel
RF	Rheumatoid Factor
Anti-CCP	Anti-cyclic citrullinated peptide
ESR	Erythrocyte Sedimentation Rate
CRP	C-reactive protein
MMPs	Matrix metalloproteinases
CII	anti-type II collagen
LPS	Lipopolysaccharide
FLNA	Filamin A
SEs	Shared epitopes
IFNG	Interferon-γ
MPO	Myeloperoxidase

1. Background

1.1 Rheumatoid arthritis

Human rheumatoid arthritis (RA) is a major autoimmune disease, pathologically characterized by proliferative synovitis, manifesting in joint inflammation, edema, and progressive destruction of articular cartilage and bone (Feldmann, Brennan et al. 1996), as well as fatigue and joint pain. RA is a systemic disease, with symptoms varying from person to person, usually starting in the joints. Depending on disease progression, a number of extra-articular manifestations may develop, including vasculitis, subcutaneous nodule formation, inflammatory eye disease, and lung disease (Shaw, Collins et al. 2015). Furthermore, it is estimated that the risk of heart attack increases by 60% in patients with RA within one year post diagnosis (Nicola, 2006), and patients with RA are estimated to be twice as likely to suffer from depression (Widdifield, Paterson et al. 2014).

While the pathogenesis of RA is not yet completely understood, various genetic, and environmental factors, as well as a complex interplay between many elements of the immune system, are implicated in its pathophysiology. Two major subtypes of RA have been identified according to the presence or absence of anti-citrullinated protein antibodies (ACPAs/anti-CCP) as well as rheumatoid factor (RF). These subsets are seropositive RA and seronegative RA. Seropositive RA diagnosis refers to positive ACPA and/or RF blood tests. Seronegative RA refers to RA diagnoses where ACPA and RF are absent. Anti-citrullinated protein antibodies (ACPAs) are antibodies to citrullinated peptides (CP), they are cross-reactive in nature and can recognize many citrullinated proteins. CP leads to the activation of immune responses and the generation of specific anti-citrullinated protein antibodies (ACPA). Rheumatoid factors (RF) are

antibodies that attach to the Fc region of other antibodies; they can be any isotope but are mostly IgG or IgM.

While the presence of RF or ACPA alone is not indicative of RA, seropositive RA is considered to be more progressive and severe than seronegative RA. Seropositive RA is associated with greater joint damage, rheumatic nodules, deformity, lung issues, development of vasculitis and extra-articular manifestations (Malmström, Catrina et al. (2017), (Choi and Lee 2018). The autoimmune response in seropositive RA is presumably initiated by the citrullination of self-peptides, leading to alterations of their shape and the activation of immune responses and generation of specific ACPAs (Catrina, Krishnamurthy et al. 2021). ACPA generated by citrulline-specific B cells may react with various citrullinated autoantigens, such as fibrinogen, fibrin, vimentin, type II collagen,α-enolase, and histones (Catrina, Krishnamurthy et al. 2021).

1.1.1 Diagnosis and Therapies. RA, and other forms of inflammatory autoimmune diseases, cannot be detected through one single diagnostic test. Rather, bloodwork, imaging and physical exams are all required. Blood work tests could include: complete blood count (CBC), comprehensive metabolic panel (CMP), Rheumatoid Factor (RF, autoantibody against IgG Fc), antibodies to citrullinated peptides including (ACPAs, autoantibodies against cyclic citrullinated peptides), Erythrocyte Sedimentation Rate (ESR, elevated in RA), and C-reactive protein (CRP, marker of inflammation) (Heidari 2011). While newer studies have demonstrated that joint pain and joint inflammation in RA is not completely correlated (Krock, Jurczak et al. 2018, Lopes, Vicentini et al. 2020), reducing the inflammatory burden may be responsible for prolonging survival in women, as well as reducing disease severity and slowing down disease progression (Kasman N 2004, Jacobsson, Turesson et al. 2007, Widdifield, Paterson et al. 2014). This is why

early, aggressive treatment is recommended to prevent joint damage (Widdifield, Paterson et al. 2014).

Current treatment goals focus on 1) reducing pain and 2) stopping or slowing further damage (Widdifield, Paterson et al. 2014). To reduce pain, the first group of treatments includes: Nonsteroidal Anti-Inflammatory Drugs (NSAIDs), which primarily work to reduce pain by reducing inflammation, but do not inhibit the progression of RA (Kidd, Langford et al. 2007); and corticosteroids, which work to quickly decrease inflammation; ideally for short-term usage (Vonkeman and van de Laar 2010). To stop or slow further damage, the second group of treatments includes Disease-Modifying Antirheumatic Drugs (DMARDs), and Biologic DMARDs. DMARDs are the most standard RA treatment and work to slow down the progression of RA (Kasman N 2004), however, they may cause moderate to severe adverse effects (Bullock, Rizvi et al. 2018). Biologic Response Modifiers (biologic DMARDs), often used in combination with DMARDs, work to modify immune systems that have trouble responding to DMARDs (Kasman N 2004). However, these therapies have shown limited efficacy in certain patient cohorts with 1 in 3 patients not responding adequately to treatment (Vonkeman and van de Laar 2010, Tarnowski, Paradowska-Gorycka et al. 2016, Bullock, Rizvi et al. 2018). Consequently, there is a need for more diverse and safe treatments that can be used broadly among multiple RA patient cohorts.

1.1.2 Pathology. In the past two decades, there has been a great advance in the development of available RA therapies thanks to a better understanding of the pathogenesis of RA, its key cells, and cytokines (Bullock, Rizvi et al. 2018). In both subsets of RA, while there is no exact timeline for the progression, without effective treatment, the condition tends to worsen over time, progressing through specific stages (Heidari 2011); first as an autoimmune disease,

then evolving into a chronic inflammatory joint disease complicated by recurrent episodes of systemic acute-phase reactions (Badolato and Oppenheim 1996). Several studies have shown a significant decline in the risk of death, as well as a reduction in disease severity and progression, following anti-inflammatory treatments (Kasman N 2004, Jacobsson, Turesson et al. 2007, Widdifield, Paterson et al. 2014). It is important, therefore, to modulate and understand the inflammation in the joint to prevent disease progression.

The pathology of RA is characterized by (a) acute and chronic/acute inflammation, (b) cell proliferation, and (c) tissue destruction/fibrosis. Joint inflammation and damage in RA are mediated by the influx of innate and adaptive immune cells into the synovial joint space (Wright, Moots et al. 2014). The usual course of RA progression, for most people, includes flare-ups of high disease activity (Bullock, Rizvi et al. 2018). One of the main characteristics of this acute stage and flares is the formation of the pannus. In RA joints are typically swollen and contain an inflamed and hyperplastic synovial lining and excess synovial fluid (Wright, Moots et al. 2014), as can be observed in **Figure 1**. The pannus, or invasive tissue, is then formed, which contains CD4+ T cells, lymphocytes, neutrophils, macrophages, activated synovial fibroblasts and others. These in turn secrete proinflammatory mediators, such as chemokines, cytokines, and prostaglandins, which perpetuate inflammation.

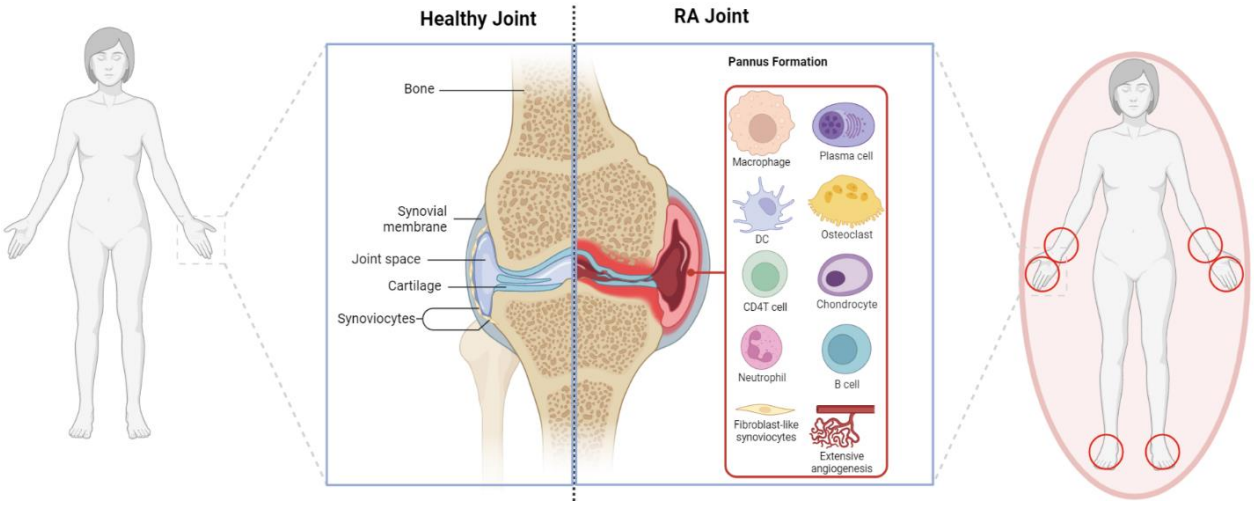

Figure 1) Representation of healthy vs rheumatoid joint indicating major cell types and sites of joint destruction. Representation of inflammation and pannus formation, with infiltrated and activated immune cells. Adapted from (Wright, Moots et al. 2014, Wright, Lyon et al. 2020). Created with BioRender.com

1.2 Inflammation

The damage caused by inflammation can be broken down into the work of both cytokines and immune complexes, the initial stages of inflammation can be described as follows (**Figure 2**): after an (as of yet) unknown trigger, a protein is citrullinated and taken in by antigen-presenting cells, such as dendritic cells (DC). Inflammation starts with the presentation of self-peptide to a naïve T-cell, which differentiates depending on the cytokines present. These in turn induce macrophages (Mθ) to produce more pro-inflammatory cytokines (such as IFN-γ, IL-6) further inducing Th1 and Th17 cells. At the same time, we have B-cell help (Th1 activating B cells) producing antibodies like RF and ACPAs. Differentiation into plasma cells promotes the immune complex formation and further Mθ activation. This leads, finally, to the activation of osteoclasts and chondrocytes which secrete cartilage and bone destructive enzymes (Smolen, Aletaha et al. 2018).

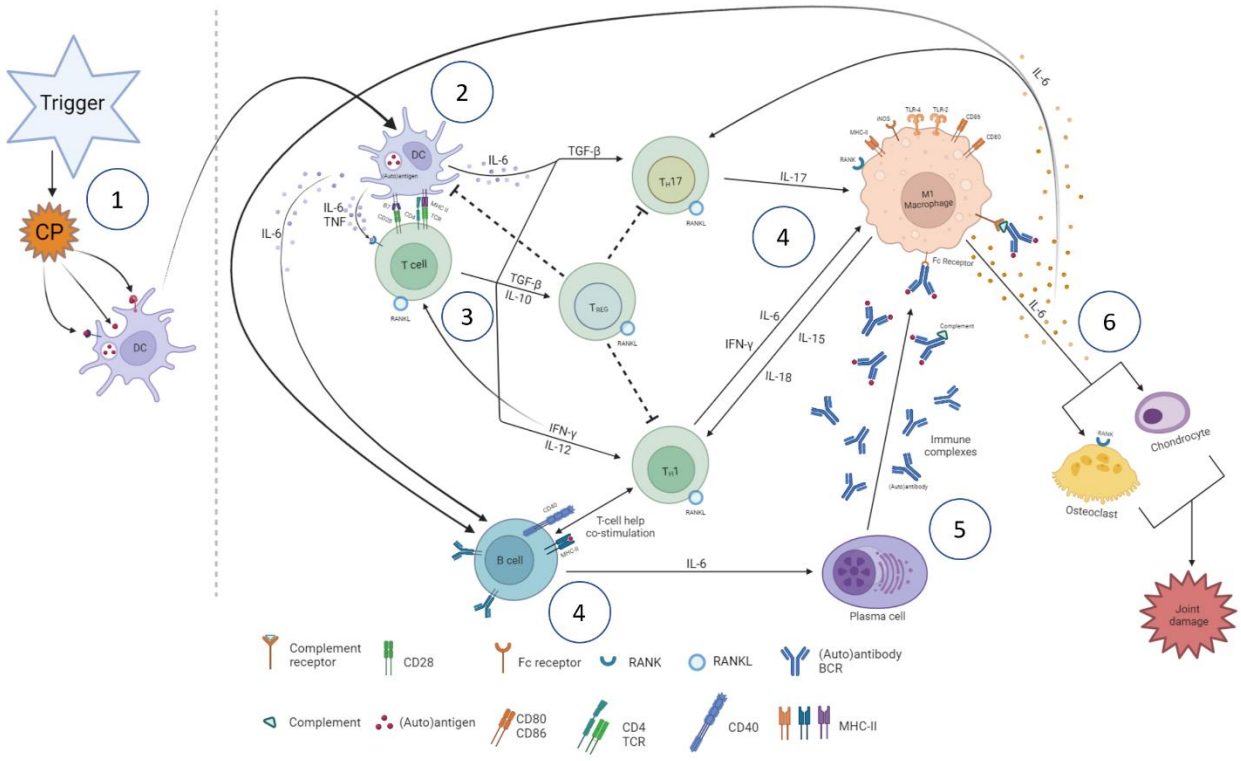

Figure 2) Initiation of inflammation. Schematic representation of initiation of acute inflammation in the pannus. Following an unknown trigger and protein citrullination, antigen-presenting cells present self-peptide to naïve T-cells, this results in the activation and recruitment of inflammatory cells into the joint and the local production of inflammatory mediators. This leads to the activation of osteoclasts and chondrocytes which secrete cartilage and bone destructive enzymes promoting cartilage degradation and amplifying the vicious cycle of inflammation. Adapted from Smolen *et al.* 2018. Created with BioRender.com

The recurrence of these triggers leads to the activation of immune responses in joints and the deposition of immune complexes, causing the formation of the pannus (i.e., mass infiltration of inflammatory cells into the synovium). As an effective trigger for inflammation, immune complexes and autoantibodies activate Fc receptors, which are trapped in a narrow space in the joint, causing synovium inflammation (Smolen, Aletaha et al. 2018).

1.2.1 Neutrophils. Neutrophils are the most abundant type of granulocytes in humans, making up 40% to 70% of all white blood cells. They are the first cellular responders to acute pathogenic insults and are the body's first line of defense against pathogens (Kobayashi and Deleo 2009). Neutrophils follow the leukocyte adhesion cascade to move from the bone marrow and extravasate from the vasculature where they are recruited to sites of infection or

inflammation (Sandilands, McCrae et al. 2006). Amongst their three main functions are: degranulation, netosis, and phagocytosis; all of which play a role in fine-tuning the immune response and modulating the activity of innate and adaptive immunity (Tecchio and Cassatella 2016).

A vital activity of neutrophils is the release of reactive oxygen species (ROS; i.e., oxidative burst), important in both antimicrobial host defense and inflammation (Mittal, Siddiqui et al. 2014). During this oxidative burst, neutrophils consume oxygen and convert it into superoxide radicals via the NADPH oxidase 2 (NOX2) complex (Nunes, Demaurex et al. 2013, Mittal, Siddiqui et al. 2014). Under inflammatory conditions, the oxidative stress produced promotes the migration of inflammatory cells across the endothelial barrier by opening inter-endothelial junctions (Mittal, Siddiqui et al. 2014). The migrated inflammatory cells not only help in the clearance of pathogens but also lead to tissue injury.

Circulating neutrophil properties are different from inflammatory neutrophils within the tissue. Circulation neutrophils usually have a short lifespan of 24 hours (undergoing constitutive apoptosis). However, in inflamed tissue, there is lower oxygen tension and pH, as well as chemokines and inflammatory molecules which regulate chemotaxis and activation of neutrophils and other leucocytes, which upregulate neutrophil gene expression (Walmsley, Print et al. 2005, Wright, Lyon et al. 2020) and affect neutrophil function and longevity (Cross, Barnes et al. 2006). During inflammation they share macrophage-like functions such as the expression of cytokines, chemokines, and MHC class II antigens (Wright, Moots et al. 2014, Wright, Lyon et al. 2020). HLA-DR is not present on circulating neutrophils but is expressed on the surface of tissue neutrophils under specific inflammatory conditions, such as in RA synovial fluid (Sandilands, McCrae et al. 2006). Additionally, the presence of neutrophil priming agents during

inflammation, such as TNF or granulocyte-macrophage colony-stimulating factor (GM-CSF), in the peripheral blood enhances neutrophil extravasation, chemotaxis, and oxidative burst production (Amulic, Cazalet et al. 2012). With their high pro-inflammatory activity, excessive neutrophil accumulation and prolonged activation can result in tissue damage and chronic inflammation (Amulic, Cazalet et al. 2012). Further, the dysfunction of neutrophils has been associated with adverse prognoses in a variety of diseases including rheumatoid arthritis (RA).

Neutrophils in RA. One of the most prominent drivers of joint inflammation in RA is the overabundance and persistence of activated neutrophils, which release proinflammatory cytokines and cause tissue damage (Rosas, Correa et al. 2017, Cecchi, Arias de la Rosa et al. 2018, O'Neil and Kaplan 2019). They are the most abundant cell type in the pannus, constituting over 90% of cells found in the synovial fluid, and are also detected in RA synovial tissue (Palmer, Hogg et al. 1986, Tak, Smeets et al. 1997, Cascão, Moura et al. 2010, Cecchi, Arias de la Rosa et al. 2018). Neutrophils have been recognized as a major player in disease progression, demonstrating a differentiated activated phenotype characterized by delayed apoptosis, increased capacity to produce ROS, active gene expression, and membrane expression of high-affinity Fcγ receptors (Wright, Moots et al. 2014, Rosas, Correa et al. 2017, Cecchi, Arias de la Rosa et al. 2018, O'Neil and Kaplan 2019, Wright, Lyon et al. 2020). Besides this activated phenotype in peripheral blood, activated neutrophils have been found in high numbers in both synovial joints and tissues of patients with RA (Wittkowski, Foell et al. 2007, Cascão, Moura et al. 2010, Moura, Cascão et al. 2011, Turunen, Huhtakangas et al. 2016). It has also been shown that levels of ACPA in RA synovial fluid correlate with neutrophil numbers and severe disease activity, additionally synovial fluid with high ACPA titers induces high levels of ROS and NET production (Gorlino, Dave et al. 2018).

Cumulative data has demonstrated the importance of neutrophils as a potential target for treatment in RA. Injection of serum from K/B×N mice (K/BxN mice spontaneously develop inflammatory arthritis at around 3-5 weeks of age) into wild-type mice initiates a rapid development of inflammatory arthritis. Interestingly, neutrophil-depleted mice were demonstrated to be completely resistant to the disease-inducing effects of K/B×N serum transfer (Wipke and Allen 2001). Studies on anti-type II collagen (CII) antibodies and lipopolysaccharide (LPS) induced arthritis also demonstrated that neutrophil depletion completely inhibited arthritis development (Tanaka, Kagari et al. 2006). Furthermore, in mice that had already developed arthritis, neutrophil depletion ameliorated the disease (Tanaka, Kagari et al. 2006). This collective data demonstrates that neutrophils are indispensable for the development and maintenance of RA.

Neutrophil tissue damage in the joint. Within the synovial fluid neutrophils are activated by soluble immune complexes that induce neutrophil degranulation and release the of ROS and proteases, leading to the degradation of hyaluronic acid and activation of cytokines (Wright, Moots et al. 2014). Neutrophils present at the pannus–cartilage interface also become activated by locally deposited immune complexes (Figure 3). They undergo frustrated phagocytosis (deposition of immune complexes onto the joint surface resulting in an incomplete phagosome formation), releasing hypochlorous acid, ROS, and cartilage degrading enzymes within a microenvironment directly on the surface of the cartilage, leading to cartilage destruction (Figure 3) (Wright, Moots et al. 2014). At the pannus-cartilage junction, neutrophils contribute to matrix degradation by secreting neutrophil elastase, MMP-8, MMP-9, cathepsin G, and proteinase 3 (Murphy and Nagase 2008). Several chemokines responsible for regulating the inflammatory response in the joint are highly expressed in RA synovial fluid neutrophils,

including CXCL1, CXCL2, and CXCL8 (recruitment of other neutrophils), as well as CCL3, CCL4, CCL10, CXCL16, and CXCL2 (recruitment and activation of both innate and adaptive immune cells) (Wright, Lyon et al. 2020). Cumulative evidence also suggests that cytokines are crucial mediators for RA's pathogenesis. In particular, proinflammatory cytokines, such as IL-1β, tumor necrosis factor (TNF), interferon-γ (IFN-γ) and IL-6 play a pivotal role in pathogenesis (Wright, Lyon et al. 2020) as well as, GM-CSF, C5a, IL-17, LTB_4, IL-8 (O'Neil 2018), IL-1β, IL-12 and IL-23 (Rosas, Correa et al. 2017).

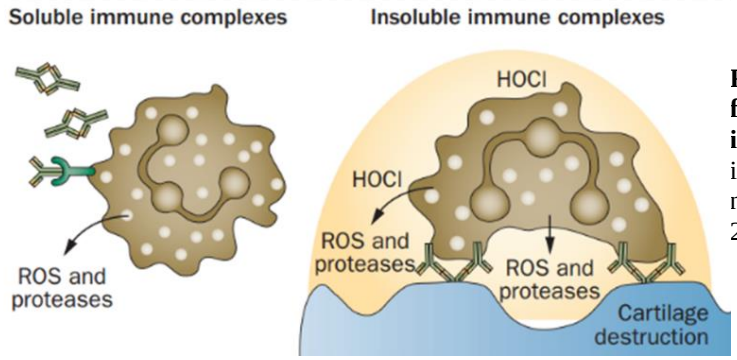

Figure 3) Representation of neutrophil frustrated phagocytosis in pannus-cartilage interface. Representative summary of inflammatory role by RA synovial fluid neutrophils (Edited from (Wright, Moots et al. 2014) (Wright, Lyon et al. 2020).

1.3 Animal Models of Arthritis

Several murine models of RA have been developed to study different mechanisms of the disease. From a historical perspective, the models most widely used in the past decades include collagen-induced arthritis, adjuvant-induced arthritis, antigen-induced arthritis, collagen antibody-induced arthritis, *streptococcal* cell wall-induced arthritis, as well as serum transfer from K/BxN transgenic mice, and tumor necrosis factor (TNF)-transgene mice (Bendele, McComb et al. 1999, Wipke and Allen 2001, Nandakumar and Holmdahl 2006, Baddack, Hartmann et al. 2013, Bas, Su et al. 2016, Castañeda-Lopez, Garza-Veloz et al. 2018). This study

will focus on the Antigen Induced Arthritis (AIA) murine model due to its ability to replicate acute inflammation of the joint in a T-cell-mediated monoarthritic manner.

It is important to keep in mind that key differences exist between mouse and human immune systems. Whereas mouse neutrophils represent around 10–20% of circulating white cells, human neutrophils represent 40–70% of blood leucocytes (Wright, Moots et al. 2014). Key differences between mice and human immune systems exist, including subtle differences in the phenotype of neutrophils (Wright, Moots et al. 2014). Key differences between mice and human surface molecule expression, including MHC class II antigens, FcγR, TLRs, and chemokine receptors have also been described by Mestas *et al*. (2004).

1.3.1 Antigen Induced Arthritis. Antigen-induced arthritis (AIA) is a well-characterized, experimental model of joint disease. AIA is a T-cell mediated monoarthritis model commonly used in mice and rats (Brackertz, Mitchell et al. 1977, Coelho, Pinho et al. 2008, Lopes, Coelho et al. 2011, Krock, Jurczak et al. 2018). This model is induced by first immunizing mice with methylated bovine serum albumin (mBSA) and Freund's complete adjuvant (CFA) in an oil emulsion inoculated at the base of the tail; 14 days after immunization mBSA is injected into the joint (Lopes, Coelho et al. 2011). It is evaluated by articular leukocyte trafficking and levels of cytokines (TNF) and chemokine (CXCL-1) in the periarticular tissue (Noviello Mde, Batista et al. 2013).

The model is characterized by an acute phase that involves joint swelling and immune cell infiltration (Krock, Jurczak et al. 2018). Joint inflammation is caused by local antigen-specific T-cell hyperreactivity and deposition of immune complexes (Cooke, Richer et al. 1975, van den Berg and van de Putte 1985), similarly to human RA. Intraarticular injection of mBSA

into the knee joint results in local inflammation characterized by swelling, immune cell infiltration, damage to the joint, and pain (Lopes, Graepel et al. 2016). After mBSA challenge, the acute inflammation and resolution kinetics of AIA have been well characterized; with a peak of neutrophil recruitment at 12-24 hours and resolution at 48 hours (Lopes, Coelho et al. 2011). Further, the pathological outcome of AIA is regulated by the presence of cytokines, such as TNF, and chemokines, such as CXCL-1, in the synovium (Coelho, Pinho et al. 2008, Shiozawa, Tsumiyama et al. 2011). These chemokines and cytokines amplify the inflammatory response by activating resident cells that attract neutrophils into the synovial cavity (Kagari, Doi et al. 2002, Shiozawa, Tsumiyama et al. 2011, Noviello Mde, Batista et al. 2013). Other important markers in AIA include cytokine IFN-γ and myeloperoxidase (MPO). These markers, chemokines, and cytokines will be further explored in the following section.

TNF. Tumor necrosis factor (TNF) is a multifunctional cytokine secreted by inflammatory cells, with a primary role in immune cell regulation. As an adipokine, cytokine, or endogenous pyrogen, it plays an important part in cell differentiation, survival, proliferation, and death. As a cytokine, TNF is used in cell signaling. Macrophages release TNF to alert other immune cells and initiate the inflammatory response, which leads to the production of chemokines, this in turn bind to proteoglycans and forms a gradient in the inflamed tissue and along the endothelial wall (Hall J, 2011). This affects a wide variety of cells to induce inflammatory reactions such as fever, chemotaxis, production of cytokines, fibroblasts activation, and leukocyte adherence (Hall J, 2011). TNF affects the pathological outcome of inflammatory arthritis, playing an important part in AIA, in a similar manner to RA, activating resident cells to attract neutrophils into the synovial cavity and amplifying the inflammatory response (Noviello Mde, Batista et al. 2013, Wright, Lyon et al. 2020). Further, TNF has also

been linked as a key mediator of chronic pain and depression-like behavior after remission of joint inflammation in AIA (Lopes, Vicentini et al. 2020).

IFN-γ. Interferon-gamma (IFN-γ), or type II interferon, is important in both innate and adaptive immunity against viral, bacterial, and protozoan infections. IFN-γ works as both an important autocrine signal, for professional APCs in early innate immune response, and a paracrine signal, in the adaptive immune response (Luckheeram, Zhou et al. 2012). It is the primary cytokine that defines Th1 cells, these cells further secrete IFN-γ in a positive feedback loop that further activates more undifferentiated CD4+ cells to differentiate into Th1 cells (suppressing Th2 cell differentiation) (Luckheeram, Zhou et al. 2012). IFN-γ is secreted by T-helper cells (specifically, Th1 cells, once antigen-specific immunity develops), cytotoxic T-cells (TC cells), mucosal epithelial cells, NK cells, and macrophages. Not only is it involved in the activation of CD4+ Th1 cells, but also in inducing proinflammatory effects. It is an important activator of macrophages, as well as an inducer of MHC-II molecule expression (Luckheeram, Zhou et al. 2012). Abnormal IFN-γ expression has been associated with several autoinflammatory and autoimmune diseases, such as EAE (experimental autoimmune encephalitis) (Brüstle, Heink et al. 2007). Further, an interaction between IFN- γ, IL-17, and neutrophil recruitment was demonstrated by Irmler, Gajda et al. (2007), who observed an exacerbation of AIA in IFN-γ-deficient mice as a result of unrestricted IL-17 response (Irmler, Gajda et al. 2007). IL-17-producing Th-cells are also known to play a major role in the inflammatory pathogenesis of AIA (Irmler, Gajda et al. 2007).

CXCL-1. As previously mentioned, a number of chemokines have been recognized as major players in regulating the inflammatory response in the joint and are also highly expressed in RA synovial fluid neutrophils. A key chemokine important in the recruitment of neutrophils

for both RA and AIA is chemokine C-X-C motif ligand 1(CXCL1). CXCL-1 acts as a chemoattractant for various immune cells or other non-hematopoietic cells at a site of injury or infection, but especially for neutrophils (Schumacher, Clark-Lewis et al. 1992). Thus, it plays an important role in regulating immune and inflammatory responses. It is produced by a variety of immune cells such as neutrophils, macrophages, epithelial cells, or Th17-cells, and is not expressed constitutively upon normal conditions (Becker, Quay et al. 1994). Additionally, its expression can be indirectly induced by IL-1, TNF, or IL-17. It is mainly triggered by the activation of NF-κB or C/EBPβ signaling pathways, which are predominantly involved in inflammation leading to further production of other inflammatory cytokines (Ma, Yang et al. 2018; Silva, Lopes et al. 2017). CXCL1 is expressed at higher levels during these inflammatory responses, thus contributing to the process of inflammation (Silva, Lopes et al. 2017). These inflammatory events are also observed in the murine model of AIA in a similar manner to RA (Coelho, Pinho et al. 2008, Shiozawa, Tsumiyama et al. 2011, Noviello Mde, Batista et al. 2013).

Myeloperoxidase. A number of the intracellular components of neutrophils, as well as neutrophils themselves, have been linked to the pathophysiology of RA (Rosas, Correa et al. 2017). Myeloperoxidase (MPO) is the most cytotoxic and abundant enzyme expressed in neutrophil granulocytes and has also been linked to RA (Strzepa, Pritchard et al. 2017). In the context of AIA, MPO is used to indirectly measure the infiltration of neutrophils into the periarticular tissue (Barcelos, Talvani et al. 2004, Lopes, Coelho et al. 2011).

MPO plays a well-known role in immune responses, has direct anti-bacterial properties, and has emerged as a modulator of the adaptive immune response (Strzepa, Pritchard et al. 2017), for example, it participates in the activation of T-cells as well as the elimination of pathogens (Strzepa, Pritchard et al. 2017; Cecchi, Arias de la Rosa et al. 2018). MPO triggers the

production of inflammatory cytokines and interacts with endothelial cells, leading to an increased endothelial cell permeability and activating dendritic cells (this is mediated by nitric oxide consumption and nitrite anion generation) (Eiserich, Baldus et al. 2002, Klinke, Nussbaum et al. 2011). Increased MPO activity and protein levels have been observed in many inflammatory conditions and autoimmune diseases, including in the joints of rheumatoid arthritis (RA) patients, and in the central nervous system of multiple sclerosis (MS). They have also been linked to coronary artery disease (Strzepa, Pritchard et al. 2017). Further, a specific role for MPO in both the K/BxN and CIA models of RA was indicated by reduced disease severity in $MPO^{-/-}$ mice (Odobasic, Kitching et al. 2013). Demonstrating that depleting MPO in a mouse model of arthritis reduces the severity of the disease, and further indicates that MPO may have a direct impact on inflammation in the joint, which is independent of the underlying immune response (Strzepa, Pritchard et al. 2017).

1.4 Helminth regulation of inflammation

Many epidemiological studies have drawn a link between the incidence of helminth infection and a reduction in allergic and inflammatory diseases (Cooper 2009, Wiria, Djuardi et al. 2012, Rajamanickam, Munisankar et al. 2020). Helminth parasites have been found to be effective in inducing regulatory pathways that reduce inflammatory responses within their hosts, thus allowing chronic infection to occur whilst also suppressing bystander atopic or autoimmune diseases (Cooper 2009, Smith, Hochweller et al. 2011, McSorley and Maizels 2012, Maizels, Smits et al. 2018). Consequently, infection with parasitic helminths is currently being studied to treat and limit the severity of diabetes, multiple sclerosis, arthritis, atopic conditions, airway inflammation and IBD (Weinstock and Elliott 2009, Fleming 2013, Lopes, Matisz et al. 2016,

Steinfelder, O'Regan et al. 2016). Some examples of helminths used in different models of RA as potential experimental treatments are listed in Table 1, together with their respective effects and potential mechanisms.

Table 1. Summary of Experimental Models for Helminths in RA

Helminth Species	**Treatment**	**Effect of Treatment**	**Mice model**	**Proposed Mechanism**	**Ref.**
Acanthocheilonema viteae	ES-62; SMAs	Modify bone remodeling by altering bone marrow progenitors and thus impacting osteoclastogenesis.	Collagen-induced arthritis (CIA)	Inhibits functional osteoclast differentiation *in vitro* by induction of antioxidant response gene expression, resulting in reduction of ROS production.	(Doonan, Lumb et al. 2018)
Nippostrongylus brasiliensis	Infection	Th2 and eosinophil accumulation in the joints associated with robust inhibition of arthritis and protection from bone loss.	K/BxN serum transfer arthritis; tumor necrosis factor (TNF) transgenic (hTNFtg) mice	Dependent on IL-4/IL-13-induced STAT6 pathway	(Chen, Andreev et al. 2016)
Heligmosomoides polygyrus bakeri	Infection	Attenuates the development of arthritis and positively impacts systemic bone metabolism	Collagen-induced arthritis (CIA); Collagen antibody-induced arthritis (CAIA)	Inhibits the differentiation of osteoclasts in vitro, no mechanism	(Sarter, Kulagin et al. 2017)

Helminth therapy can be approached from three broad perspectives: (1) the use of viable ova/larvae, (2) the administration of helminth-derived extracts or purified molecules, and (3) cellular immunotherapy with helminth extract/antigen-pulsed immune cells (Lopes, Matisz et al. (2016)). The use of (1) viable ova/larvae has been demonstrated in several different settings of infection with a variety of helminth species. Of note is a study by Correale et al (2007), who observed that 12 adult multiple sclerosis (MS) patients with intestinal helminth infections remained in remission, while uninfected subjects with similar disease scores at the initial time point experienced repeated relapses and exacerbations. They went on to demonstrate that there was increased production of IL-10 and TGF-β, together with the induction of CD25+CD4+

FoxP3+ T cells; suggesting that Treg cells induced during parasite infections can alter the course of MS (Correale and Farez 2007).

However, while promising, the use of viable ova/larvae is still a topic of debate, with disbenefits such as compromised responses to certain microbial infections (Salgame, Yap et al. 2013; DiNardo, Nishiguchi et al. 2018) and vaccination (LaBeaud, Malhotra et al. 2009). Alternatively, the (2) administration of helminth-derived extracts or (3) cellular immunotherapy with helminth extract/antigen-pulsed immune cells, have risen as potential resources of more universally effective treatments, and as a way to understand the helminth-driven regulatory pathways involved in anti-inflammatory properties; this way reproducing the effect of live parasites without exposing patients to the detrimental effects of infection (Segura, Su et al. 2007, Jang, Cho et al. 2011, Rzepecka, Coates et al. 2014, Lopes, Matisz et al. 2016, Hiemstra, Klaver et al. 2014). Owing to the advances made in this research in the last couple of years, we have a better understanding of the mechanisms by which helminths induce anti-allergenic or anti-inflammatory effects.

Helminth-induced regulatory T and B cells (Tregs and Bregs, respectively) have been linked to the dampening of responses to allergens (Logan, Navarro et al. 2018, Maizels 2020) such as ovalbumin (OVA) (Mangan, van Rooijen et al. 2006, Amu, Saunders et al. 2010), house dust mites (Wilson, Taylor et al. 2005, Qiu, Fan et al. 2017), and peanuts (Bashir, Andersen et al. 2002). They have also been linked to the amelioration of inflammation in several disease models, including experimental autoimmune encephalitis (Wilson, Taylor et al. 2010), colitis (Elliott, Setiawan et al. 2004, Metwali, Setiawan et al. 2006, Hang, Blum et al. 2013), diabetes (Hübner, Shi et al. 2012, Morimoto, Azuma et al. 2017), and prevented arthritis in a murine model of RA (Sarter, Kulagin et al. 2017). One of the most potent examples of helminths with such immuno-

modulatory effects is the murine intestinal nematode *Heligmosomoides polygyrus* (Monroy and Enriquez 1992), which has a remarkable record of modifying a wide spectrum of host immune responses (Maizels, Hewitson et al. 2012).

1.4.1 *Heligmosomoides Polygyrus bakeri.* *Heligmosomoides polygyrus bakeri* (Hpb; also known as *H. polygyrus* or H. *bakeri*) is a naturally occurring intestinal roundworm of mice. It is a widely applied murine model used to study host-parasite interactions in gastro-intestinal helminth infection (Monroy and Enriquez 1992, Camberis, Le Gros et al. 2003, Behnke, Menge et al. 2009, Maizels, Hewitson et al. 2012). Hpb belongs to the Strongylida order together with the human hookworm parasites *Ancylostoma duodenale* and *Necator americanus*. While the Hpb life cycle does not follow that of human hookworms, such as skin penetration and lung migration before entering the intestinal lumen (unlike *N. brasiliensis*), primary infection with Hpb can establish a chronic infection in most strains of laboratory mice and thus represents a useful model for chronic intestinal helminthiases (Barron and Wynn 2011).

Life cycle. Hpb has five developmental forms (L1-L5). Under natural conditions, Hpb is transmitted via the fecal-oral route, while under experimental conditions infection is initiated by oral gavage (Valanparambil, Segura et al. 2014). A diagram of the life cycle can be seen in Figure 4.

The cycle starts when mice ingest infective L3-stage larvae. These larvae penetrate the duodenum mucosa of the small intestine and migrate to the muscularis externa settling in the tunica muscularis within 24 hours. Here, they further differentiate into L4-stage larvae and develop into male and female adult worms. These stages elicit inflammation, local tissue damage, and the formation of granulomatous infiltrates, L4-larvae are surrounded by

inflammatory cells (mostly eosinophils) and can be seen nestled in nodules on the surface of the small intestine. Eight to ten days after infection they emerge as adult worms into the lumen where they anchor tightly to the intestinal villi, mate, and produce eggs, which are excreted in the feces. The eggs hatch under favorable external conditions and develop into L1-larvae, these differentiate into L2 and eventually infective L3 within seven to nine days after expulsion; capable of infecting a new host after ingestion and continuing the life cycle (Valanparambil, Segura et al. 2014, Progatzky, Shapiro et al. 2021).

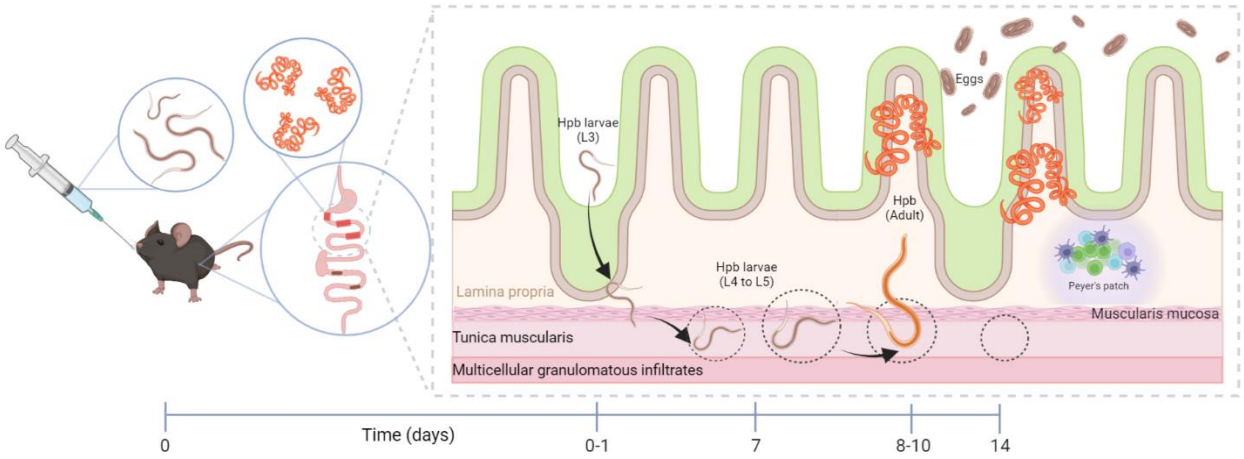

Figure 4) Schematic of intestinal cross-section illustrating the life-cycle of H. polygyrus (Image adapted from Progatzky et al 2021, and Valanparambil et al. 2014). Created with BioRender.com

Immunomodulatory effects. Hpb has been documented to have a wide spectrum of effects on host immune responses, from modulation of systemic immune pathologies including airway hyperresponsiveness (Wilson, Taylor et al. 2005, Kitagaki, Businga et al. 2006), intestinal food allergy (Bashir, Andersen et al. 2002), and bystander inflammatory responses to bacterial pathogens (Fox, Beck et al. 2000), to amelioration of inflammation in several disease models including, colitis (Elliott, Setiawan et al. 2004, Hang, Setiawan et al. 2010), experimental autoimmune encephalitis (Wilson, Taylor et al. 2010, White, Johnston et al. 2020), contact hypersensitivity (Filbey, Mehta et al. 2020), Type I diabetes (Saunders, Raine et al. 2007, Liu,

Sundar et al. 2009) and Type II diabetes (Morimoto, Azuma et al. 2017), as well as experimental models of RA (Sarter, Kulagin et al. 2017).

Importantly, primary Hpb infection induces an immune-regulatory network involving regulatory T cells (Tregs), tolerogenic dendritic cells (TolDCs), alternatively activated macrophages (AAMθ), and regulatory B cells (Bregs), as well as the anti-inflammatory cytokines IL-10 and TGF-β; all of which exert widespread immunomodulatory effects on both the innate and adaptive immune system of the host (Su, Segura et al. 2005, Weng, Huntley et al. 2007, Blum, Hang et al. 2012, Maizels, Hewitson et al. 2012, Reynolds, Filbey et al. 2012, Valanparambil, Segura et al. 2014). Several Hpb-derived excreted secreted products have been isolated, and while they reproduce the effect of live parasites without infection, there are differences between some of their immune-modulatory effects *in-vitro* when compared to the *in-vivo* Hpb infection (Segura, Su et al. 2007, Jang, Cho et al. 2011, Rzepecka, Coates et al. 2014, Lopes, Matisz et al. 2016, Maizels, Hewitson et al. 2012). A representation of the immunomodulatory *in-vitro* and *in-vivo* effects of Hpb is observed in Figure 5**)** Representation of

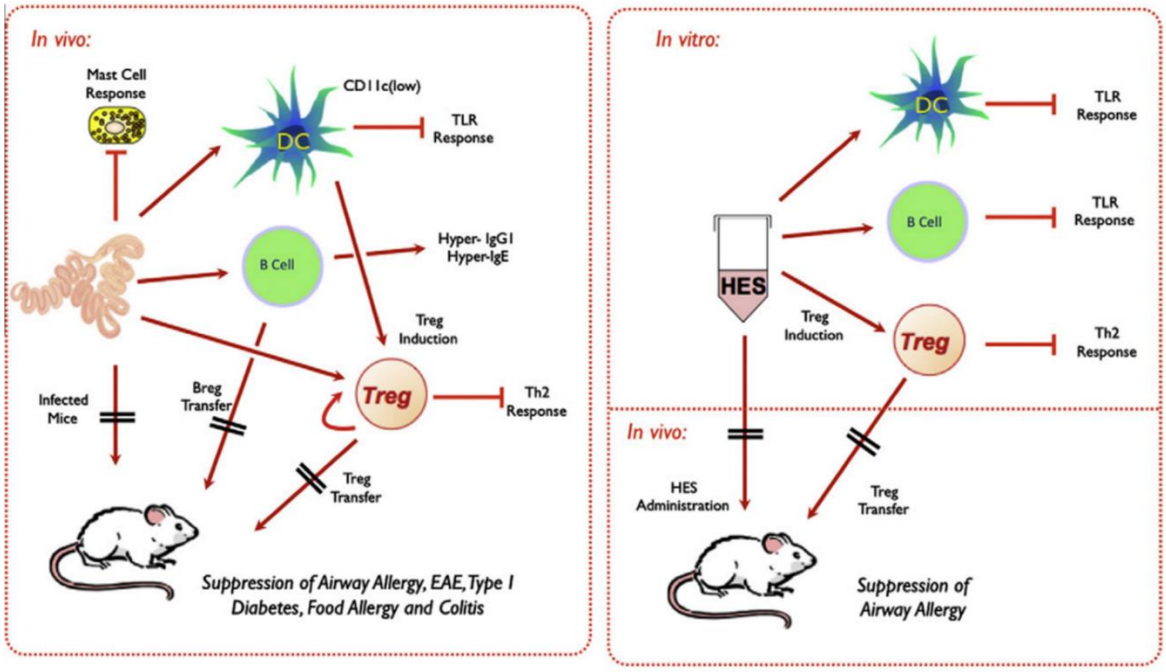

Figure 5) Representation of immunoregulatory effects of *H. polygyrus* A) *In-vivo* and B) *In-vitro* (Maizels 2012).

immunoregulatory effects of *H. polygyrus* A) *In-vivo* and B) *In-vitro* (Maizels 2012)..

While the majority of our understanding on the immune-modulatory and therapeutic role of Hpb has mainly been described for the adult stage, different Hpb life cycle stages secrete different products that could affect immunomodulatory effects (Maizels, Hewitson et al. 2012). In the next section, we will dive into the modulatory effects of both Hpb larvae and adult stages.

Recently, the L4-larvae stage of Hpb has risen as a crucial source of new compounds with immunomodulatory properties with potential therapeutic roles in the treatment of inflammatory diseases (Hewitson, Harcus et al. 2011, Moreno, Gros et al. 2011, Donskow-Łysoniewska, Krawczak et al. 2012, Donskow-Łysoniewska, Majewski et al. 2012, Maruszewska-Cheruiyot, Donskow-Lysoniewska et al. 2019). Further demonstrating the immunomodulatory properties of the L4 stage, the treatment effect of Hpb in autoimmune disorders has been observed before larval maturation (Donskow-Łysoniewska, Majewski et al. 2012, Maruszewska-Cheruiyot, Donskow-Lysoniewska et al. 2019, Maruszewska-Cheruiyot, Szewczak et al. 2021). In the early phase of Hpb infection, while in the lamina propria, the activation and expansion of $CD4^{+}Foxp3^{+}$ Tregs in the mesenteric lymph nodes, and CD8+ regulatory populations, have been reported (Finney et al., 2007; Rausch et al., 2008; Metwali et al., 2006). On the 7^{th} day of infection, several effects of L4 larvae have been reported: the larvae can polarize type 2 cytokine response (Filbey, Grainger et al. 2014), they also increase myeloid-derived suppressor cells in the lamina propria and systemic lymphoid tissues (Valanparambil, Tam et al. 2017), and that nuocyte population is subdued (Smith, K.A. et al., personal communication). *In-vitro* L4 larvae have been demonstrated to prevent the maturation of JAWS-II-DC and the Th2 regulatory response (Maruszewska-Cheruiyot, Donskow-Lysoniewska et al. 2019); with a suppressed CD4+ Th2 (GATA3+) response (Valanparambil, Tam et al. 2017).

On the 8^{th}-10^{th} day of infection, the adult worms emerge. This life stage is associated with Hpb immunomodulatory capabilities previously describes, including the induction of Tregs, TolDCs, AAMθs, and Bregs. In these later stages, Hpb-induced AAMθ have been associated with intestinal granulomas and protective immunity (Weng, Huntley et al. 2007, Maizels, Hewitson et al. 2012). A distinctive characteristic of this type of macrophage is its ability to suppress the proliferation of other cells with which it is co-cultured, as well as its ability to impair nitric oxide (NO) production and increase the expression of the transferrin receptor, supporting the intracellular growth of Mycobacterium tuberculosis (Kahnert, Seiler et al. 2006, Weng, Huntley et al. 2007). This life stage is also associated with Hpb modulation of microbiota, Walk et al. (2010) quantified the effects of Hpb on the composition of gastrointestinal tract microbiota in C57BL/6 (WT) mice and found that members of the bacterial family *Lactobacillaceae* significantly increased in abundance in the ileum of infected mice (Walk, Blum et al. 2010). Hpb adult stage has also been associated with an increase of B-reg cells expressing the low-affinity IgE receptor (CD23) in primary infection, these Bregs when transferred to uninfected hosts can suppress both airway allergic reactivity and experimental autoimmune encephalomyelitis (Wilson et al., 2010, Maizel 2012). Additionally, the production of TolDCs induces tolerogenic dendritic cells that block colitis and prevent antigen-specific gut T-cell responses (Blum 2012, Hang 2019). Finally, Hpb-derived excreted-secreted (ES) products have been shown to modulate CD4+ Th cell responses by suppressing DC function (Valanparambil, Segura et al. 2014).

Other known immunomodulatory molecules from the Hpb adult stage include: HpARI, an alarmin release inhibitor that blocks human and mouse IL-33 (Osbourn, Soares et al. 2017); TGM (TGF-β mimic), ligates TGF-β receptor on T-cells leading to induction of Treg cells

(Grainger, Smith et al. 2010, Johnston, Smyth et al. 2017); HpCPI, cystain inducing IL-10 producing macrophages, hyporesponsive T-cells and compromised APC function (Sun, Liu et al. 2013); and extracellular vesicles (EVs) with micro RNAs targeting epithelial cells and macrophages, leading to loss of IL-33 (Buck, Coakley et al. 2014, Coakley, McCaskill et al. 2017). These identified molecules have been summarized in Table 2, together with their modulatory effects.

Table 2. Summary of Hpb identified molecules.

Molecule	**Abbreviation**	**Effect of molecule**	**References**
Alarmin release inhibitor	**HpARI**	Suppresses Interleukin-33. Suppresses type 2 immunity in both infection and allergy.	Osbourn et al.,2017
Cysteine protease inhibitor (Cystain)	**HpCPI**	Modulates differentiation and activation stages of BMDC. Interferes with antigen and MHC-II molecule processing and Toll-like receptor signaling pathway (results in functionally deficient DC).	Sun et al., 2013
Extracellular vesicles	**EV**	Targets macrophage activation and IL-33 pathway. Downregulates type 1 and type 2 immune-response-associated molecules (IL-6 and TNF, and Ym1 and RELMa) and inhibits expression of the IL-33 receptor subunit ST2.	Buck 2014; Coakley 2017

1.5 Metabolomics

Metabolomics refers to the large-scale study of small molecules (or metabolites) within biofluids, organisms, cells, or tissues. Metabolites are separated chromatographically based on polarity, they are also ionized, and the resulting ions are separated and quantitated by mass spectrometry. Currently, metabolomics has been playing an increasing role in biological (Nicholson and Lindon 2008, Palsson 2009) and pharmaceutical research (Wei, Xie et al. 2011, Xu, Chang et al. 2022). While many methods exist to separate and study metabolites, one particularly sensitive and specific method is liquid chromatography-mass spectrometry (LC-MS).

Metabolomics methodologies fall into two distinct groups: targeted metabolomics and untargeted metabolomics. Targeted metabolomics measures defined groups of chemically characterized and biochemically annotated metabolites. Targeted metabolite quantitation is useful for building a comprehensive matrix of the quantitative response of known metabolites to a perturbation (Mark Ritchie and Mainak Mal 2012). One effective approach to quantify known metabolites is multiple reaction monitoring (MRM, or targeted MS/MS) on a triple-quadrupole instrument (Clasquin, Melamud et al. 2012). This, together with isotope labeling, can provide insight into metabolic pathway activities and is a prerequisite to the quantitation of metabolic fluxes. (Clasquin, Melamud et al. 2012). Untargeted metabolomics involves an intended comprehensive analysis of all the measurable analytes in a sample including chemical unknowns. Untargeted analysis is useful for identifying metabolites that differ between two or more sets of biological samples; for example, drug-treated versus control patient samples (Dunn, Erban et al. 2013).

1.5.1 Metabolomics in RA. In recent years many reports have been published reviewing the metabolome of RA, providing great advances in our understanding of RA metabolomics. The metabolic profiles of patients with RA are being determined using targeted and untargeted metabolomics technology. Thus far, metabolomics has enabled the discovery of biomarkers for clinical risk factors, subgroups, and predictors of treatment response. For example, a study by Hur et al. (2021) identified biochemical features predictive of quantitative disease activity using plasma metabolomic profiling from patients with RA (Hur, Gupta et al. 2021). More specifically, they identified eight metabolites significantly associated with Disease Activity Score-28 using C-reactive protein (DAS28-CRP): “abundances of mannose, beta-hydroxy isovalerate, (14 or 15)-

methyl palmitate (a17:0 or i17:0), erucate (22:1n9), 10-undecenoate (11:1n1), N-acetyl citrulline were higher in high-CRP, while those of serine and linoleoylcarnitine (C18:3) were lower in high CRP" (Hur, Gupta et al. 2021). Elevated levels of CRP (C-reactive protein) in the blood are well known to indicate increased inflammatory conditions (Nehring Sara 2022). Studies such as this are providing insight into circulating pro- or anti-inflammatory metabolic signatures that reflect disease activity and inflammatory status in RA patients (Hur, Gupta et al. 2021).

These metabolomic technologies have been used on patient biospecimens, this way patients with RA were classified according to their disease activity categories (Hur, Gupta et al. 2021). Such as the work by Li J et al. who used LC-MS-based serum metabolomics to reveal a distinctive signature in patients with RA (Li, Che et al. 2018, Li, Ma et al. 2022). Likewise, Teitsma et al. identified metabolites and metabolic pathways significantly associated with sustained, drug-free remission after tocilizumab- or methotrexate-based therapy using metabolomic profiling in serum samples from early RA patients (Teitsma, Yang et al. 2018). Furthermore, Sasaki et al. identified differentially abundant metabolites between active RA and inactive RA, with 15 in plasma and 20 and in urine (Sasaki, Hiraishi et al. 2019).

This metabolic profiling is possible due to the metabolic changes that have been observed in the different cell types involved in RA and their metabolic pathways. This includes metabolic changes in lipid, amino acid, and glucose levels that are involved in glycolysis; the arachidonic acid metabolic pathway; the tricarboxylic acid cycle; amino acid metabolism; and the pentose phosphate pathway (Xu, Chang et al. 2022). Such metabolic pathways and metabolite alterations can drive inflammatory mediator secretion, mediate leukocyte infiltration, induce joint destruction and muscle atrophy and promote or regulate cell proliferation, all of which may reflect the etiologies of RA (Xu, Chang et al. 2022).

Recent data have implicated metabolic mis-regulation as a fundamental pathogenic pathway in all phases of RA due to metabolic signals acting as decisive determinants in T-cell fate and behavior (Qiu, Wu et al. 2021). For example, research has shown that RA T-cells fail to repair mitochondrial DNA, resulting in malfunctioning metabolic machinery, and that this is in turn aggravated by the mis-trafficking of the energy sensor AMPK away from the lysosomal surface (Wen, Jin et al. 2019, Weyand, Wu et al. 2020, Qiu, Wu et al. 2021). An important metabolite is lactate, since lactate concentrations are high and glucose concentrations are distinctly low in the inflamed joint in RA, and T cells lose their mobility and are trapped in the tissue niche when they sense tissue lactate (Ciurtin, Cojocaru et al. 2006). Also increasing these lactate levels are tissue-residing macrophages, T cells, B cells, and stromal cells which are chronically activated in RA and under high metabolic stress; this creates a microenvironment poor in oxygen and glucose, but rich in metabolic intermediates, such as lactate (Qiu, Wu et al. 2021).

On account of these and many other findings linking autoimmunity, tissue inflammation in RA, and misbalanced metabolic pathways, it has been proposed that "defining and targeting metabolic abnormalities provides a new paradigm to treat or even prevent the cellular defects underlying autoimmune disease" (Qiu, Wu et al. 2021).

1.5.2 Metabolomics and Helminths. Helminth infection may affect the aforementioned immune metabolic pathways. Researchers such as Michla et al. (2022) have hypothesized that nutrient competition between host and helminths may have prevented chronic inflammation in the past, and they also argue that a detailed understanding of the metabolic restraints imposed by helminth infections may offer new therapeutic avenues in the future (Michla and Wilhelm 2022).

For example, helminths favor glucose over amino acids (AA) as their primary nutrition source (Bueding 1950, Hansen, Hansen et al. 2016, Michla and Wilhelm 2022). Another example of helminths affecting cell metabolism may be seen in their effect on type 2 innate lymphoid cells (ILC2). ILC2 function is controlled by amino acid (AA) metabolism and glycolysis is regulated by high expression of arginase-1 (Arg1) cleaving L-arginine into urea and ornithine.

Further, *Trichuris muris* infection induces an increase in the amount of amino acids (AA) found in the feces of mice (Houlden, Hayes et al. 2015), this potentially indicates a reduced absorption and depletion of AA as a general mechanism of host metabolic manipulation by helminths (Michla and Wilhelm 2022) to limit the activation and expansion of ILC2 (in response to helminth infections) and prevent expulsion. Furthermore, in the chronic stage of liver infections with *Opisthorchis felineus*, a metabolomic analysis of the serum showed a shift towards lipid metabolism followed by a depletion of AA (Kokova and Mayboroda 2019).

In short, research shows that metabolic changes associated with therapeutic responses can improve our understanding of drug induced mechanisms (Xu, Chang et al. 2022), that metabolomic studies can be used for the discovery of biomarkers for clinical risk factors, subgroups, and predictors of treatment response (Xu, Chang et al. 2022); and that metabolic homeostasis and regulation present new therapeutic strategies for RA (Qiu, Wu et al. 2021). Helminth infection may shift these immune metabolic pathways, but the clinical consequences of helminth infections on the metabolome, as well as on inflammation in relation to AIA have not yet been explored.

2. Rationale

Canada has one of the highest incidences of rheumatic diseases in the world (Widdifield, Paterson et al. 2014) which includes gout, rheumatoid arthritis and psoriasis, among other conditions. Rheumatoid arthritis (RA) is estimated to affect one out of every 100 adult Canadians (Widdifield, Paterson et al. 2014). RA is an autoimmune inflammatory disorder characterized by joint inflammation, fatigue, and joint pain. RA does not only affect joints; there are a several extra-articular manifestations of the condition, including vasculitis, subcutaneous nodule formation, inflammatory eye disease, cardiovascular disease and lung disease (Shaw, Collins et al. 2015). One of the prominent joint inflammation drivers in RA is the overabundance and persistence of neutrophils (Rosas, Correa et al. 2017, Cecchi, Arias de la Rosa et al. 2018, O'Neil and Kaplan 2019). While the prevalence of RA is increasing, there is currently no available cure, and current therapies such as steroids, broad-spectrum immunosuppressive drugs and anti-TNF have limited efficacy and can result in severe side effects in certain patient cohorts (Tarnowski, Paradowska-Gorycka et al. 2016). There is a need, therefore, for safe and diverse treatments to be developed.

H. polygyrus bakeri (Hpb) has demonstrated to be one of the most potent immunomodulatory helminths in mice (Maizels, Hewitson et al. 2012). Infection with helminth parasites or treatment with helminth extracts (Helminth Excreted-Secreted products, HES) have been shown to limit the severity of autoinflammatory disease models (Cooper 2009, McSorley and Maizels 2012, Wiria, Djuardi et al. 2012, Rajamanickam, Munisankar et al. 2020). There are, however, relatively few pre-clinical studies linking helminth infection in mice to inflammatory responses in the joints. We have therefore chosen to investigate the influence of infection with Hpb on the outcome of murine Antigen-induced-arthritis (AIA).

AIA has been widely used as a model of human RA in view of similar histopathological features and chronicity (Brackertz, Mitchell et al. 1977, Coelho, Pinho et al. 2008, Lopes, Coelho et al. 2011, Krock, Jurczak et al. 2018), previous studies have shown that chronic infection with Hpb results in immunomodulatory dampening of inflammatory immune response in mice (Elliott, Setiawan et al. 2004, Saunders, Raine et al. 2007, Liu, Sundar et al. 2009, Hang, Setiawan et al. 2010, Wilson, Taylor et al. 2010, Morimoto, Azuma et al. 2017, Sarter, Kulagin et al. 2017, Filbey, Mehta et al. 2020, White, Johnston et al. 2020). We hypothesize, therefore, that infection with Hpb will limit inflammation in AIA; with a focus on the potential effects of Hpb-infection on AIA acute phase modulators.

3. Study Objectives

Hypothesis: We hypothesize that *Heligmosomoides polygyrus bakeri* infection will limit immunopathology in AIA, dampening inflammation in the knee joint by decreasing/preventing neutrophil infiltration to the joint and inhibiting the expression of inflammatory cytokines. We also aim to determine the effects of Hpb infection on the host metabolome as it pertains to AIA.

Objective 1: Characterize the effects of Hpb infection on the outcome of AIA *in vivo*. We postulate that Hpb infection will lead to a decrease in inflammation by modulating inflammatory mediators in the knee joint of AIA-mice.

- For this, we first validated that AIA was reproducible in our group, and further characterized its inflammatory kinetics.
- We further assessed whether cell infiltration and inflammatory mediators (cytokines, chemokines, MPO) in the knee are affected by Hpb infection.
- Finally, we validated that our findings were due to Hpb having a direct effect on inflammatory mediators, by assessing T-cell derived cytokines from the spleen, worm burden, whether Hpb infection affects mBSA immunization or neutrophil viability, and total blood leukocytes after Hpb infection before mBSA challenge.

Objective 2: Characterize the mechanisms by which Hpb modulates AIA. We further wanted to determine the effect of Hpb infection on the AIA host metabolome.

- For this, untargeted metabolomics were performed on serum samples by LC-MS/MS to assess metabolic alternations of mice in different groups.
- Further statistical and enrichment pathway analyses were performed comparing “Ctl vs AIA” and “AIA vs AIA-infected” groups to identify potential metabolic pathways affected as well as potential compounds of interest.

4. Methods

The following chapters will outline the process by which we tested our hypothesis, from AIA induction and Hpb infection to sample collection and processing, as well as metabolomic processing and the protocols used.

4.1 Mouse Colony and Hpb life cycle setup

4.1.1 Animals. To create the mouse colony, eight-to-10-week-old C57Bl/6 wild type (WT) mice were obtained from Charles River Laboratories (Saint-Constant, Quebec, Canada) and maintained in the Small Animal Research Unit (SARU) at the Macdonald Campus. An in-house mice colony was bred and maintained with filtered water and food *ad libitum* and in a controlled environment (temperature and humidity). Animal care and handling procedures were undertaken in accordance with the guidelines of the Canadian Council on Animal Care and the Animal Ethics Committee of McGill University, and had prior approval from the local animal ethics committee (Protocol #2018-8066).

C57Bl/6 (WT) mice were chosen due to their known susceptibility to AIA (Brackertz, Mitchell et al. 1977, Nandakumar and Holmdahl 2006, Lopes, Graepel et al. 2016) as well as their precisely defined onset and mechanism of disease. They were also chosen due to their genetic background, which is completely genotyped, with many transgenic animals bred from this background; this will enable examination of different molecular pathways (Atkinson and Nansen 2017). Hpb is known to persist for varying lengths of time in different inbred mice strains, and C57BL/6 is a well-established fully susceptible model of chronic infection with Hpb (Filbey, Grainger et al. 2014, Johnston, Robertson et al. 2015).

4.1.2 Infection Protocol. *Heligmosomoides polygyrus*-infective larvae were provided by Dr. Irah King (McGill University) and life cycle was maintained in stock C57Bl/6 (WT) mice as previously described (Valanparambil, Segura et al. 2014). For life cycle maintenance, female C57Bl/6 (WT) mice were infected by oral gavage with 400 infective third-stage larvae (L3) (**Figure 6**). Male C57Bl/6 (WT) mice were used for all experimental procedures due to observations of high variability in cell numbers and cytokine concentrations when using female mice. For all experiments investigating the immune modulation of Hpb against AIA, male mice were infected by oral gavage with 200 infective third-stage larvae (L3) (Valanparambil, Segura et al. 2014) as this dose commonly shows non-overt pathology with a moderate worm burden in most mice. Processed modeled in **Figure 6**.

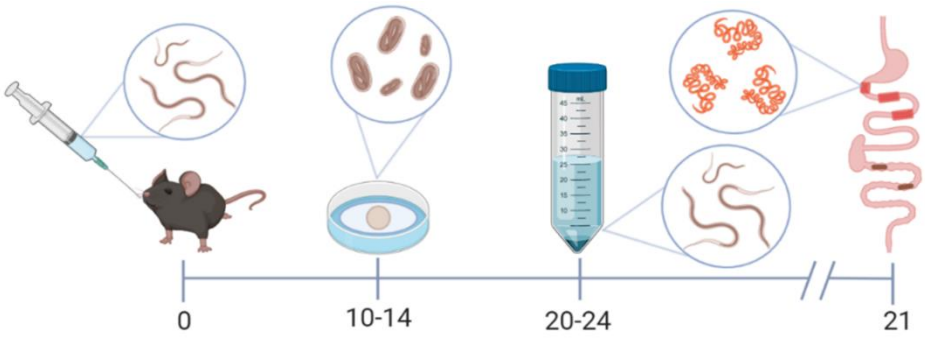

Figure 6) In-lab Hpb life cycle representation. Infection (Day 0), Egg collection (Day 10-14), L4 larvae collection from eggs (Day 20-24), and adult worm from mice small intestine (Day 21). Created with BioRender.com

4.2 Preliminary Tests and Optimization

To assess whether cell infiltration and inflammatory mediators in the knee are affected by Hpb infection, we first standardized our AIA model and sought to determine the kinetics of inflammation. Animals were immunized with mBSA and CFA, 14 days later, mice were challenged with antigen (mBSA) or PBS in the right knee joint. The peak of inflammation was determined by counting neutrophils and mononuclear cells in the knee cavity, as well as evaluating cytokines, chemokines, and myeloperoxidase (MPO) in the peri-articular tissue.

4.2.1 Antigen Induced Arthritis Induction. This first experiment was designed to verify the induction of inflammation during the AIA model in our group. The AIA model was used for a pilot study with 10 mice (n=10; five males, five females) because of its short-lived, self-resolving features, as previously described (Cunha, Verri et al. 2004, Coelho, Pinho et al. 2008, Cunha, Barsante et al. 2008, Lopes, Coelho et al. 2011, Lopes, Graepel et al. 2016, Gonçalves, Rezende et al. 2020). Animals were immunized intra-dermally at the base of the tail with 500 mg of methylated BSA (mBSA) in 100 mL of an emulsion of saline and an equal volume of complete Freund's adjuvant (CFA) (Coelho, Pinho et al. 2008, Lopes, Coelho et al. 2011). Fourteen days later, the mice were challenged with antigen (10 µg mBSA in 10 µL sterile saline) or PBS in the right knee joint and divided into two groups: (i) PBS control and (ii) mBSA challenge (AIA) (**Figure 7**). Mice were necropsied by Carbon dioxide (CO_2) euthanasia and their knee cavities were washed 24 h later with phosphate-buffered saline (PBS) and 3% BSA (2 X 5 mL), and peri-articular tissues were removed for evaluation of cytokines, chemokines and myeloperoxidase (MPO) evaluation.

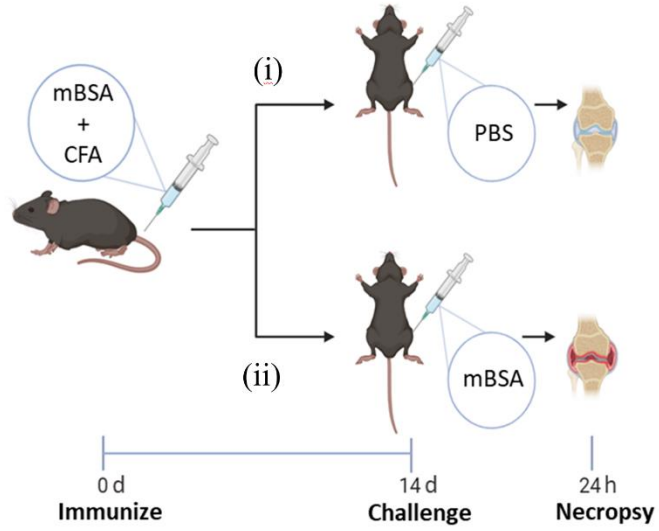

Figure 7) Representation of AIA induction. Immunization at day 0, challenge at 14 days, and necropsy 24 hours after challenge. Created with BioRender.com

4.2.2 Kinetic of Antigen Induced Arthritis. To determine the kinetic of inflammation in AIA, a time course experiment was done. Twenty male mice were immunized as described above and challenged with antigen, or PBS, after 14 days. Mice were necropsied at 12 h, 24 h and 48 h after challenge (**Figure 8**), then the knee cavities were washed and peri-articular tissues were harvested for evaluation of cytokines, chemokines and myeloperoxidase (MPO) evaluation. The samples from the 24hr group were separated and periarticular tissue was prepared for further ELISA's.

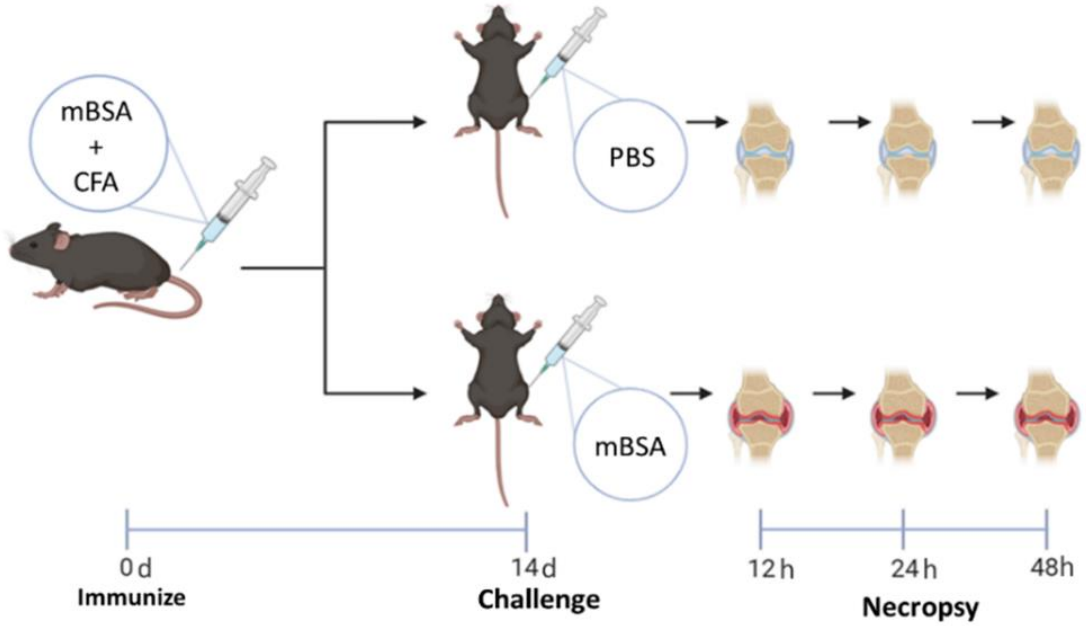

Figure 8) Representation of AIA time course. Immunization at day 0, challenge at 14 days, and necropsy 12, 24, and 48 hours after challenge. Created with BioRender.com

4.3 *In vivo* experiments

To evaluate the effects of Hpb infection on AIA, the same model was followed, with groups receiving 200 L3 larvae seven days after immunization. Mice were then challenged with antigen as described above, and 24 hours later the knee cavity was washed, and peri-articular tissues were removed for evaluation. Samples of spleen were taken to determine T cell-derived cytokines, as were small intestines for worm burden and blood samples for metabolomic processing.

4.3.1 Hpb Modulation of Antigen Induced Arthritis Model. To evaluate the effects of Hpb infection on AIA, 20 male mice were immunized as described above and divided into four groups: (i) PBS (Control), (ii) mBSA (AIA), (iii) Hpb infection + PBS (Hpb control) and (iv) Hpb infection + mBSA (Hpb + AIA). To assess the effect of Hpb on AIA inflammation, groups iii and iv received 200 L3 larvae seven days after immunization. Mice were then challenged with antigen as described above, 14 days after immunization (**Figure 9**).

This challenge time point also corresponds to the seventh day of infection with Hpb (when L4 larvae have develop). Peak inflammation of AIA is 12 to 24 hours after challenge, with resolution at 48 hours, as described in Lopes 2011. For this reason, samples were harvested 24 hours after challenge. A point of note is that the life cycle of Hpb is at the eighth day after infection, when adult worms begin to emerge into the lumen. This life stage is associated with Hpb immunomodulatory capabilities (Walk, Blum et al. 2010).

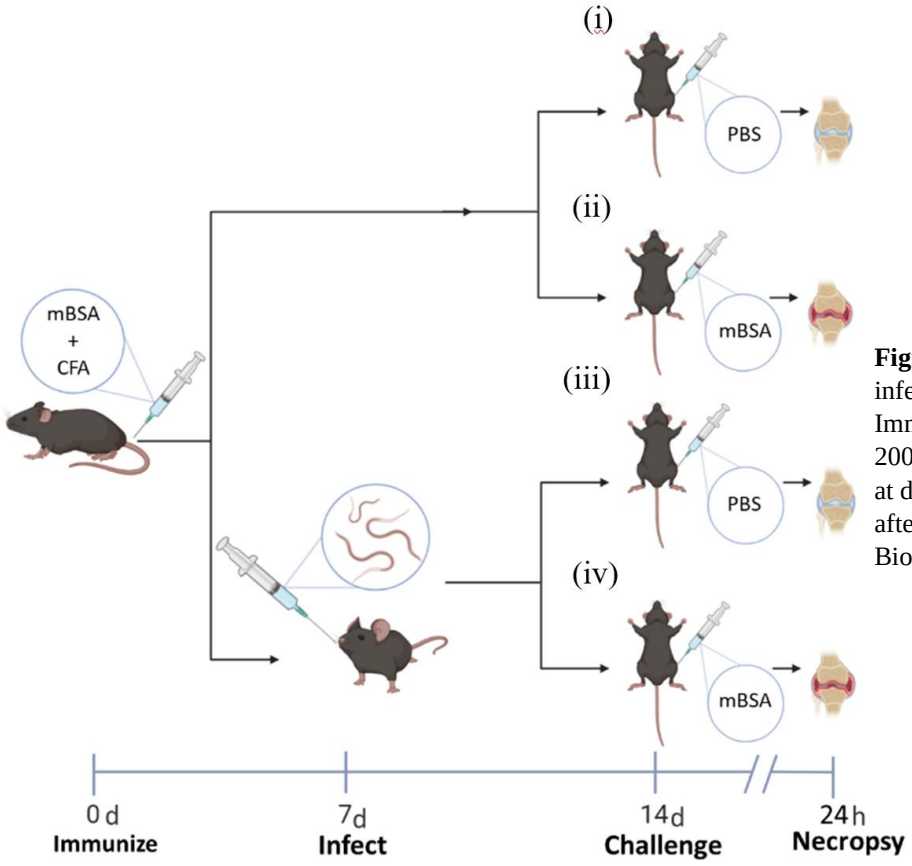

Figure 9) Representation of infection and AIA model. Immunization at day 0, infect with 200 L3 larvae at day 7, challenge at day 14, and necropsy 24 hours after challenge. Created with BioRender.com

Splenocytes were isolated at 5×10^6 cells in 1 ml of RPMI medium and were activated with the T-cell mitogen concanavalin A (ConA; 2 μg/ml) for 48 hours. Culture media was then collected for cytokine determination (Johnston, Wang et al. 2010). The concentrations of IL-4 and IL-10 were determined using commercially available ELISA assays, following the instructions supplied by the manufacturer (R & D systems, Minneapolis, MN, USA).

Blood smears were obtained on the day of the challenge to determine the percentage of leukocytes in the peripheral blood. To assess total cell migration, the knee cavity was washed, and peri-articular tissues were harvested. Small intestines were collected for adult worm burden determination and blood samples were collected for metabolomic analysis. Spleens were also collected and processed for evaluation of cytokines and chemokines.

To assess infection levels, worm burden was determined from small intestines, as previously described (Valanparambil, Segura et al. 2014). Tail blood was collected by vertical a puncture of the tail with a needle to prepare blood smears (Bjorner and Zhu 2019). To assess percentage of leukocyte, blood smears were then stained with May-Grünwald-Giemsa, as previously described (Lopes, Graepel et al. 2016).

Determination of intra-articular inflammation. The total number of leucocytes was determined by hemocytometer counting after staining with Turk's solution. Differential counts were obtained from cytospin (Thermo Shandon Cytospin 3 Centrifuge) preparations by evaluating the percentage of each leucocyte on a slide stained with May-Grünwald-Giemsa, as previously described above (Lopes, Graepel et al. 2016). The proportion of cells with distinctive apoptotic morphology was also assessed.

Quantification of neutrophil accumulation in the tissue. Neutrophil activity and accumulation in the tissue was measured by assaying MPO activity (Barcelos, Talvani et al.

2004, Lopes, Coelho et al. 2011). This test is specific for neutrophils over macrophages and lymphocytes. Periarticular tissue was collected and frozen at -80 °C. Upon thawing, the tissue (0.1 g of tissue per 1.9 mL of buffer) was homogenized and processed to determine MPO levels. The assay employs 25 μL of 3,3′-5,5′- tetramethylbenzidine (TMB, Sigma, St Louis, MO, USA) in PBS (pH 5.4) as the colour reagent, read in spectrophotometer at OD 450 nm. Results are expressed by optical density.

Cytokine concentrations. The concentrations of TNF, CXCL-1, IFN-γ and IL-10 were measured in periarticular tissues using commercially available ELISA assays, following the instructions supplied by the manufacturer (R & D systems, Minneapolis, MN, USA). Periarticular tissue was processed in the proportion of 100 mg of tissue to 1 mL of PBS (0.4 M NaCl and 10 mM de NaPO4) containing (0.1 mM phenylmethylsulphonyl fluoride, 0.1 mM benzethonium chloride, 10 mM EDTA, 20 KI mL-1 aprotinin A) and 0.05% Tween 20. The samples were then centrifuged for 10 min at 3000X g and the supernatant was used for ELISA assay. Samples were assayed in duplicate.

Antigen Induced Arthritis Immunization and Hpb. To determine whether Hpb infection affects mBSA immunization in AIA, the same experimental model was repeated on a separate cohort of mice following the same steps and timepoints for immunization: Hpb infection seven days after, and challenge 14 days after immunization [n=6]. Blood was collected 24 hours after challenge in a BD Vacutainer blood collection tube (3.6mg EDTA, Ref# 367841).

To assess mBSA immunization, blood was incubated at room temperature for between 30 minutes and one hour, and then centrifuged at 2,000 rpm for 10 minutes. Serum was then collected and stored at -80 °C until further analysis. Titers of anti-mBSA IgG were measured following ELISA protocol. Flat-bottomed 96-well plates were coated with 100μl of dilute mBSA

(8 mg mBSA/ml in 0.1 M sodium carbonate buffer [pH 9.6] and incubated overnight at 4°C. Plates were washed and serum from both control and infected mice was added (serum samples were diluted at 1:10 with PBS-1% BSA reagent dilutant) and incubated overnight at 4°C. The plates were washed and incubated with anti-mouse IgG conjugated to horseradish peroxidase (1:5,000) for two hours. Following this, the incubation plates were washed again and incubated with 100µl of tetramethylbenzidine for 15 minutes. Finally, 50µl of Stop Solution was added and the plates were read at OD 405nm.

ELISA Statistical analysis. Data were analyzed using GraphPad Prism (version nine; GraphPad, San Diego, CA, USA). Results are shown both as individual data points and as the mean ± SEM. Student's t-test was used for two group comparisons. The difference among groups was evaluated by using a one-way analysis of variance, followed by Tukey's paired post-hoc statistical tests. The level of significance was set at $P < 0.05$ (*).

Reagents/Drugs. Methylated bovine serum albumin (mBSA) and Freund's complete adjuvant (CFA) were purchased from Sigma Chemical Co. (St Louis, MO, USA). All compounds were dissolved in saline.

4.4 Metabolomics Methods

To determine the effects of Hpb infection on the host metabolome and its effect on AIA, untargeted metabolomics were performed on serum samples by LC-MS/MS. Further, statistical and enrichment of pathway analysis were performed in MetaboAnalyst to assess metabolic alternations of mice in different groups.

4.4.1 Model. To investigate the potential mechanisms of Hpb infection in AIA, serum samples for metabolomic analyses were taken from the same mice cohort and grouped into: (i)

Naive (PBS control), (ii) mBSA challenge (AIA), (iii) Naïve plus Hpb infection (Hpb control) and (iv) mBSA challenge plus Hpb infection (AIA + Hpb). Blood from six mice was also collected as non-immunized controls and divided into two groups: (v) Naïve non-immunized (naïve control), and (vi) Infected non-immunized (Hpb control). HPLC grade methanol was added to the serum at a 1:1 ratio and centrifuged at 10,000 rpm (for 10 min at 4 °C). Supernatant was then collected and sent for metabolomic analysis.

4.4.2 Metabolite analysis. Untargeted metabolite analysis was performed as previously described in Michi et al. 2021. Hydrophilic Interaction Liquid Chromatography (HILC) and ultra-high-pressure liquid chromatography-mass spectrometry (UHPLC-MS) were performed on a Q Exactive™ HF Hybrid Quadrupole-Orbitrap™ Mass Spectrometer coupled to a Vanquish™ UHPLC System. Chromatographic separation was used to separate metabolites using a Syncronis HILIC UHPLC-MS column (2.1 mm × 100 mm × 1.7 μm). While liquid chromatography separates mixtures with multiple components, mass spectrometry provides the structural identity of the individual components with high molecular specificity and detection sensitivity. Metabolite analyses can then be completed using El Maven (v.0.12.0), a mass spectrometry data analysis software package (Clasquin, Melamud et al. 2012).

Metabolites were identified by matching observed m/z signals (±10 p.p.m.) and chromatographic retention times to those observed from the reference Mass Spectrometry Metabolite Library. Metabolomic analyses and statistical figures were generated using MetaboAnalyst 5.0. Metabolic pathways and compounds were identified by matching observed m/z signals (±10 p.p.m.) and chromatographic retention times with those observed from the reference Mass Spectrometry Metabolite Library (Table in Supplemental File).

5. Results

5.1 Preliminary Results and Optimization

5.1.1 Mice Colony and Hpb life cycle setup. Hpb life cycle was set up for optimizing L3 larvae and adult worm collection as described in the methods (Valanparambil, Segura et al. 2014). The life cycle of Hpb was confirmed with egg collection 14 days after infection (**Figure 10**A) and adult worms were counted 21 days after infection (**Figure 10**C). Five mice were infected with 200 L3 larvae (**Figure 10**B) and ~9000 L3 larvae were obtained from feces collected from those five mice. Two of these mice were maintained for further egg/L3 collection from feces and Hpb life cycle continuation. Three mice were necropsied, and adult worms collected from them for Helminth Excreted Secreted product production.

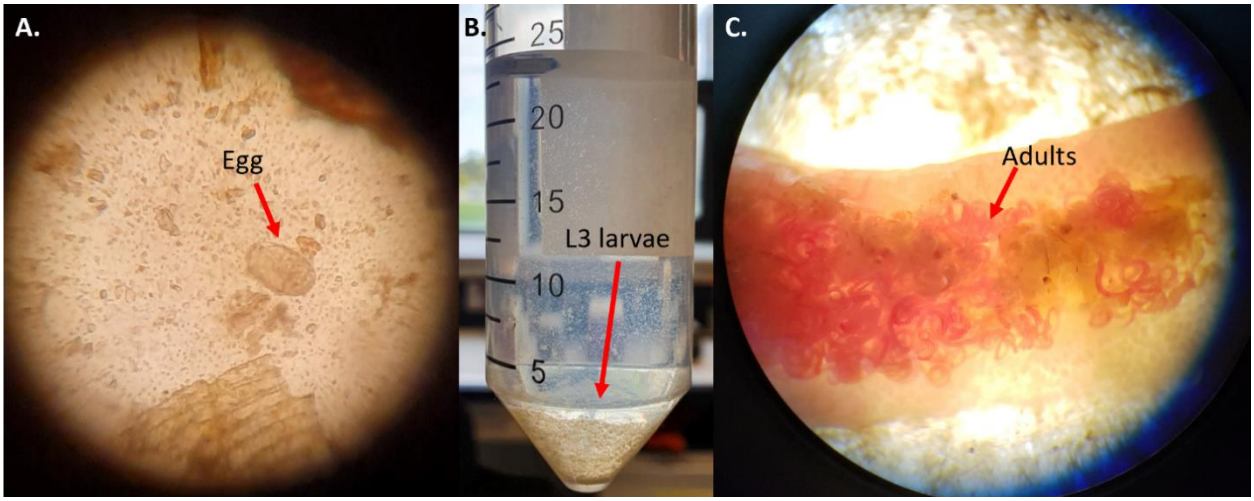

Figure 10) *H. polygyrus* life cycle confirmation. (A.)Egg from feces (Day 0), (B) L3 larvae (Day 20-24), and (C) adult worm from mice small intestine (Day 21).

5.1.2 Antigen Induced Arthritis Induction. This first experiment was designed to verify the induction of inflammation during the AIA model in our group. The study was completed with a sample of 10 mice (n=10; five males, five females). We observe virtually no cells after PBS injection, and a significant leukocyte recruitment at 24 h after mBSA challenge (**Figure 11**A).

There was a significant neutrophilic inflammation at 24 h after mBSA challenge (**Figure 11**B), and a smaller but significant number of mononuclear cells present in knee cavities 24 h after mBSA challenge (**Figure 11**C). There was, however, a high level of variability.

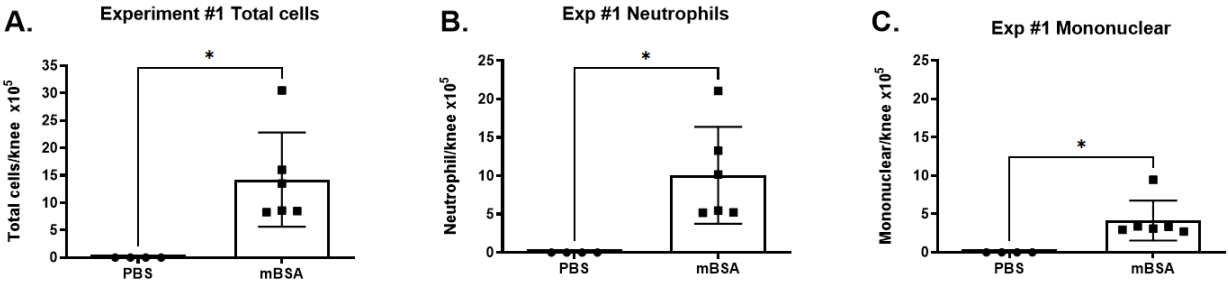

Figure 11) Characteristics of knee inflammation of mice with AIA. (A) Number of total leukocytes, (B) neutrophils and (C) mononuclear cells in the synovial cavity 24 h after injection with 10 μg of mBSA or 10 μL sterile PBS (control) into the knee joints of immunized mice [n=4-6]. Each symbol represents an individual animal, with results expressed as mean ± SEM; *$p < 0.05$.

Due to the observed differences, we separated the groups into male and females to assess whether the variability derived from sex differences. When the data was plotted as a group, no statistically significant difference was observed in neutrophil numbers between PBS and mBSA challenge in the male group (**Figure 12**A). When the plots were separated, however, we observed significant neutrophil inflammation at 24 h after mBSA challenge in both female (**Figure 12**B) and male (**Figure 12**C) groups, with a higher number of neutrophils in the female group (peak of 5.49 X 10^5 for males and 21.05 X 10^5 for females). The estimation plots gave further insight into the variability for each group with female mice having a greater difference between means of 14.83 (± 2.707; Figure 2B), compared to the male's less variable difference between means of 5.310 (± 0.07592; Figure 2C). These observations are in accordance with other published reports of increased BM and splenic neutrophils in female mice (Hensel, Khattar et al. 2019); as well as sex-related differences in the course and destructive effects of AIA (van Beuningen, van den Berg et al. 1989). There is also a possibility that neutrophil numbers were affected by the age difference of the female mice, which previously been reported to affect the

immune response and neutrophil numbers in female C57Bl/6 mice (van Beuningen, van den Berg et al. 1989).

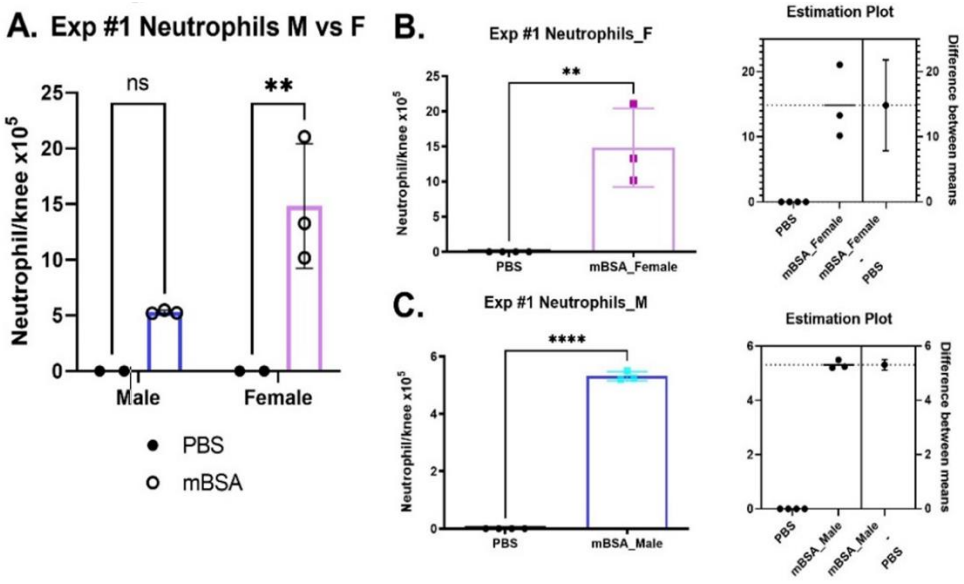

Figure 12) Knee inflammation of mice with AIA in male vs females. (A) Number of neutrophils in the synovial cavity 24 h after injection with 10 µg of mBSA or 10 µL sterile PBS (control) into the knee joints of immunized mice grouped by sex. Number of neutrophils (B) female and (C) male number of neutrophils with corresponding estimation plots [n=3]. Each symbol represents an individual animal, with results as mean ± SEM; *p < 0.05.

Further experiments analyzing cytokine profiles, increasing the n value of each group, would be needed to fully understand the mechanisms of sex differences in AIA, which is not within the scope of this project. For these reasons, and the observations of high variability in cell numbers and cytokine concentrations when using female mice, only male C57Bl/6 mice will be used for future experimental procedures, even that we will validate the findings in females.

5.2 Standardization and *In-vivo* results

5.2.1 Antigen-Induced Arthritis: peak and resolution. Next, we assessed the kinetics of the inflammation in our model. It has been previously reported that after injection of antigen (mBSA) into the knee joints of immunized mice, recruitment of neutrophils peaks 12 to 24 hours after challenge, and is reduced to basal levels (> 80% decrease in neutrophil influx) at 48 h after antigen challenge (Lopes, Coelho et al. 2011). For this experiment, 20 male mice were immunized and challenged, as previously described. After various points in time after challenge with antigen or PBS, the mice were necropsied. To characterize AIA model kinetics, knee lavages and periarticular tissue were obtained at 12, 24 and 48 hours after challenge.

Virtually no cells were observed after PBS injection, compared to 12, 24 and 48 hours after mBSA challenge (**Figure 13**A, B). Neutrophil infiltration into the synovial cavity peaked at 12 to 24 hours after challenge and resolved by 48 hours (> 77% decrease in neutrophil influx) after antigen challenge (**Figure 13**A). Mononuclear cells were first detected at 12 hours, peaking at 24 and 48 hours (**Figure 13**B). **Figure 13**C represents both neutrophil and mononuclear cell numbers superimposed. Increased MPO levels were observed in periarticular tissue at 12 and 24, and persisted 48hours after challenge ($p < .01$) (**Figure 13**D). TNF in periarticular tissue followed a similar trend as neutrophils in synovial cavity, with a peak at 12 to 24hours and a resolution at 48 hours (**Figure 13**E). These observations follow previous reports of peak inflammation at 12h and resolution at 48h as seen in Lopes et al. (2011, 2020). The neutrophil resolution index was approximately 16 hours after mBSA challenge (**Figure 13**F).

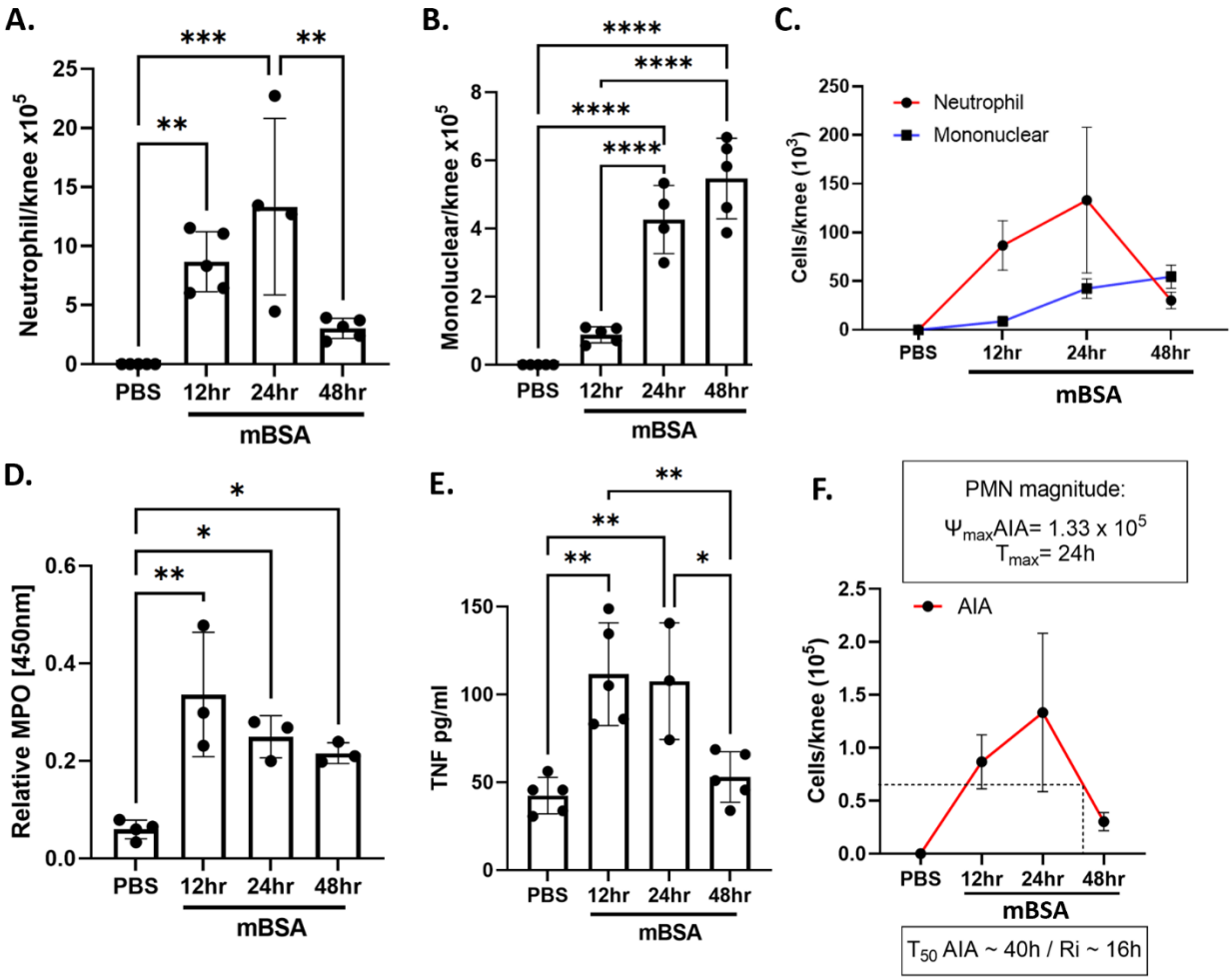

Figure 13) Kinetics of knee inflammation of mice with AIA. (A) Number of total neutrophils and (B) mononuclear cells in the synovial cavity 12, 24, and 48 hours after injection with 10 µg of mBSA or 10 µL sterile PBS (control) into the knee joints of immunized mice [n=5]. (C) Myeloperoxidase and (D) TNF levels following mBSA challenge in periarticular tissue. Each symbol represents an individual animal, with results expressed as mean ± SEM; *p < 0.05. (E) neutrophil and mononuclear cells combined kinetics; each symbol represents a group. (F) Neutrophil resolution index.

5.2.2 Antigen Induced Arthritis 24 hours after challenge. We further observed the 24hr time point, at which point both the peak neutrophil infiltration and cytokine levels were observed. **Figure 14**A shows a schematic of the AIA model followed. At 24 hours post mBSA challenge, as expected we observe virtually no neutrophils or monocytes after PBS injection, as well as significant infiltration of both into the synovial cavity (**Figure 14**B, C). One sample from the AIA group was excluded due to insufficient amount of sample for counting. Increased levels of MPO (indirect measurement of neutrophil tissue infiltration) were observed in the periarticular

tissue after mBSA challenge (**Figure 14**D), as well as a respective increase in TNF, neutrophil chemokine CXCL-1, and IFN-γ (**Figure 14** E, F, and G respectively). IL-10 levels were found to be not statistically different from the control (**Figure 14**H).

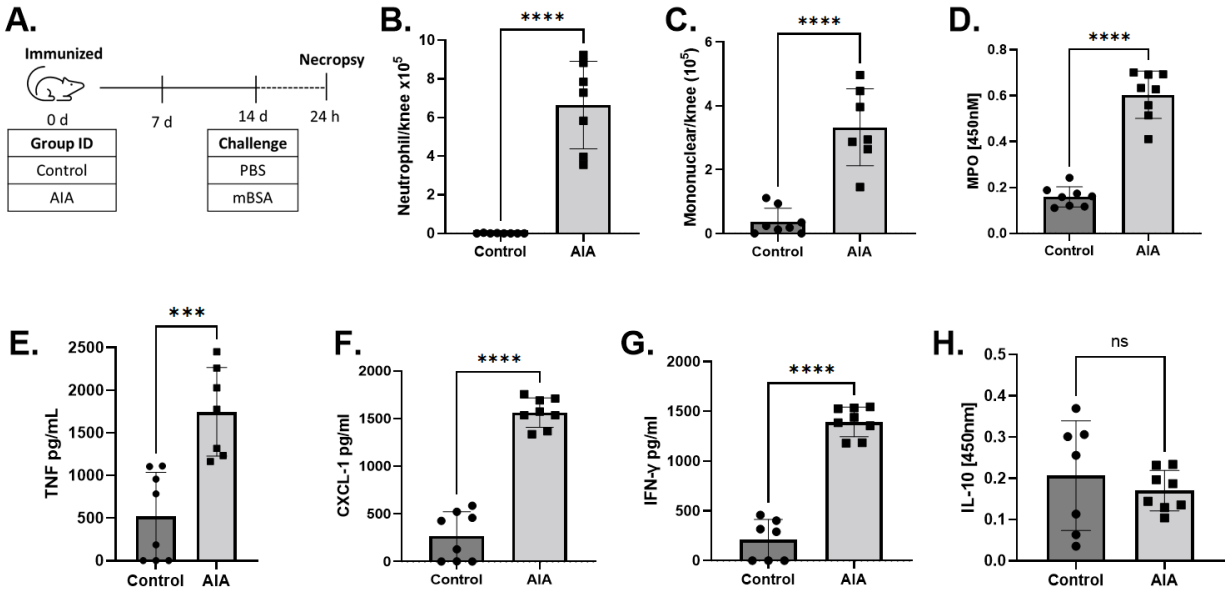

Figure 14) Characterization of AIA model at 24hrs. Knee inflammation of mice with AIA 24hours after challenge. (A)Schematic of AIA model. (B) Number of neutrophils and (C) mononuclear cells in the synovial cavity 24 hours after injection with 10 μg of mBSA or 10 μL sterile PBS (control) into the knee joints of immunized mice. (D) Myeloperoxidase [MPO, as measured by MPO assay], (E) TNF, (F) CXLCL-1, (G) IFN-γ, and (H) IL-10 in periarticular tissue, as measured by ELISA 24 h after challenge with mBSA. Each symbol represents an individual animal, with results expressed as mean ± SEM; *p < 0.05.

5.2.3 Characterization of Hpb infection on AIA 24 hours after challenge. To evaluate the effects of Hpb infection on AIA, the mice were separated into four groups: PBS (Control), mBSA-challenged (AIA), PBS + Hpb infection (Hpb control), and mBSA + Hpb infection (AIA + Hpb). A schematic representation of the model is shown in **Figure 15**A. Twenty-four hours after challenge, virtually no cells were observed after the PBS injection in both the control and Hpb-control groups (**Figure 15**B, C). An increased number of neutrophils in the synovial cavity of both AIA challenged and AIA + Hpb groups was observed, with no significant differences between AIA and Hpb infected AIA (**Figure 15**B). An increase in monocyte numbers was also

observed in both the AIA challenged and AIA+Hpb groups, with a statistically different [$p<0.0001$] increase of 35% in mononuclear cells for the AIA+Hpb group (average $9.27x10^5$ neutrophils/knee) when compared to AIA (average $3.33x10^5$ neutrophils/ knee), indicating a greater recruitment of mononuclear cells into the synovial cavity with Hpb infection (**Figure 15**C).

Analysis of the periarticular tissue revealed differences in MPO, as well as different cytokine levels. As previously mentioned, MPO is used here as an indirect measurement of neutrophil tissue infiltration. As expected from an mBSA challenge, we observed an increase of MPO after challenge in AIA compared to controls ($p<0.0001$), while both the control and Hpb-control groups contained undetectable levels. Interestingly, we observed a significant decrease of MPO in the AIA+Hpb group ($p<0.0001$) with a 65.77% decrease when compared to AIA (**Figure 15**D). This is consistent with our previous observations indicating an increase of mononuclear cells (**Figure 15**C) and may also indicate a faster clearance of neutrophils in AIA when infected.

We next assessed cytokine levels in the periarticular tissue. As expected from the mBSA challenge, we observed an increase in TNF ($p=0.0002$), CXCL-1 ($p<0.0001$), and IFN-γ ($p<0.0001$) after challenge in the AIA group compared to the controls, while both of the PBS challenged control groups (control and Hpb-control) contained low TNF levels, with no significant differences between the two (**Figure 15**E, F, and G respectively). Correlating to the decrease in MPO (infiltrating neutrophils to the periarticular tissue), as well as the increase of mononuclear cells in the knee cavity, a significant decrease in TNF ($p=0.0231$), CXCL-1 ($p= 0.0011$), and IFN-γ ($p= 0.0001$) was observed in Hpb infected-AIA mice when compared to the AIA group (**Figure 15**E, F, and G). This indicates a decrease in inflammatory cytokines and

chemokines in the periarticular tissue in infected challenged animals. There was no observable difference in IL-10 levels between non-infected groups, with a statistically significant increase in IL-10 in the Hpb control group, as expected. Interestingly, the AIA-Hpb group did not show an increase in IL-10 in the periarticular tissue (**Figure 15**G).

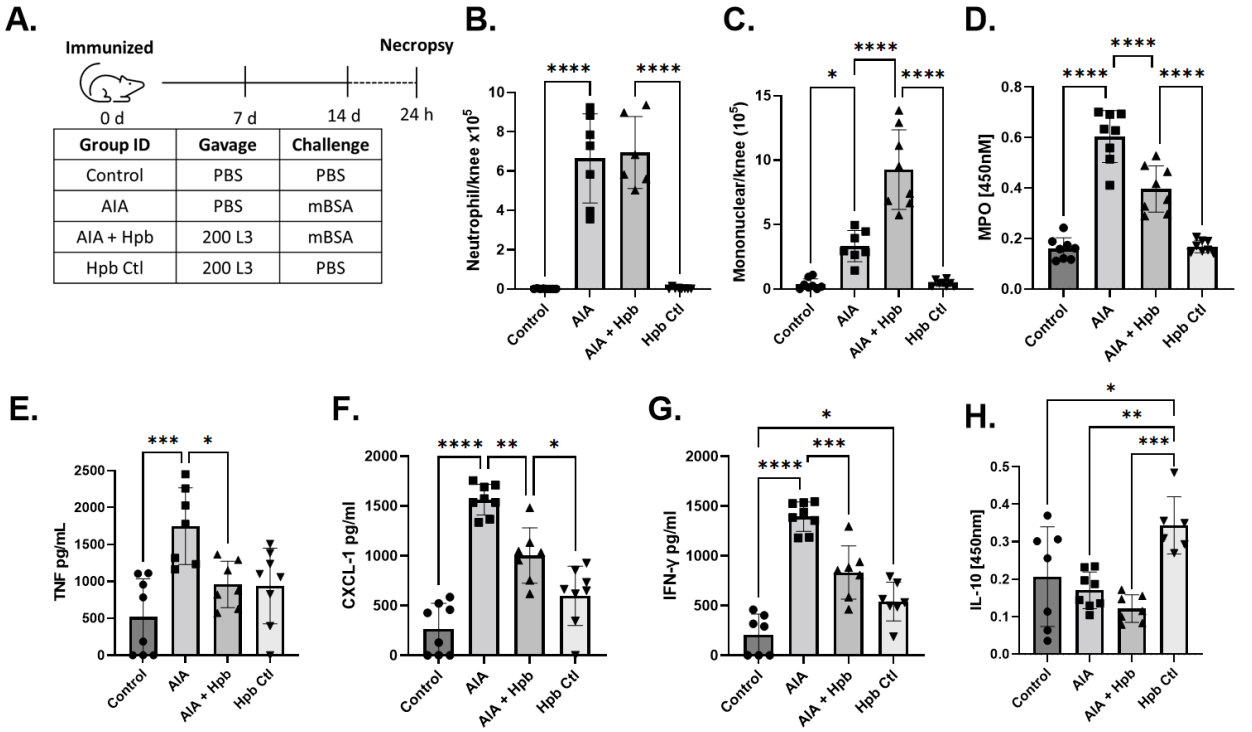

Figure 15) Hpb Infection in AIA. Knee inflammation of mice with AIA following Hpb infection. (A) Schematic of AIA model with infection. Infected groups received 200 L3 larvae 7 days after immunization. (B) Number of neutrophils and (C) mononuclear cells in the synovial cavity 24 hours after injection with 10 μg of mBSA or 10 μL sterile PBS (control) into the knee joints of immunized mice. (D) Myeloperoxidase [MPO, as measured by MPO assay], (E) TNF, (F) CXLCL-1, and (G) IL-10 in periarticular tissue, as measured by ELISA 24 h after challenge with mBSA. Each symbol represents an individual animal, with results expressed as mean ± SEM; *p < 0.05.

T cell-derived cytokines in the spleen were also assessed. Hpb is known to increase both IL-4 and IL-10 in the mucosa (Setiawan, Metwali et al. 2007). We observed that while non-infected groups did not differ in IL-4 levels between control and AIA, there was a decrease of IL-4 in the AIA-Hpb infected mice when compared to the control Hpb-infected group (**Figure 16**A). IL-10 was increased for both Hpb-infected groups (**Figure 16**B), and no difference in IL-10 was observed between Hpb infected-AIA mice and Hpb control mice (**Figure 16**B). Notably we observed that while IL-10 was increased in the spleen, it was unaffected in the periarticular

tissue of infected mice (**Figure 15**H). Hpb is known to increase IL-10 in the intestinal mucosa and spleen (Valanparambil, Segura et al. 2014, Hang, Kumar et al. 2019). Future experiments will be needed to assess the mechanisms through which Hpb affects cytokine levels in the periarticular tissue.

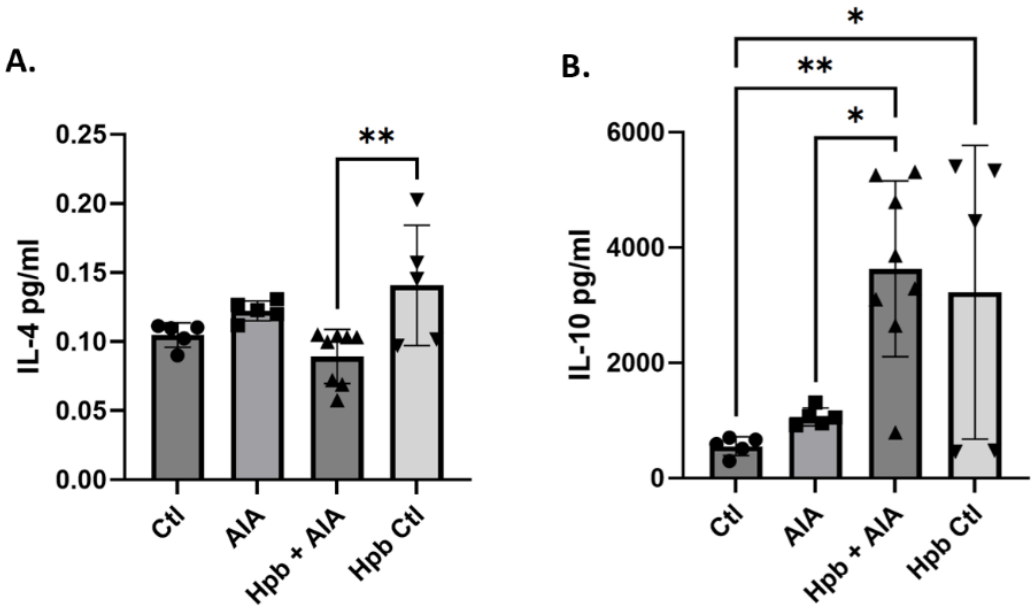

Figure 16) Spleen cytokine levels of AIA following Hpb infection. (A) IL-4 and (B) IL-10 in splenic tissue, as measured by ELISA 24 h after challenge with mBSA, 7 days after Hpb infection [n=5-8]. Each symbol represents an individual animal, with results expressed as mean ± SEM; *p < 0.05.

To assess whether neutrophil viability was affected by Hpb infection, the proportion of cells with distinctive apoptotic morphology in the knee cavity was counted from cytospin preparations stained with May-Grünwald-Giemsa. There was no observable difference in the number of viable or apoptotic cells between AIA and Hpb+AIA groups (**Figure 17**).

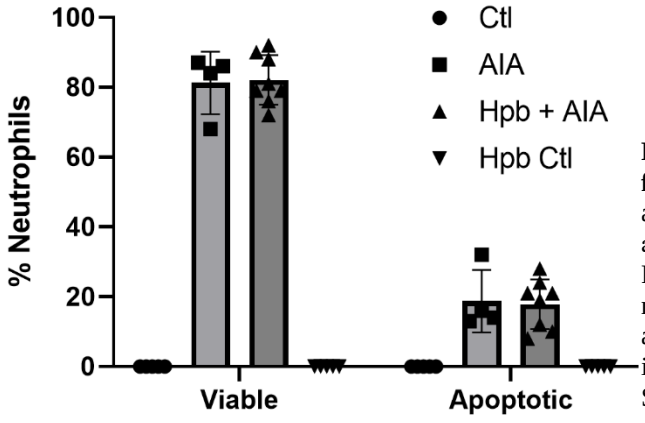

Figure 17) Knee neutrophil viability in AIA following Hpb infection. Percent of viable vs apoptotic neutrophils in the synovial cavity 24 hours after injection with 10 µg of mBSA or 10 µL sterile PBS (control) into the knee joints of immunized mice. Infected groups received 200 L3 larvae 7 days after immunization. Each symbol represents an individual animal, with results expressed as mean ± SEM; *p < 0.05.

Different Hpb life cycle stages secrete different products that could affect immunomodulatory effects (Maizels, Hewitson et al. 2012). To assess infection levels, worm burden was determined from infected mice small intestine, as previously described (Valanparambil, Segura et al. 2014). As seen in **Figure 18** the worm burden stayed relatively uniform between groups, indicating that the previously observed changes are not due to differences in worm burden or life cycle stage.

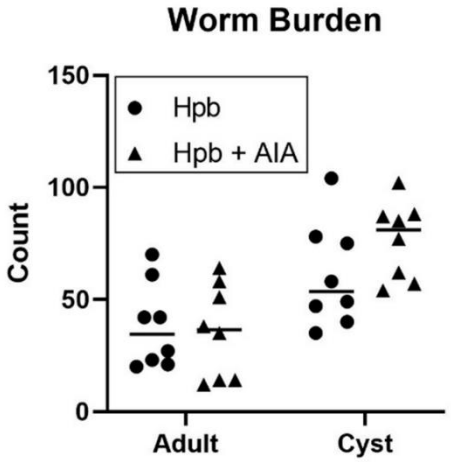

Figure 18) AIA worm burden. Differences in *H. polygyrus bakeri* adult and L4 (cyst) burden in small intestines 8 days after infection; 24hrs after mBSA knee challenge. Left demonstrates differences in adult worm burden and right demonstrates L4 burden. (•) represents control infected mice, (▲) represents infected mice challenged with mBSA. Data are presented as mean ± SEM.

If immunization were affected, this would affect the model, since immunization titers and antigen retention are correlated to pathology of AIA (Brackertz, Mitchell et al. 1977, Bas, Su et al. 2016). To assess whether the results we observed were specifically due to the effect of Hpb on AIA inflammation, rather than the infection inhibiting mBSA immunization, we performed the same experimental model on a separate cohort of mice, following the same steps and timepoints for immunization: Hpb infection seven days, and challenge 14 days after immunization [n=9]. To assess mBSA immunization, serum was collected 24 hours after mBSA challenge, and titers of anti-mBSA IgG were measured following ELISA protocol. As observed in **Figure 19**, both immunized groups had an increase in anti-mBSA IgG compared to the control, with no statistically significant difference between immunized and immunized+Hpb groups, confirming that Hpb infection did not interfere with mBSA immunization.

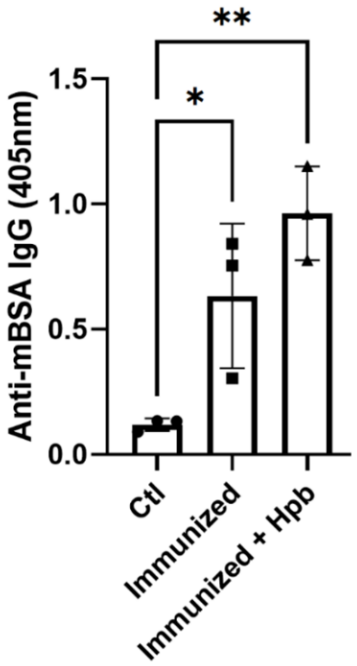

Figure 19) mBSA IgG. Differences in anti-mBSA IgG levels, 14 days after immunization (Hpb group infected 7th day after immunization). As measured by ELISA 24 h after challenge with mBSA. Each symbol represents an individual animal, with results expressed as mean ± SEM; *p < 0.05.

Blood smears were also obtained before mBSA challenge in order to assess whether Hpb infection affects the percentage of leukocytes in peripheral blood. This was done to determine whether the results we observed were specifically caused by the effects of Hpb on AIA inflammation, rather than to the effects of the infection on white-blood cell numbers in peripheral blood. Following the same model, the mice were all immunized and separated into Control and Hpb infected groups (infected with Hpb seven days after immunization). Tail blood was collected by vertical puncture of the tail before mBSA challenge on the 14th day after immunization. To assess the percentage of leukocytes, blood smears were stained with May-Grünwald-Giemsa. A summary of all leukocytes counted can be observed in **Figure 20**A. We observed that the percent of neutrophils (**Figure 20**B) did not differ between uninfected and Hpb-infected groups. Interestingly there was a slight increase in mononuclear (**Figure 20**C, p=0.045), eosinophil (**Figure 20**E, p=0.0006) and basophil numbers (**Figure 20**F, p=0.0001), as well as a decrease in lymphocyte numbers (**Figure 20**F, p=0.046) in the peripheral blood of Hpb-infected groups when compared to the uninfected control.

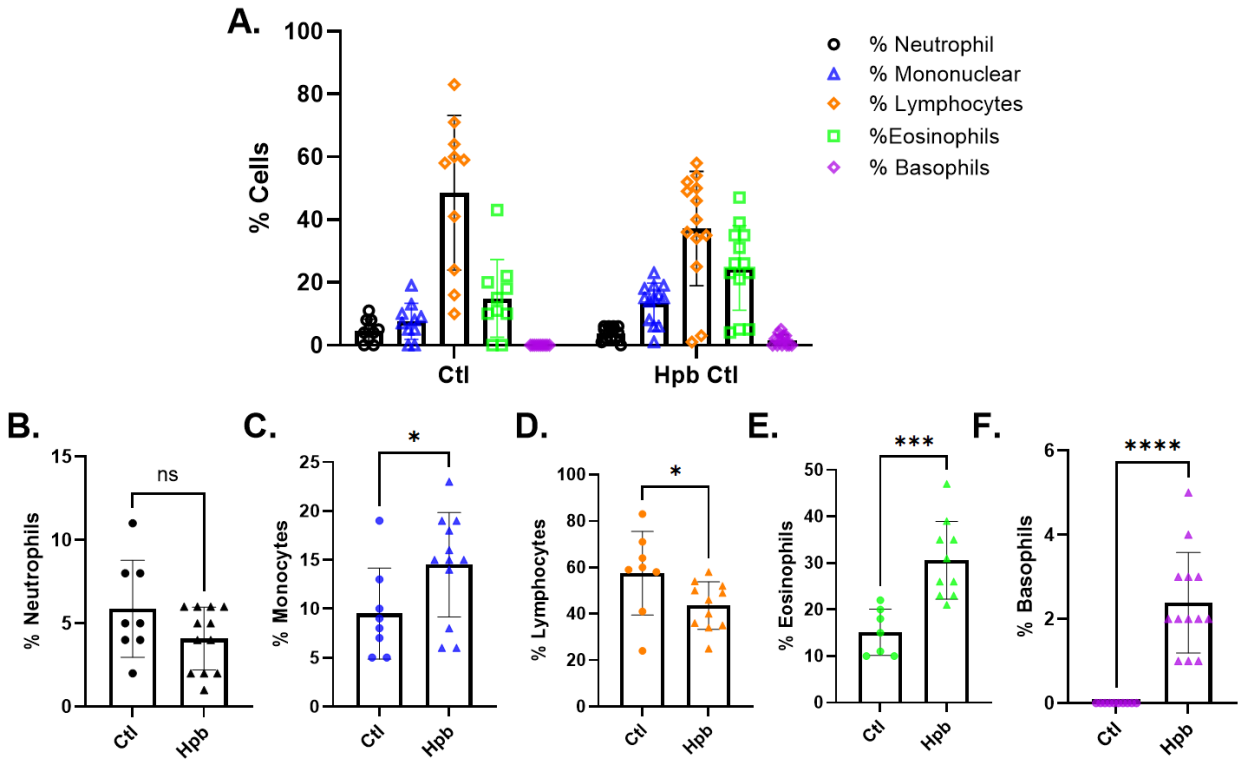

Figure 20) Hpb infection effect on peripheral blood leukocytes. (A) Total percent of leukocytes in peripheral blood of both control and Hpb infection. Infected groups received 200 L3 larvae 7 days after immunization, blood smears collected 14 days after immunization. Percent of (B) Lymphocytes, (C) Neutrophils, (D) Mononuclear cells, (E) Basophils, and (F) Eosinophils, as measured before challenge with mBSA. Each symbol represents an individual animal, with results expressed as mean ± SEM; *p < 0.05.

5.3 Metabolomic results

To assess the effects of Hpb and AIA and their metabolic alternations, untargeted metabolomics were performed on serum samples by LC-MS/MS; following the same protocol and model as seen in Figure 5A. Serum was collected from the following groups: PBS (Control), mBSA-challenged (AIA), PBS + Hpb infection (Hpb control), and mBSA + Hpb infection (AIA + Hpb), with the serum of naïve (non-immunized) and naïve-infected mice acting as controls. We found that serum samples contained 3,645 unique features **[Supplemental file]**. The peaks were selected using a two-fold change cut-off against naïve non-immunized control samples, to create a hierarchy of relevant metabolic changes, in which 2048 features were identified. Statistical analysis was performed in MetaboAnalyst (**Supplementary Figure 1**). Here we

observed a clear clustering of naïve groups, separate from immunized groups (**Supplementary Figure 1**A). This separation is made clearer when viewed using principal component analysis (PCA) (**Supplementary Figure 1**B). To further assess the effects of Hpb infection on AIA and its metabolic alternations on either PBS or AIA groups, both naïve (non-immunized) groups were separated. Further results focused on comparisons between the following groups: PBS-challenged control mice [Imm], mBSA-challenged mice [AIA or Imm_mBSA], mBSA-challenged + Hpb infected mice [AIA+Hpb or Imm_Hpb_mBSA] and control PBS+Hpb infected mice [Imm_Hpb]. Serum untargeted metabolomic data identified 2047 unique features. Statistical analysis was performed in MetaboAnalyst. We observed through a heatmap hierarchical clustering analysis that all four groups clustered individually, separate from one another (**Figure 21**A). The PCA plot demonstrated distinct clustering of features (**Figure 21**B), especially in the Hpb infected-mBSA challenged group. Supplementary figure two demonstrates the 50 most statistically significant features that are most upregulated or downregulated between each group, with 763 features identified as the most statistically significant ($p>0.1$) amongst all groups (**Supplementary Figure 2**). To further identify potential compounds that significantly differed between AIA and control mice, and between AIA mice and AIA *Hpb* infected mice, metabolomic data were analyzed using an unpaired univariate analysis, which performed on (A) PBS (control) vs mBSA (AIA), and (B) mBSA (AIA) vs mBSA+Hpb (Hpb infected AIA) and presented as volcano plots (**Figure 22**). Features that met an FDR-adjusted p-value (i.e., q value) threshold of less than 0.1 were regarded as features of interest. Based on this threshold, a total of 81 features were found to significantly differ between the PBS control mice and AIA mice (64 downregulated and 17 upregulated). Similarly, a total of 777 features were found to differ between the AIA vs AIA+Hpb mice (452 downregulated and 32 upregulated) (**Figure 22**).

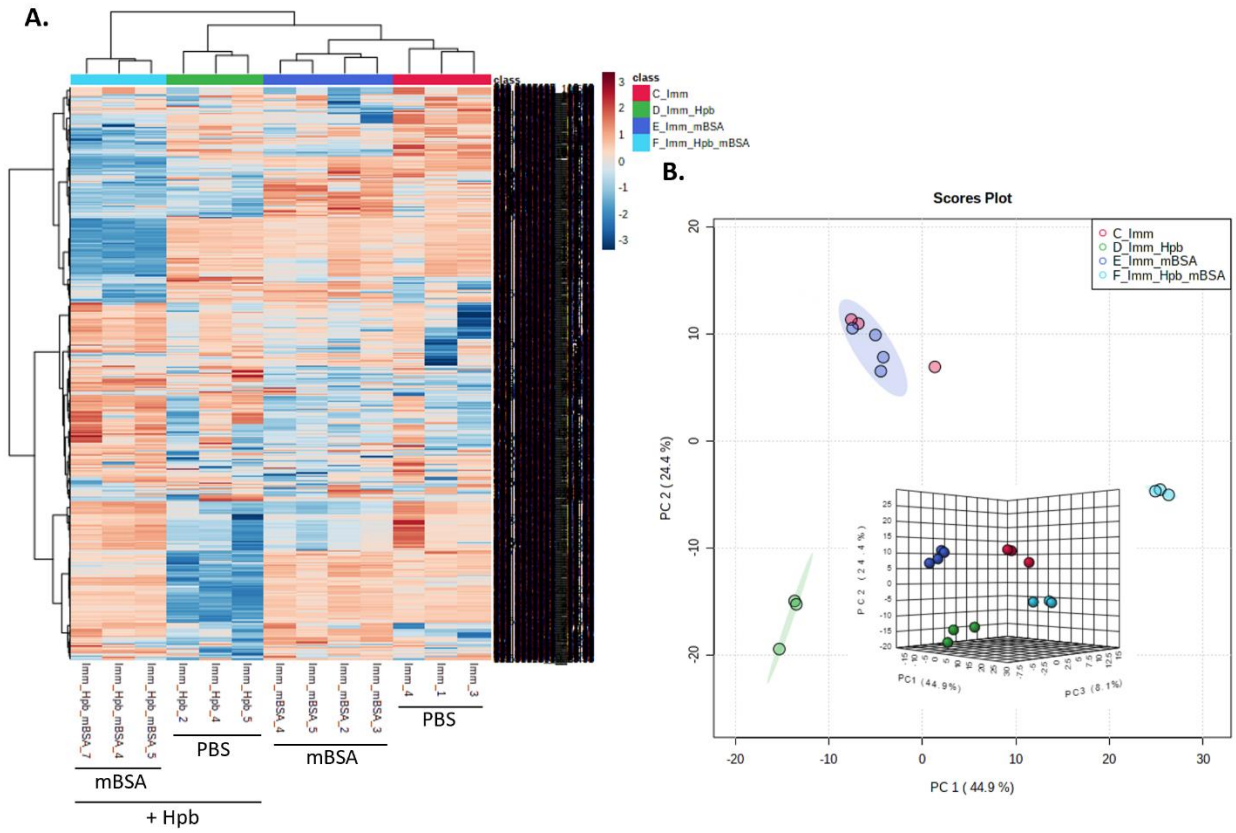

Figure 21) Metabolomic characterization of Hpb infection on AIA. (A) Heat map representation of metabolome from PBS control [Imm], AIA [Imm_mBSA], AIA+Hpb [Imm_Hpb_mBSA], and control PBS Hpb [Imm_Hpb] groups. (B) Principal Component Analysis plot of all groups. Red represents PBS control samples, Green PBS control-Hpb infected samples, Dark blue mBSA challenged (AIA) samples, and Clear blue mBSA challenged-Hpb infected samples

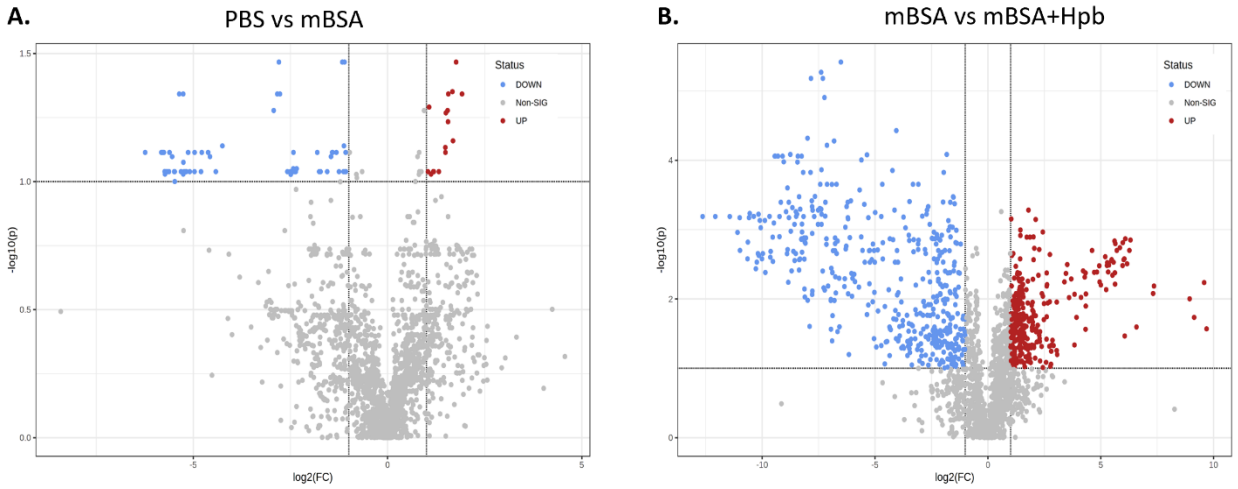

Figure 22) Different metabolomic profiles in AIA and Hpb+AIA. (A) Volcano plot control vs mBSA (p-value 0.01); (B) Volcano plot mBSA vs mBSA+Hpb (p-value 0.1)

Thirty-nine features were identified as most significantly differentiated and shared between both comparisons. Of this, 35 were present in **Supplementary Figure 2**'s statistical comparison between all groups; in other words, they were present in the 763 features identified as most statistically significant ($p>0.1$) amongst all four groups. Of these 35 features, the majority were found to be upregulated in both the PBS control and AIA+Hpb groups, with 29 features displaying this pattern, with four found to be increased in AIA (mBSA challenged mice) and downregulated on all other groups and one increased in the PBS control and downregulated in all other groups.

5.3.1 Metabolomic profiling of AIA serum 24hrs after challenge. To further observe the difference between PBS control and AIA groups 24 hours after mBSA challenge, we will now show the results of the statistical analysis of the groups and their features of interest. This will be followed by an enrichment of pathway analysis, which will identify affected metabolic pathways and possible metabolites of interest.

As expected, a heatmap hierarchical clustering analysis clustered the PBS control group separately from the AIA group, as demonstrated by dendrograms at the top of the map (**Figure 23**A). The unsupervised principal components analysis [PCA] model more clearly demonstrates this clustering (**Figure 23**B), with a distinct clustering of metabolites apparent for both groups. This shows that all groups are distinctive from one another, which demonstrates that the model of RA has been successfully established. A PLS-DA was used to extract the variation information among groups to find different compounds. The results of the PLS-DA score plots show that the classification effect was significant, and that each group is separate from the others (**Figure 23**C), indicating the possibility of identifying each group through metabolomic analysis. Further, 93 features were identified as most significantly different ($p>0.1$) (**Figure 23**D).

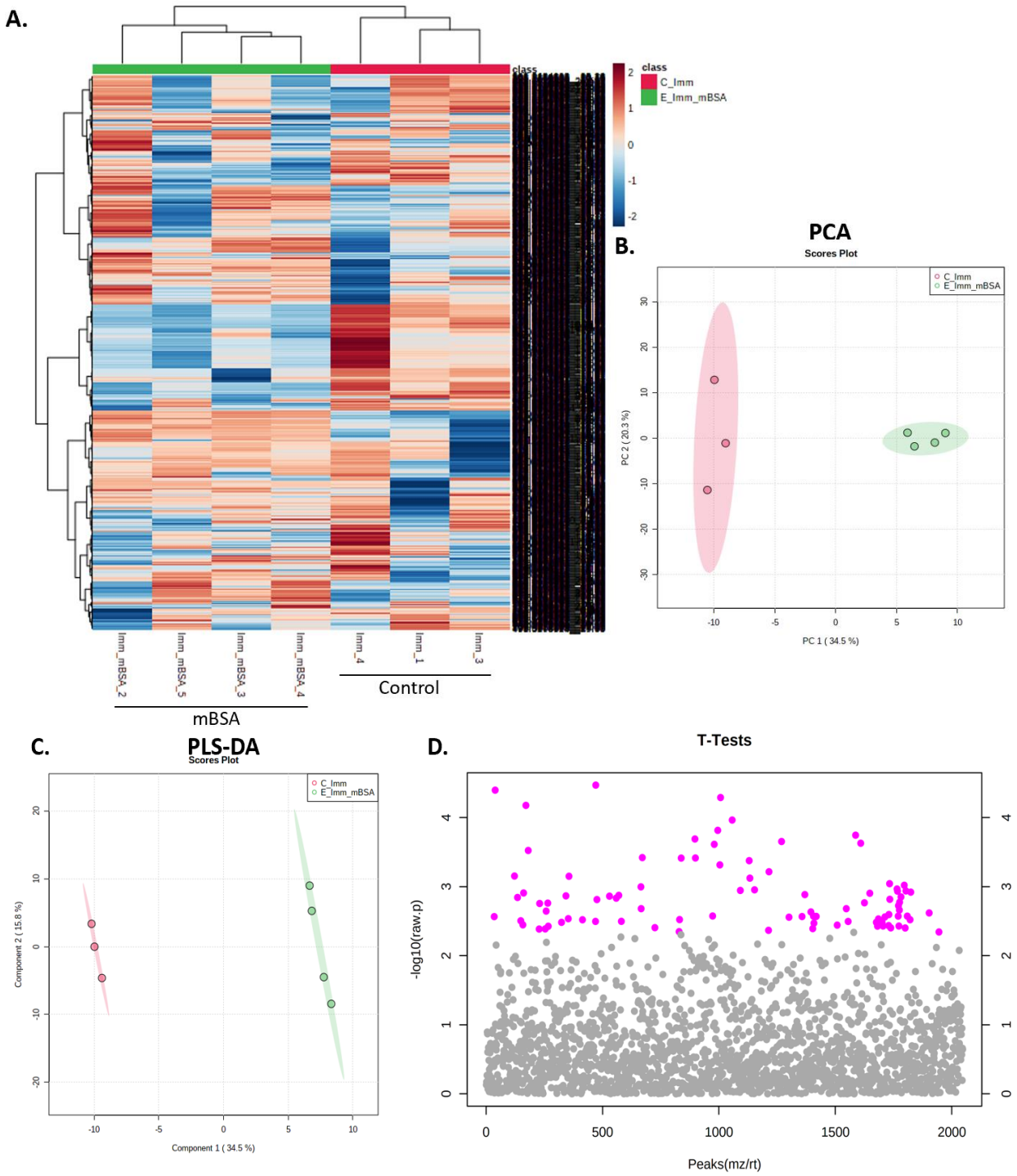

Figure 23) Statistical analysis of Control group vs AIA group. Statistical analysis of PBS vs mBSA groups before enrichment pathway analysis. (A) heat map for discriminating the serum metabolome from control and AIA groups. (B) Principal Component Analysis plot and (C) Partial Least Squares Discriminant Analysis between control and AIA groups D) 93 features identified as most statistically p>0.1 different metabolites.

Functional analyses were performed to infer pathways related to the differentially enriched metabolites using Mummichog enrichment and a KEGG database. **Figure 24** shows the enrichment of the pathway analysis results, predicting a total of 49 pathways and 1471 matched compounds. Of these, mBSA was found to primarily affect four pathways, namely, sphingolipid metabolism, arginine biosynthesis, Lysine degradation and Pyrimidine metabolism. A heatmap representation of the pathway analysis demonstrating the upregulation and downregulation of features and their corresponding pathways can be found in **Supplementary Figure 3**.

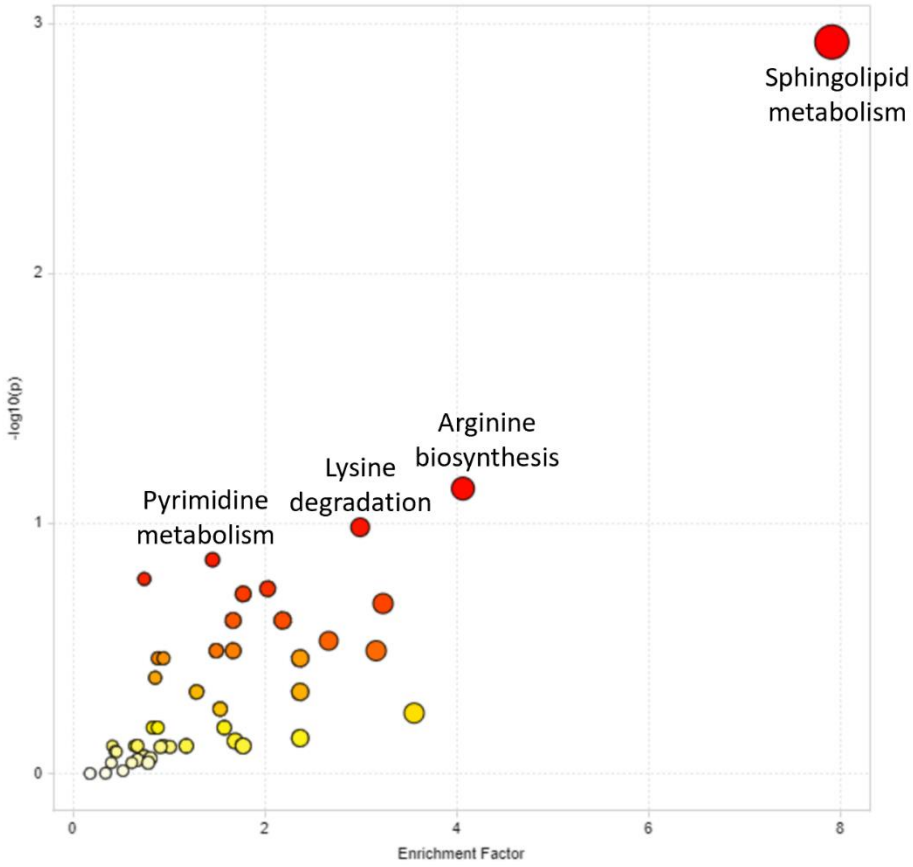

Figure 24) Enrichment of pathway analysis of AIA. Enrichment of pathway analysis of control vs AIA groups with MetaboAnalyst5.0.1

5.3.2 Metabolomic characterization of infected AIA serum 24hrs after challenge. To further identify compounds of interest and the differences between AIA (mBSA challenged) and AIA+Hpb infection (Hpb infected + mBSA challenged), a statistical analysis was done 24hours after mBSA challenge to identify their metabolic differences, which was followed by an enrichment of pathway analysis to identify affected metabolic pathways and possible metabolites of interest. The statistical analysis was performed in MetaboAnalyst. **Figure**A demonstrates the full-length hierarchical clustering heatmap between each group, showing the upregulation and downregulation of features, with both groups clustered separately from one another. As expected, the PCA plot also demonstrates the distinct clustering of both groups (**Figure**B), and 1045 features were identified as most statistically different (p>0.1) (**Figure**D).

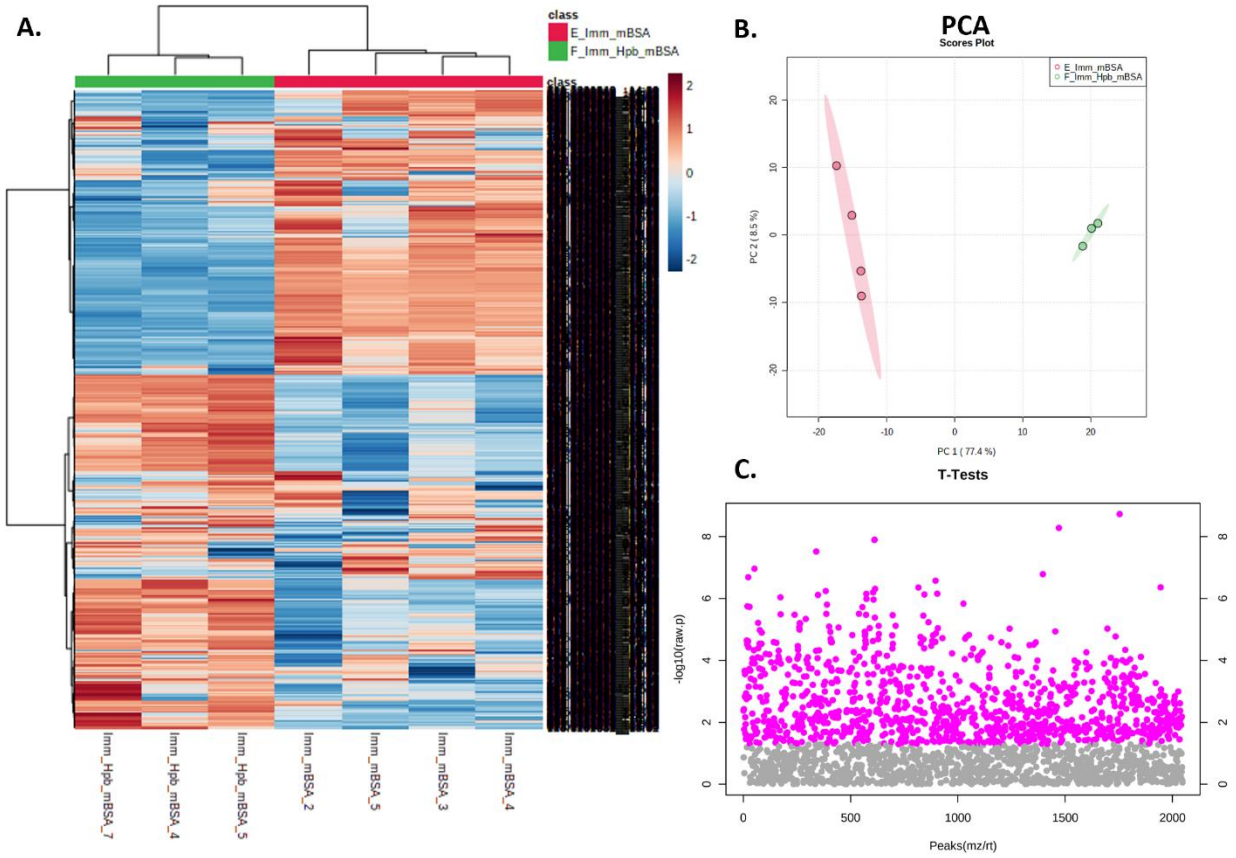

Figure 25) Statistical analysis of AIA group vs AIA+Hpb group. Statistical analysis of mBSA vs mBSA+Hpb groups before enrichment pathway analysis. (A) heat map for discriminating the serum metabolome from mBSA+Hpb and AIA groups. (B) Principal Component Analysis plot mBSA+Hpb, and AIA groups. (C) 1045 metabolites identified as most statistically p>0.1 different metabolites.

Statistical analysis was followed by functional analyses to identify metabolic pathways and metabolites of interest. An enrichment of pathway analysis was completed using Mummichog enrichment and KEGG database. The results predicted a total of 43 pathways and 489 matched compounds (**Figure**). Of these, Hpb infection was found to affect the following: steroid biosynthesis, valine, leucine and isoleucine biosynthesis, alpha-Linolenic acid metabolism, Porphyrin and chlorophyll metabolism, Linoleic acid metabolism, Biosynthesis of unsaturated fatty acids, Arginine and proline metabolism, Valine, leucine and isoleucine degradation, Lysine degradation, Glutathione metabolism, D-Arginine and D-ornithine metabolism, Folate biosynthesis, Steroid hormone biosynthesis, Tryptophan metabolism and Sphingolipid metabolism, to name a few. A heatmap representation of the pathway analysis, demonstrating the upregulation and downregulation of features with their respective pathways, can be found in **Supplementary Figure 4**.

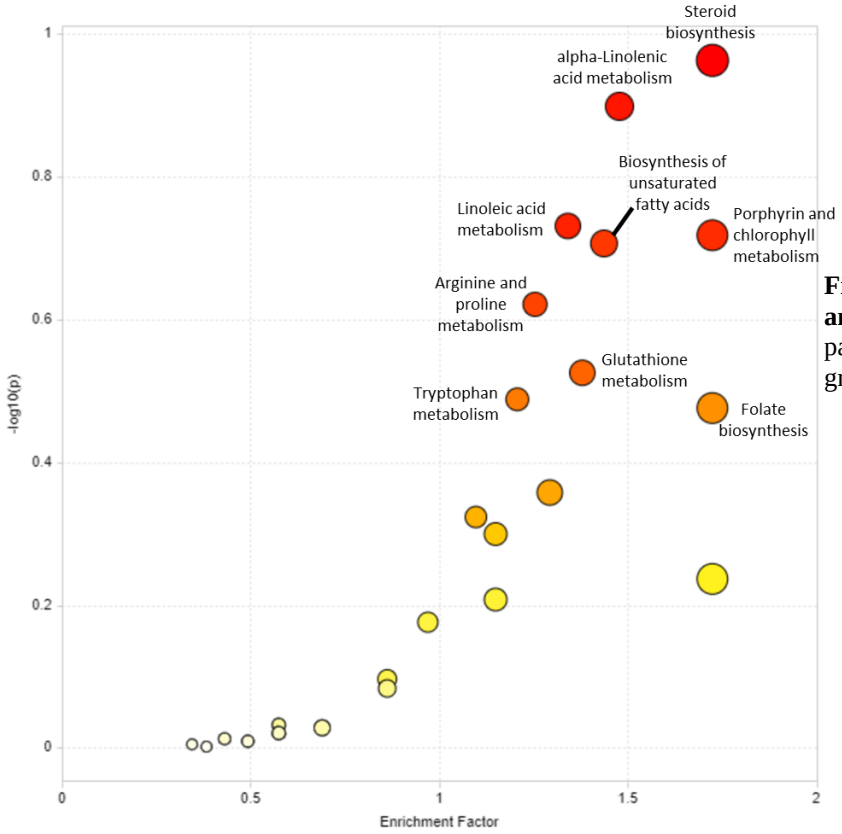

Figure 26) Enrichment of pathway analysis AIA+Hpb. Enrichment of pathway analysis of AIA vs AIA+Hpb groups with MetaboAnalyst5.0.1

5.3.3. Identified metabolomic compounds. Based on both the statistical analysis of Ctl vs AIA and AIA vs AIA+Hpb, and the enrichment analysis results, eight features were identified between both groups to be on the topmost statistically significant in all analyses (Supplementary table 1). Of these, only three features were found to be upregulated by AIA and downregulated in AIA+Hpb and only two were identified during enrichment analysis with potential compound hits. These two features are further discussed below:

Feature 244.0939099__14.86531667 which was upregulated in AIA mice when compared to the PBS control and downregulated with Hpb infection (**Figure 27**). This compound was identified in KEGG database library as Cytidine (KEGG ID: C00475; M+H[1+]; Formula: $C_9H_{13}N_3O_5$) and is involved in pyrimidine metabolism for both Ctl vs AIA and AIA vs AIA+Hpb, which can be observed in both enrichment analysis heatmaps (**Supplementary Figure 3**, **Supplementary Figure 4**).

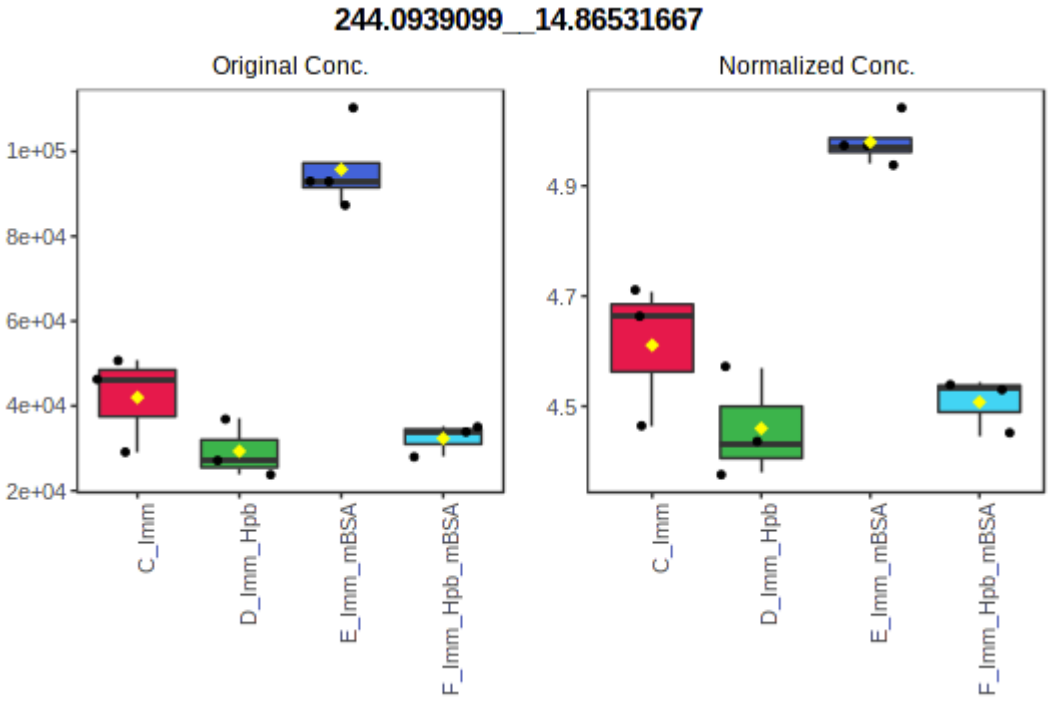

Figure 27) Box and *whisker* plots of plasma metabolite levels. For feature 244.0939099__14.86531667 identified as altered in (A) Ctl vs AIA, and (B) AIA vs AIA+Hpb.

Feature 302.3048794__19.6885 was also upregulated in AIA mice when compared to the PBS control and downregulated with Hpb infection (**Figure 28**). This compound was identified in KEGG database library as Sphinganine (KEGG ID: C00836; M+H[1+]; Formula: $C_{18}H_{39}NO_2$) and is involved in sphingolipid metabolism for both Ctl vs AIA and AIA vs AIA+Hpb, as can be observed in both enrichment analysis heatmaps (**Supplementary Figure 3**, **Supplementary Figure 4**).

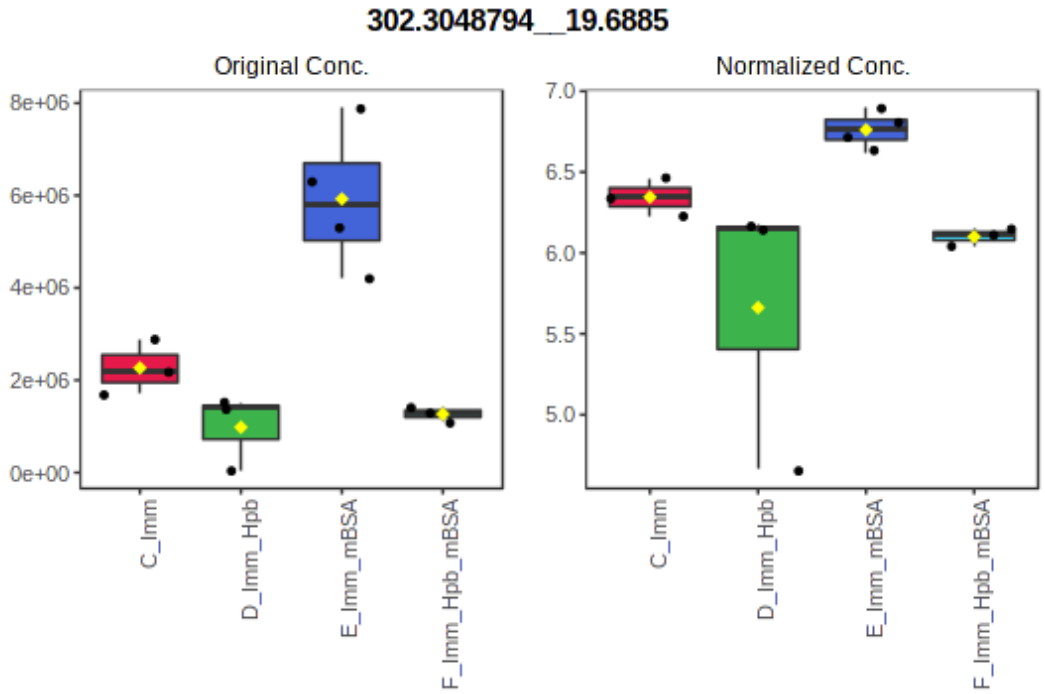

Figure 28) Box *and whisker* plots of plasma metabolite levels. For feature 302.3048794__19.6885 identified as altered in (A) Ctl vs AIA, and (B) AIA vs AIA+Hpb.

6. Discussion

Rheumatoid arthritis is a cause for worldwide concern, affecting 0.5–1% of the global population, making it the most common chronic inflammatory joint disease on the planet, as well as a leading cause of disability worldwide. Canada has one of the highest incidences of rheumatic diseases (Widdifield, Paterson et al. 2014), with RA affecting approximately 374,000 Canadians aged 16 and older (Hayter and Cook 2012), (Widdifield, Paterson et al. 2014). In other words, RA is estimated to affect one out of every 100 Canadian adults (Widdifield, Paterson et al. 2014). The prevalence and incidence of diagnosed rheumatoid arthritis generally increases with age, and it affects women two to three times more often than men (Widdifield, Paterson et al. 2014). It is estimated that around 60% of patients with RA who are inappropriately treated are unable to work within 10 years of the onset of the disease, which costs the Canadian economy more than $6.4 billion annually in medical expenses and indirect costs, such as decreased productivity and quality of life (Widdifield, Paterson et al. 2014). Given the increasing prevalence of RA increasing and the existence of no available cure, as well as the severe side effects of existing treatments for certain patient cohorts, we seek to broaden and diversify the list of safe and effective treatments available for RA.

To this aim, we focused on the effects of Hpb on the acute phase of a murine model of Antigen-induced arthritis (AIA). AIA is a well-characterized, experimental model of joint disease (Mauri, Williams et al. 1996); characterized by an acute phase marked by joint swelling and immune cell infiltration (Krock, Jurczak et al. 2018). This model was picked for this study due to its short-lived nature and self-resolving features, and also because the mechanisms and kinetics of AIA inflammation and resolution have been well characterized (Cunha, Verri et al.

2004, Coelho, Pinho et al. 2008, Cunha, Barsante et al. 2008, Lopes, Coelho et al. 2011, Lopes, Graepel et al. 2016, Gonçalves, Rezende et al. 2020).

As mentioned, *Hpb* has been shown to be immunomodulatory and can limit the severity in models of certain inflammatory diseases, with a chronic infection of Hpb resulting in the immunomodulatory dampening of the inflammatory immune response, thus attenuating the development of collagen-induced arthritis (Sarter, Kulagin et al. 2017). There are, however, relatively few pre-clinical studies linking helminth infection in mice to inflammatory responses in the joints. Consequently, it was of interest to determine if infection with Hpb would limit immunopathology in AIA. With this in mind, we focused on the effects of Hpb infection on the acute phase of AIA. We hypothesized that *Heligmosomoides polygyrus bakeri* infection would limit immunopathology in AIA, dampening inflammation in the knee joint by attenuating neutrophil infiltration to the joint and inhibiting expression of inflammatory cytokines. We also aimed to determine the effect of Hpb infection on the host metabolome as it pertains to AIA.

To evaluate the effects of Hpb infection on AIA, we first standardized the model in our group. In our pilot study, 10 mice (five males, five females) were immunized and challenged with mBSA to induce AIA. While we were able to confirm the induction of inflammation in the joint, we also observed a high level of variability, especially when it came to neutrophil numbers. Sex-related differences in antigen-induced arthritis in mice are understudied, as young adults are mainly used in such studies, and sex-related differences appear to be most remarkable in older mice (van Beuningen, van den Berg et al. 1989). Most of these studies on sex-specific factors affecting RA have focused on human studies, and specifically on the potential effects of sex hormones (Liu, Jia et al. 2020). For example, RA often improves during pregnancy, and male

patients with RA generally have a less severe course of illness and better response to therapy than female patients (Ostensen and Villiger 2007, Förger, Marcoli et al. 2008, Sokka, Toloza et al. 2009). We separated the mice into males and females to assess if any variability was due to sex-differences.

When separated, we observed that while both groups presented significant neutrophil inflammation 24 hours after mBSA challenge, the females had a higher number of neutrophils, as well as higher variability, with a 14.83 (± 2.707) difference between means, compared to the males' less variable difference between means of 5.310 (± 0.07592). These results corroborate previous data that demonstrates that there are sex-related differences in the inflammatory response, course and destructive effects of antigen-induced arthritis (van Beuningen, van den Berg et al. 1989). There is also the possibility that neutrophil numbers were affected by the age difference of the female mice, as age has previously been reported to affect the immune response and neutrophil numbers in female C57Bl/6 mice (van Beuningen, van den Berg et al. 1989).

We also observed an elevated number of neutrophils in females when compared to males, with peak of 5.49 X 10^5 for males and 21.05 X 10^5 for females. This data corroborates the findings of Hensel *et al.* (2019), who characterized immune cell subtypes by sex, as well as strain-specific variations, and observed that neutrophils in female mice are elevated within the bone marrow of 129/SvHsd mice and within the spleen of C57BL/6NCr and BALB/cAnNCr mice when compared to male mice (Hensel, Khattar et al. 2019). Another study, which used the anti-homocitrullinated (HomoCitJED) immune model of RA, showed that immunized female mice display a more proinflammatory state compared to male mice (Cairns, Saunders et al. 2020). Due to these variabilities, further experiments that analyze cytokine profiles and increase the n value of each group would be needed to fully understand the mechanisms of sex differences

in AIA, which is not within the scope of this project. For these reasons, only male C57Bl/6 mice were used for our experimental procedures.

To further standardize our model, we assessed the kinetics of the inflammation 12 hours, 24 hours and 48 hours after challenge. Peak inflammation of AIA is expected to occur at 12-to-24 hours after challenge, with resolution at 48 hours, as described in Lopes 2011. As expected, we observed a peak in neutrophil infiltration into the synovial cavity at 12-to-24 hours after challenge, which resolved by 48 hours (> 77% decrease in neutrophil influx) post-antigen challenge. We also observed the initiation of resolution in the synovial cavity with an increase in mononuclear cells that increases at 48hrs. Additionally, as expected and previously reported (Lopes 2011), neutrophil infiltration (MPO) in the periarticular tissue has a slower resolution than neutrophils in the in the synovial cavity, peaking at 48 hours, while TNF follows the same progression as neutrophils in the synovial cavity, peaking at 12-to-24 hours. Based on these results, we chose the 24 hour timepoint for further experiments.

In the first part of our study, we investigated whether localized arthritis in the knee joint was affected by Hpb infection. To evaluate the effects of Hpb infection on AIA inflammation, the same model of AIA was used with four groups of mice. All four groups were immunized at day zero, challenged with mBSA or PBS on day 14, and necropsied 24 hours after challenge. Hpb-infected groups received 200 L3 larvae seven days after immunization. The life cycle stage of Hpb is worth noting. The challenge time point (day 14) coincides with the seventh day of infection with Hpb, when L4 larvae have developed and can be seen nestled in nodules on the surface of the small intestine, surrounded by inflammatory cells consisting mostly of eosinophils (Monroy and Enriquez 1992, Finkelman, Shea-Donohue et al. 1997, Camberis, Le Gros et al.

2003, Gause, Urban et al. 2003), and a strongly polarized type 2 cytokine response (Filbey, Grainger et al. 2014). Necropsy day, i.e., 24 hours after challenge, coincides with the eighth day of infection, when the adult worms begin to emerge into the lumen of the intestine and anchor tightly to the intestinal villi (Monroy and Enriquez 1992). This life stage is associated with Hpb immunomodulatory capabilities, as well as the modulation of microbiota (Walk, Blum et al. 2010).

One question of special interest was whether Hpb infection had any effect on neutrophils during AIA. This is noteworthy because, as previously mentioned, the overabundance and persistence of activated neutrophils is one of the most prominent drivers of joint inflammation in RA (Rosas, Correa et al. 2017, Cecchi, Arias de la Rosa et al. 2018, O'Neil and Kaplan 2019). While our data shows that Hpb infection did not affect neutrophil numbers in the knee cavity, infection reduced MPO (neutrophil infiltration) in the periarticular tissue by 65.77% compared to AIA group. Indicating a decrease, or faster clearance, of neutrophil infiltration in the periarticular tissue of Hpb infected + mBSA challenged animals.

The decrease in MPO could be due to a decrease in neutrophil cytotoxic activity, since MPO is the most cytotoxic and abundant enzyme expressed in neutrophil granulocytes (Strzepa, Pritchard et al. 2017), or it could show that Hpb affects neutrophil differentiation/activation. While this has not yet been observed in neutrophils, a 2017 study by Sarter and Kulagin et al. demonstrated that Hpb infection attenuates the development of collagen-induced arthritis (CIA) and collagen antibody-induced arthritis (CAIA) by inhibiting the differentiation of osteoclasts *in vitro* (Sarter, Kulagin et al. 2017). As mentioned in the introduction, an increased MPO activity has been observed in many inflammatory conditions and autoimmune diseases, such as MS and

RA (Strzepa, Pritchard et al. 2017). MPO may play a bigger role in AIA, as it has been shown to play a role in both K/BxN and CIA models, in which reduced disease severity was observed in $MPO^{-/-}$ mice (Odobasic, Yang et al. 2014). We hypothesize that a decrease in MPO (as was observed with Hpb infection in our model) could lead to reduced disease severity with Hpb infections, but future experiments evaluating disease scores and MPO levels are needed to further assess the effect of Hpb on AIA disease severity. These results corroborate the observation by Odobasic et al. (2014) that MPO may have a direct impact on inflammation in the joint which is independent of the underlying immune response (Odobasic, Yang et al. 2014).

The decrease of MPO in the periarticular tissue led us to the hypothesis that Hpb infection could block neutrophil migration or chemotaxis by blocking activity of CXCR1/CXCR2 receptors. Correspondingly, we also observed a decrease in CXCL-1, as well as in TNF and IFN-γ in the periarticular tissue. The decrease of CXCL-1 in Hpb-infected AIA, compared to AIA, corresponds with the decrease of MPO (infiltrating neutrophils) into the periarticular tissue in this group, indicating that Hpb infection may be blocking CXCL-1-based neutrophil migration. However, neutrophil functions may be affected through several pathways, and it is yet to be determined whether *Hpb* infection affects neutrophils directly or indirectly through the activation of other regulatory cell types discussed below. Further tests, such as *in-vitro* chemotaxis and intravital microscopy, could provide further insights into the effects of Hpb on neutrophil migration.

We also observed decreased levels of IFN-γ and TNF in the Hpb+AIA group when compared to AIA. This indicates that CD4+ T cells infiltration/activation in the periarticular tissue may be being inhibited by Hpb infection, and this is of note since CD4+ T cells infiltrating the RA synovial membrane have been found to have a notably high IFN-γ production

(Frederique Ponchel and El-Sherbiny 2012). Further, the lower level of IFN-γ is in accordance with previous reports of decreased IFN-γ levels in the spleen and mesenteric lymph nodes of mice infected with Hpb (Setiawan, Metwali et al. 2007, Maizels, Hewitson et al. 2012). This finding also corroborates with observations from Classon et al, stating that Hpb infection induced long term H-poly specific CD4+ Th2 cells homing to skin; this in turn decreased the IFN-γ response to mycobacterial antigens (Classon, Li et al. 2022). This indicates that Hpb may have a more systemic effect than previously thought with infection causing durable changes to the composition of skin T-cells; with our results indicating this response may be occurring at the 7^{th} or 8^{th} day of infection, earlier than previously indicated.

Our observations of lower TNF levels also concur with previous reports of decreased inflammatory cytokine levels in mice infected with Hpb (Setiawan, Metwali et al. 2007, Maizels, Hewitson et al. 2012) with protection in these infections mostly being attributed to Th2 immune deviation and suppressed levels of TNF, IFN-γ and IL-17A. Of note is that these reports are mainly of mucosal, peripheral blood or intestinal cytokines during the 14th day of Hpb infection. Here, we observe a decrease in TNF levels in the joint eight days post-infection, indicating that this earlier time point of infection plays a role in the early prevention of inflammation. TNF levels have been associated with variable apoptotic neutrophil levels, with an increase in TNF has been shown to accelerate MCL-1 turnover (Adams and Cooper 2007, Cross, Moots et al. 2008), suggesting that apoptotic rate may be affected. To rule out that our observed decrease in neutrophils in the periarticular tissue was due to higher neutrophil turnover, or due to neutrophil survival being affected by Hpb infection, the distinctive apoptotic morphology was estimated from cytospin preparations stained with May-Grünwald-Giemsa. We did not observe a difference

in the number of viable or apoptotic cells between AIA and Hpb+AIA groups, thus confirming that the decrease in inflammatory cytokines and MPO was not due to a difference in viability.

While Hpb infection did not affect neutrophil numbers in the knee cavity, we did observe a 35% increase in mononuclear cell numbers in the knee cavity, indicating a greater recruitment of mononuclear cells into the synovial cavity of AIA-mice infected with Hpb compared to AIA. An increase in mononuclear cells in this model is linked to the start of inflammation resolution, as the resolution of inflammation involves apoptosis and the subsequent clearance of activated inflammatory cells. This increase in mononuclear cells in the knee cavity could lead to the clearing out of more debris and neutrophils faster from periarticular tissue. In RA, neutrophils have been recognized as a major player in disease progression, presenting an activated phenotype (Wright, Moots et al. 2014, Rosas, Correa et al. 2017, Cecchi, Arias de la Rosa et al. 2018, O'Neil and Kaplan 2019, Wright, Lyon et al. 2020) as well as being found in high numbers in both the synovial joints and tissues of patients with RA (Wittkowski, Foell et al. 2007, Cascão, Moura et al. 2010, Moura, Cascão et al. 2011, Turunen, Huhtakangas et al. 2016). Clearance of these activated neutrophils could lead to faster resolution. However, further experiments looking into mononuclear cell number in the periarticular tissue and their phenotype, as well as Hpb effect on immuno-histological/histological scores and inflammation kinetics, are needed.

Ultimately, while Hpb infection did not affect neutrophil infiltration into the knee cavity, the results indicate a reduction of MPO (neutrophil infiltration) in the periarticular tissue, as well as an increase in mononuclear cells in infected groups and a decrease of inflammatory cytokines. This indicates a faster resolution of inflammation. There are other cell types that could be affecting cytokine levels as well as increasing mononuclear cell numbers, which will be discussed below.

Heligmosomoides polygyrus bakeri (Hpb) is known to induce regulatory T cells (Tregs), tolerogenic dendritic cells (TolDC), alternatively activated macrophages (AAMθ) and regulatory B cells (Bregs) (Maizels 2012, Valanparambil 2017, Hang 2019), as well as the anti-inflammatory cytokines IL-10 and TGF-β, which exert widespread immunomodulatory effects on both the innate and adaptive immune system of the host (Su, Segura et al. 2005, Weng, Huntley et al. 2007, Blum, Hang et al. 2012, Maizels, Hewitson et al. 2012, Reynolds, Filbey et al. 2012, Valanparambil, Segura et al. 2014). The majority of data described above, however, describes the adult stage of Hpb, and different Hpb life cycle stages secrete different products that could have different immunomodulatory effects (Maizels, Hewitson et al. 2012). As mentioned above, our mBSA challenge time point (the 14th day after immunization) coincides with the seventh day of Hpb infection. At these timepoints, both L4 larvae and young adults are present, which each have different effects on immune response. L4 larvae have a strongly polarized type 2 cytokine response (Filbey, Grainger et al. 2014), and have been shown to prevent the maturation of DC (JAWS-II-DC), leading to a semimature status and Th2 and regulatory response *in vitro* (Maruszewska-Cheruiyot, Donskow-Lysoniewska et al. 2019). Day seven-post Hpb infection also increases myeloid derived suppressor cells in the lamina propria and systemic lymphoid tissues, with suppressed CD4+ Th2 (GATA3+) response *in vitro*. (Valanparambil, Tam et al. 2017). Another interesting effect observed on the seventh day post-infection is that the nuocyte (IL-25-responsive innate lymphoid cell) population is subdued (Smith, K.A. et al., personal communication). Nuocytes contribute to the expulsion of helminth worms, as well as the pathology of colitis and allergic airway disease (Neill, Wong et al. 2010, Barlow, Bellosi et al. 2012, Camelo, Barlow et al. 2012). Necropsy day (24 hours after mBSA challenge) coincides with the eighth day of infection. On the eighth day of infection, adult

worms emerge. This life stage is associated with the Hpb immunomodulatory capabilities mentioned above. All of these immunomodulatory changes and the induction of Tregs, TolDCs, AAMθs and Bregs by Hpb exert widespread immunomodulatory effects on both the innate and adaptive immune system. While important to keep in mind, this goes beyond the scope of this project.

Keeping the effects of Hpb infection in mind, we further evaluated the effects of Hpb infection on AIA T cell derived cytokines. In this AIA model, the arthritic inflammation depends on the degree of antigen retention in the joint, and the accumulation, retention and local proliferation of mBSA-specific arthritogenic T-cells (van den Berg, Joosten et al. 2007).]. Hpb Th2 induction may, therefore, decrease Th1 response from mBSA-specific arthritogenic T-cells. A splenocyte proliferation assay was conducted to assess T cell derived cytokines in the spleen. This is a way to determine whether T-cells are triggered to divide after exposure to a specific stimulus. After isolation, solenocytes were activated using ConA (concanavalin A). ConA is a lectin that acts as a surrogate for antigen-presenting-cells in T-cell proliferation assays, which leads to general T-cell polyclonal proliferation. Depending on the cytokines produced by T-cell types, we can infer which is more prominent. Since Hpb is known to increase IL-4 as well as IL-10 in the mucosa, mesenteric lymph nodes and spleen at the 14th day of infection (Setiawan, Metwali et al. 2007) we assessed the level of both of these cytokines in the spleen on day eight of infection, 24 hours after mBSA challenge. We observed that non infected groups did not differ in IL-4 levels (control vs AIA); unexpectedly, however, while there was an increase in IL-4 in the Hpb-control group, there was no increase of IL-4 in AIA-Hpb-infected mice when compared to control Hpb-infection.

The AIA model is CD4+ T-cell dependent, as is the response to Hpb infection (Valanparambil, Segura et al. 2014). Immunity to Hpb has been shown to be dependent on CD4+ T cells and ILC2 (group-2 innate lymphoid cells) dependent IL-4 (Pelly, Kannan et al. 2016). Further Hpb-infected mice suppressed OVA-specific CD4+ T-cell proliferation via a nitric oxide-dependent mechanism and parasite-specific IL-4 secretion *in vitro* (Valanparambil, Tam et al. 2017). The decrease in IL-4 in the AIA-infected mice (compared to the control-infected) suggests that the AIA immunization/challenge may be affect Hpb infection, which may in turn affect our model, if the Hpb life-stage or expulsion is also being affected. Different Hpb life cycle stages secrete different products, which could have immune-modulatory effects (Maizels, Hewitson et al. 2012). It would be interesting, therefore, to study whether immunization or mBSA-induced-inflammation has any effect on the life cycle of Hpb. Based on our observed worm burden, there were no statistical differences in either life cycle stage burden. However, there was a slight (i.e., non-statistically significant) increase in observable cystic larvae in the Hpb+AIA when compared to the Hpb control. This change may affect early Hpb-cell type activation, such as LC2s, which were shown to expand early during Hpb infection in both the intestinal lamina propria (LP) and in the draining mesenteric lymph nodes (MLNs) in concert with early TH2 cell differentiation (Pelly, Kannan et al. 2016).

IL-10 was increased for both Hpb-infected groups when compared to the non-infected group, with no difference in IL-10 observed between both infected groups, the Hpb-AIA mice and Hpb control mice. These observations corroborate previous reports, in which Hpb is shown to increase IL-10 in the intestinal mucosa and spleen (Valanparambil, Segura et al. 2014, Hang, Kumar et al. 2019). The mechanism through which Hpb induces IL-10 has been identified and described by Hang Kumar et al. (2019), who show that Hpb infection decreases Smad7

expression in intestinal CD4+ T cells, leading to TGF-β induction of IL-10-producing regulatory T cells (Hang, Kumar et al. 2019). In addition, Treg cells represent a potential source of IL-10 and reduce the expression of IL-4 (Rausch, Huehn et al. 2008). Further, the use of Tregs as RA treatments has been considered, with the transfer of Tregs from *H. polygyrus*-infected mice being shown to confer protection from airway allergy in sensitized mice (Wilson, Taylor et al. 2005, Maizels, Hewitson et al. 2012). We also observed that while IL-10 had increased in the spleen of both Hpb-infected groups, it was unaffected in the periarticular tissue of AIA-Hpb infected mice but increased in the Hpb-control, thus indicating that while infection does have systemic effects, it affects distinct areas differently. This increase in IL-10 does, however, suggest an increase in Treg cells, which represented a potential source of IL-10 and may explain the reduced expression of IL-4 in the spleen of AIA-Hpb infected mice previously discussed. Future experiments will be needed to assess the mechanisms through which Hpb affects cytokine levels differently in the periarticular tissue compared to spleen, mucosa and mesenteric lymph nodes.

To prove that the results observed were specifically due to Hpb affecting inflammation and not due to a difference in infection level, infection inhibiting mBSA immunization or peripheral blood leukocyte levels, we evaluated worm burden, anti-mBSA IgG and blood smear counts. The worm burden was uniform between both AIA+Hpb and Hpb control groups, thus indicating that the previously observed results are not due to difference in worm burden or life cycle stage differences. Since mBSA titers correlate to AIA pathology (Brackertz, Mitchell et al. 1977) we also observed levels of anti-mBSA IgG. Both AIA and AIA+Hpb groups showed an increase in anti-mBSA IgG compared to the control, with a slightly higher increase in the Hpb infected group but no significant difference between the AIA and AIA+Hpb groups, confirming that Hpb infection did not interfere with mBSA immunization. Blood smears were obtained

before the mBSA challenge in order to assess whether Hpb infection affects the percentage of leukocytes in the peripheral blood. While we did not observe a difference in neutrophil numbers after Hpb infection, we observed an increase in mononuclear cells, eosinophils and basophils, as well as a decrease in lymphocyte numbers in the peripheral blood of infected animals. This indicates that previously observed results may be due to Hpb infection increasing mononuclear cell numbers before mBSA challenge or due to early Hpb-polarized type 2 cytokine responses (Filbey, Grainger et al. 2014) and the activation polarization of more regulatory cell types in tissue such as activation of regulatory cells, such as Tregs, TolDC, AAMθ and Breg (Hang, Kumar et al. 2019).

To further explore the variable effects of Hpb infection in our AIA murine model, we investigated whether Hpb infection affects the metabolome of murine-AIA. Since the identity and chemical composition of most metabolites are still undefined, we picked an untargeted approach. This is a large-scale method aimed at describing the comprehensive molecular weight profiles of potentially new metabolite biomarkers in an unbiased manner. Serum untargeted metabolomic data identified 3,645 unique features, of which 2048 were identified when compared to naïve (non-immunized) controls after a two-fold change cut-off.

To better understand the effects of Hpb infection on the metabolome of AIA, four groups were compared: PBS (Control), mBSA-challenged (AIA), PBS + Hpb infection (Hpb control) and mBSA + Hpb infection (AIA + Hpb). Through the use of heatmap hierarchical clustering analysis and principal component analysis (PCA), we observed that all four groups clustered separately from one another, indicating that all four groups exhibit changes in metabolome and can be easily distinguished from each other. Further 763 features were identified as most statistically significant between all groups (ANOVA, $p>0.1$).

In order to identify features differentially expressed between AIA and PBS-control mice, and between AIA mice and AIA-Hpb infected, the metabolomic data was analyzed using an unpaired univariate analysis and presented as volcano plots. Features that met an FDR-adjusted p-value threshold of less than 0.1 were regarded as features of interest. Between the AIA and PBS-control mice, 81 features were found to significantly differ (64 downregulated and 17 upregulated), and between the AIA and AIA+Hpb mice, a total of 777 features were found to differ (452 downregulated and 32 upregulated). Among both comparisons, 35 features were shared and were found to be statistically significant. This data can provide further insight into Hpb metabolomic changes on AIA by further finding altered metabolites upon mBSA challenge and subsequently returned towards control levels following infection with Hpb or vise-versa.

The majority of the shared features were found to be upregulated in both the PBS control and AIA+Hpb groups, and not upregulated in AIA or PBS-Hpb-control groups, with 29 features displaying this pattern. This indicates that most of the features at play in the AIA+Hpb group may be restoring the AIA metabolome back to the PBS control or preventing its change into an AIA-like metabolome. Of the 35 shared features, four were found to be increased in AIA (mBSA challenged mice) and downregulated in all other groups, potentially identifying AIA-specific features that could be targeted to prevent AIA metabolome-related-symptoms. Finally, one feature was increased in the PBS control group and not in all other groups. Identifying the compounds and pathways involved with these features could lead to identifying potential metabolite RA treatments, and this data can in turn be used as a reference for future studies that look at targeted metabolomics and *in vitro* experimentation to further explore Hpb metabolic interference as a novel RA treatment strategy during both the early stages of tolerance breakdown and the late stages of tissue inflammation.

As mentioned, it has been suggested that specific metabolic alterations could be a therapeutic target in RA (Sanchez-Lopez, Cheng et al. 2019, Qiu, Wu et al. 2021, Yoon, Jang et al. 2021). For example, glutaminolysis, glycolysis, amino acids, pyrimidine metabolism, choline metabolism, and fatty acid synthesis have been proposed as therapeutic targets for RA (Peres, Santos et al. 2017, Narasimhan, Coras et al. 2018, Sanchez-Lopez, Cheng et al. 2019, Gosselt, Muller et al. 2020, Yoon, Jang et al. 2021, Xu, Chang et al. 2022). Targeting these metabolisms can provide a chance for the restoration of homeostasis and disease modulation. In order to identify potential compounds and their associated pathways paired statistical analysis comparisons were performed on both 'PBS-control vs AIA' and 'AIA vs AIA+Hpb' groups, which was followed by an enriched pathway analysis.

To better understand the effects that Hpb exerts on the metabolome of AIA, it is necessary to first understand the impact that AIA has on the metabolome. Paired comparisons of the PBS-control vs AIA samples showed that significant changes occurred in AIA mice 24 hours after mBSA challenge. An enriched pathway analysis by KEGG predicted a total of 49 pathways and 1471 matched compounds involved after mBSA challenge when compared to the PBS-control. Most of these changes occurred in sphingolipid metabolism, arginine biosynthesis, lysine degradation and pyrimidine metabolism. Interestingly, sphingolipid metabolism in human macrophages has been associated with the resolution phase of inflammatory responses, with glycosphingolipids and cholesteryl esters sharply increasing during their resolution phase (Muralidharan, Torta et al. 2022). Furthermore, sphingolipid metabolism is essential for DC activation and production of pro-inflammatory cytokines stimulated by TLR ligands (Janneh and Ogretmen 2022). Also of interest is pyrimidine metabolism. Pyrimidine biosynthesis is necessary to maintain cellular fundamental function in DNA and RNA biosynthesis in all living organisms.

Pyrimidines are ultimately catabolized (degraded) to CO2, H2, and urea. Moreover, the inhibition of pyrimidine biosynthesis through the blocking of dihydroorotate dehydrogenase (DHODH) activity has been proven to be an effective strategy for rheumatoid arthritis (RA) treatment (Peres, Santos et al. 2017). DHODH is the prime target of leflunomide (LEF), which is a potent immunosuppressive DMARD that was approved for the treatment of RA in 1998 (Goldenberg 1999, Herrmann, Schleyerbach et al. 2000). A considerable proportion of RA patients, however, are refractory to LEF, and therefore it is desirable to discover novel DHODH inhibitors, or pyrimidine biosynthesis inhibitors, as lead compounds for the development of new RA treatment candidates.

Paired comparisons between AIA and AIA-Hpb-infected samples showed significant changes occurred in the peripheral blood metabolome of the mice 24 hours after mBSA challenge and identified 1045 features that were significantly different between both groups. Enriched pathway analysis by KEGG predicted that a total of 43 pathways and 489 matched compounds were involved in AIA-Hpb infection after mBSA challenge when compared to AIA. Hpb infection was found to primarily affect steroid biosynthesis, Valine, leucine and isoleucine biosynthesis, alpha-Linolenic acid metabolism, Linoleic acid metabolism, Biosynthesis of unsaturated fatty acids, Arginine and proline metabolism, Valine, leucine and isoleucine degradation, Lysine degradation, Glutathione metabolism, D-Arginine and D-ornithine metabolism, Folate biosynthesis, Steroid hormone biosynthesis, Tryptophan metabolism, and Sphingolipid metabolism to name a few. Sphingolipid metabolism and biosynthesis of unsaturated fatty acids were of special interest. That is because sphingolipids, in addition to their traditional roles as membrane structure, are emerging as bioactive lipids that play key roles in regulating functions (Choi and Snider 2015). The biosynthesis of unsaturated fatty acids was also

noted, since RA T cell metabolome has been reported to skew toward fatty acids (Yoon, Jang et al. 2021). This is of special interest, since the infiltration of CD4 T cells in RA patients' synovial joints has been reported to be a crucial step in RA pathogenesis, progression and development. In a study by Yoon et al. (2021) the researchers observed that retarding lipogenesis by inhibiting fatty acid synthesis reduced tissue inflammation and corrected tissue-invasive and arthritogenic behavior of RA T cells (Yoon, Jang et al. 2021), suggesting that regulating T-cell metabolism in RA is a new therapeutic target.

Of the 35 features shared between both 'PBS-control vs AIA' and 'AIA vs AIA+Hpb' only three were found to be altered upon AIA induction and subsequently returned (or inhibited) towards healthy control levels following Hpb infection and two were identified through enrichment analysis. Of special interest was feature 244.0939099__14.86531667, identified as cytidine (KEGG compound C00475, $C_9H_{13}N_3O_5$) which was found to be involved in pyrimidine metabolism. Aside from being a component of RNA, cytidine has generated interest as a potential glutamatergic antidepressant drug (Machado-Vieira, Salvadore et al. 2010) as it has been found to control neuronal-glial glutamate, with supplementation decreasing midfrontal/cerebral glutamate/glutamine levels (Machado-Vieira, Salvadore et al. 2010). Cytidine only increased in the AIA group and was inhibited (not increased) in the AIA+Hpb group, suggesting an involvement in AIA-inflammation that may be inhibited by Hpb infection. As mentioned earlier, the inhibition of pyrimidine biosynthesis has been proven to be an effective strategy for rheumatoid arthritis (RA) treatment (Peres, Santos et al. 2017). Further, several pyrimidine synthesis inhibitors are currently used in active moderate-to-severe rheumatoid arthritis and psoriatic arthritis, as well as in multiple sclerosis (e.g., Leflunomide and Teriflunomide), and they also have therapeutical uses in cancer treatment (Wang, Cui et al.

2021). Taking all of this into consideration, cytidine might present a potential target for RA treatment with Hpb (or its Excreted-Secreted products) as potential pyrimidine biosynthesis inhibitors.

The second compound upregulated in AIA mice when compared to PBS control and downregulated with Hpb infection identified through enrichment analysis was feature 302.3048794__19.6885. Identified in the KEGG database library as Sphinganine (KEGG compound C00836; $C_{18}H_{39}NO_2$), it is putatively involved in sphingolipid metabolism and found upstream of Sphingosine-1-phosphate (S1P). As mentioned earlier, targeting sphingolipid metabolism is a potential therapeutic target in RA due to its association with the resolution phase of macrophages and DC activation (Muralidharan, Torta et al. 2022). An example of a potent bioactive sphingolipid metabolite that is critically involved in both physiological and pathological processes of RA is Sphingosine-1-phosphate (S1P).

Alteration to S1P signaling in RA has been shown to lead to synovial fibroblast migration, proliferation, survival, migration and production of proinflammatory cytokines/chemokines (Zhang and Zhao 2013). The blockage of S1P, which occurs by inhibiting SphK1 (Sphingosine Kinase 1) activity in an animal arthritis model, significantly suppressed articular inflammation and joint destruction, and lead to reduced disease severity, and down-regulated proinflammatory cytokine production and inflammatory cell infiltration into the synovium (Lai, Irwan et al. 2008), thus demonstrating that lowering S1P levels may represent a therapeutic approach against RA. In our study, AIA seems to increase sphinganine levels in peripheral blood metabolome, while Hpb infection downregulates or inhibits its upregulation. Taking all of this into consideration, sphinganine presents a prospective target for RA treatment, as it is potentially involved in the metabolism of S1P and decreasing S1P levels represents a

therapeutic approach against RA, with Hpb infection (or its ESPs) serving as potential sphingolipid metabolism inhibitors.

Future studies may uncover other novel compounds and pathways through which Hpb may affect the joint inflamed metabolome by harnessing information from the list of features and compounds (both upregulated and downregulated) presented here. The therapeutic effects against these metabolites, as well as their pathways, may also be explored *in-vitro*. Further, innovative therapeutics may also be achieved through the identification and synthesis of small molecules secreted by helminths.

7. Conclusion and Future Applications

In this study, we observed—to our knowledge, for the first time—that Hpb infection has the capacity to decrease or inhibit pro-inflammatory mediators in the knee joint of mice induced with AIA, indicated by decreasing neutrophil infiltration (as measured by MPO), IFN-γ, TNF and CXCL-1 in the periarticular tissue, as well as increasing mononuclear cells in the knee cavity. This is indicative of either the inhibition and prevention, or faster resolution, of inflammation.

We also observed a clear difference in peripheral blood metabolomes between naïve, naïve-Hpb infected, PBS-control, AIA, PBS-Hpb and Hpb-AIA mice groups. We further identified two potential metabolic targets for RA treatment (Cytidine and Sphinganine) that are inhibited by Hpb infection. This could lead to a further understanding on how Hpb affects metabolism, and in turn, how the effects of helminth infection on metabolism play a role in the immune system.

This knowledge can not only better our understanding of how helminths affect disease mechanisms, but also aid in designing of more effective treatments for RA and other inflammatory diseases.

Pitfalls. The majority of the proposed studies use *in vivo* experiments, with long time intervals and limited volumes per sample, thus restricting the amount of assays possible. For example, from the articular lavage obtained during one trial, only cell counts and cytospin results were possible, with the sample not being enough for cytokine assays or flow-cytometry analysis.

While we were able to determine that Hpb infection does have an anti-inflammatory effect on AIA acute knee inflammation at an early Hpb life stage (the eighth day of infection), it is yet to be determined whether Hpb infection affects neutrophils directly, or whether it affects it

indirectly by preventing antigen presentation, or whether it affects it through the activation of regulatory T-cells (Tregs), tolerogenic dendritic cells (TolDC), alternatively activated macrophages (AAMθ) and regulatory B-cells (Bregs), which exert widespread immunomodulatory effects on both the innate and adaptive immune system (Maizels 2012, Valanparambil 2017, Hang 2019). The presence of these regulatory cell types in the knee joint during Hpb infection has yet to be determined. Additionally, the effects of Hpb infection on chronic AIA have also not been explored. Fortunately, the model used in this project has the potential to assess the effect of Hpb on arthritis flares with some minor adjustments, as described by W. B. Van Den Berg et al., 2007. It also has the ability to determine the effects of Hpb infection on AIA pain response.

Another obstacle encountered that is important to keep in mind is the fact that current available metabolome databases (such as KEGG) are currently lacking in helminth metabolome data, with no available Hpb database available to compare our metabolome to. The results of this study have only been compared against the KEGG Mus musculus (mouse) database. The methods used for this study also do not distinguish between host and parasite metabolomes. Additionally, it is worth mentioning here that the results, based on discriminatory analysis between naïve, PBS, AIA, and AIA+Hpb, are very preliminary, and that future studies on a larger cohort with targeted metabolomics are required to validate these findings.

Finally, helminth infection shifts the composition of intestinal bacteria affecting the gut microbiome, which influences arthritis susceptibility. The clinical consequences of these shifts in intestinal flora in relation to AIA are yet to be explored. While this goes beyond the scope of the current project, the microbiome interplay between Hpb and systemic immune response should be taken into consideration in future studies.

Future Applications. Throughout this project, the methodology was set for potential future projects aimed at assessing the effects of Hpb on AIA pathology score, neutrophil activation and neutrophil migration.

To determine the effects of Hpb infection on AIA pathology, the same experimental model should be followed, with immunization at day zero, Hpb infection seven days later, challenge with mBSA 14 days after immunization and necropsy 24 hours after challenge. Knees were collected for histology and pathology scoring, as seen in Lopes et al. 2020 [Appendix Supplementary Figure 5].

To assess how Hpb Excreted-secreted-products (ESP) affect neutrophil mechanisms *in vitro*, neutrophils were isolated from mice bone marrow (BM). As a pilot experiment, BM-neutrophils were cultured in the presence or absence of Urocanic acid (UCA), and a UCA and LPS dose response was tested to optimized concentrations. A similar approach can be used to test ESP. Lysates can then be assayed through ELISA or western blot and can be used to assess the direct effect of Hpb-ESP on neutrophil functions by assessing TNF production, TLR inhibition and neutrophil chemotaxis through glass agar plate chemotaxis (Appendix Methods *in vitro*).

Finally, the effect of Hpb infection on neutrophils migration can be assessed *in-vivo* through intravital microscopy of CXCL-1-induced knee inflammation. This method can also be used to assess whether Hpb infection affects other sites of inflammation and inflammatory stimuli by analyzing the effects of the infection on CXCL-1-induced cremaster inflammation. [Appendix Supplementary Figure 6].

8. Appendix

Metabolomic results

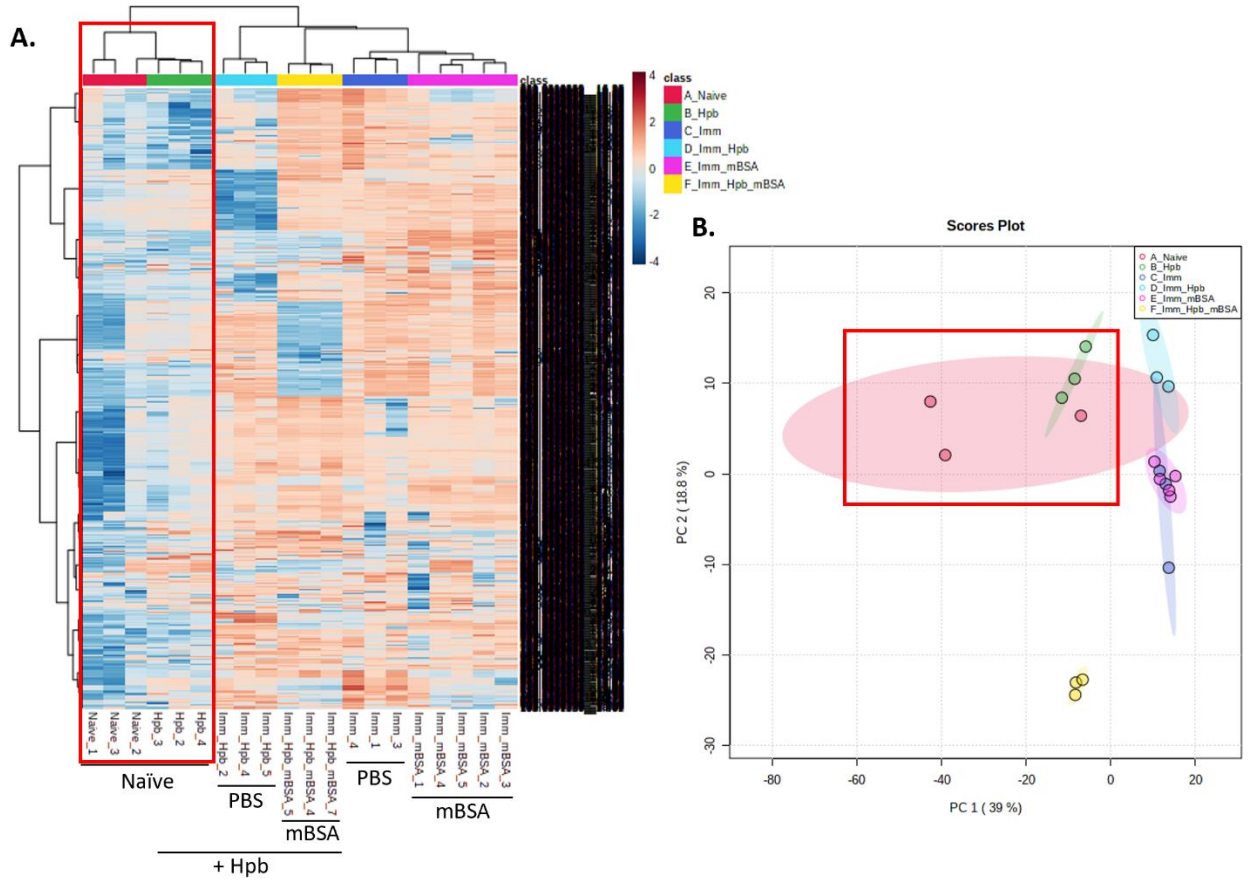

Supplementary Figure 1) Statistic analysis of all groups. (A) Heat map representation of metabolome from naïve, naïve+Hpb, PBS control [Imm], AIA [Imm_mBSA], AIA+Hpb [Imm_Hpb_mBSA], and control PBS Hpb [Imm_Hpb] groups. (B) Principal Component Analysis plot of all groups. The red squares indicate Naïve (non-immunized) groups. Red represents Naïve non-immunized controls, Green Hpb-infected non immunized controls, Dark blue PBS challenged samples, Clear blue PBS challenged-Hpb infected samples, Purple mBSA challenged (AIA) samples, and Yellow mBSA challenged-Hpb infected samples.

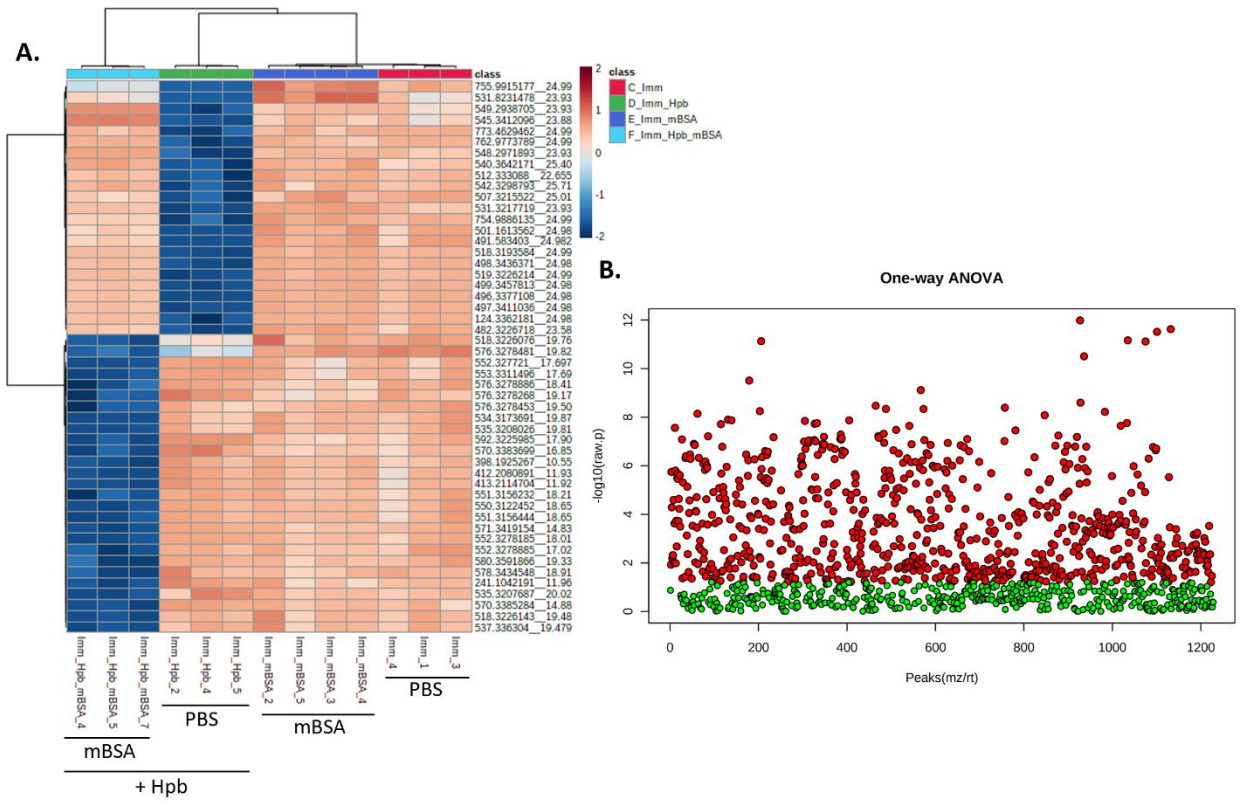

Supplementary Figure 2) Metabolomic characterization of Hpb infection on AIA. Serum untargeted metabolomic profiling of infected vs non-infected mice 24hr after challenge. (A) Heatmap representation of top 50 statistically significant metabolites from control, AIA, AIA+Hpb, and Control Hpb groups; (B) 763 features identified as most statistically significant (p>0.1). Red represents PBS control samples, Green PBS control-Hpb infected samples, Dark blue mBSA challenged (AIA) samples, and Clear blue mBSA challenged-Hpb infected samples.

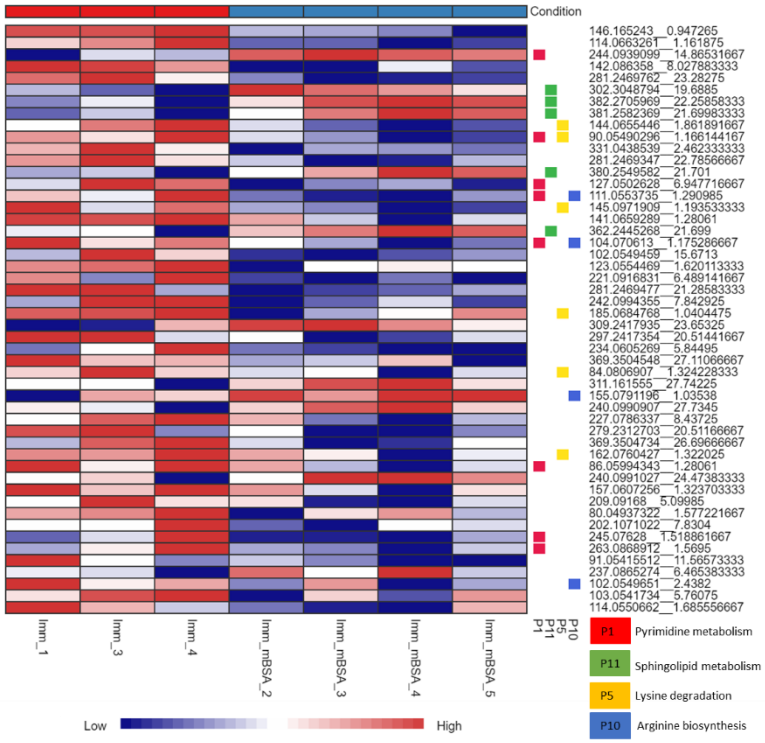

Supplementary Figure 3) Heatmap of enrichment pathway analysis of Ctl PBS vs AIA. Analyzed with MetaboAnalyst5.0.1

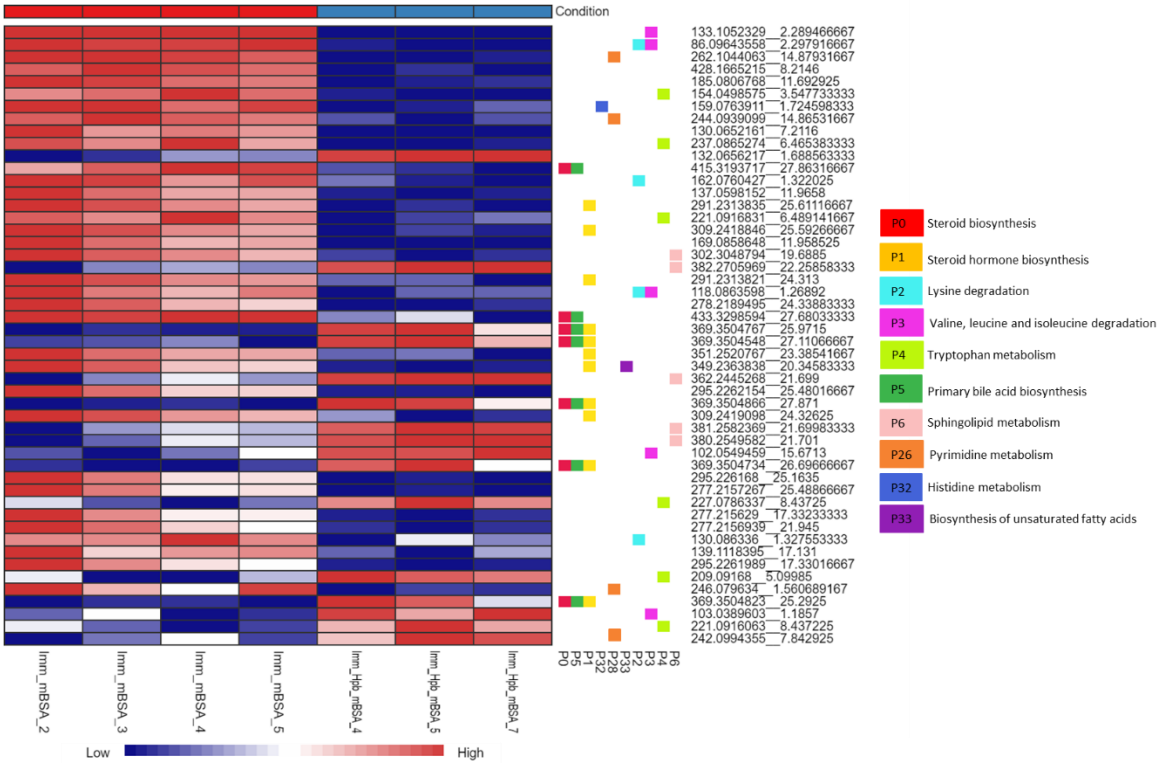

Supplementary Figure 4) Heatmap of enrichment pathway analysis of AIA vs Hpb-AIA. Analyzed with MetaboAnalyst5.0.1

Supplementary Table 1. Identified compounds of interest between AIA and AIA+Hpb

Query Mass	Matched Compound	Matched Form	Pathway	↑ or ↓ by Hpb	↑ or ↓ by AIA
244.0939	C00475	M+H[1+]	Pyrimidine metabolism	Downregulated	Upregulated
302.3049	C00836	M+H[1+]	Sphingolipid metabolism	Downregulated	Upregulated
123.0406	C01956	M+H[1+]	NA	Downregulated	Upregulated
382.2706	C01120	M+H[1+]	Sphingolipid metabolism	Upregulated	Upregulated
362.2445	C06124	M-H2O+H[1+]	Sphingolipid metabolism	Upregulated	Upregulated
381.2582	C06124	M(C13)+H[1+]	Sphingolipid metabolism	Upregulated	Upregulated
380.255	C06124	M+H[1+]	Sphingolipid metabolism	Upregulated	Upregulated
162.076	C00329	M-H2O+H[1+]	Lysine degradation	Downregulated	Downregulated

*Highlighted are features upregulated in AIA 24hrs after mBSA injection and downregulated (or inhibited) by Hpb infection (AIA+Hpb group).

9. Preliminary Future Work

Histologic Analysis (Pilot).

To determine the effect of Hpb infection on AIA pathology, the same experimental model used in Exp 3 was followed, with immunization at day zero, Hpb infection seven days later, challenge with mBSA 14 days after immunization, and necropsy 24 hours after challenge. Knees were collected for histology and pathology scoring as seen in Lopes et al. 2020. Mouse knee joints were removed and rinsed in PBS, then infused with 10% neutral buffered formalin in PBS.

After fixation, joints were incubated in Cal-Ex HCl decalcifying solution by serial immersions for 10 days (at 48 °C, with daily solution changes; Fisher Scientific, Ottawa, ON, Canada). Samples were then dehydrated and embedded in paraffin. 10-µm–thick sections will be sectioned onto superfrost slides, deparaffinized in xylene, rehydrated through graded ethanol solutions, and stained with hematoxylin and eosin. Blinded histopathological scoring of 4 parameters: synovial hypertrophy, mononuclear cell infiltration, cartilage destruction, and bone erosion will be performed. A 0–3-point scale is used for each variable, where 0 = normal, 1 = mild changes, 2 = moderate changes, and 3 = severe changes, which yielded a maximum damage score of 12 (Lopes et al., 2016).

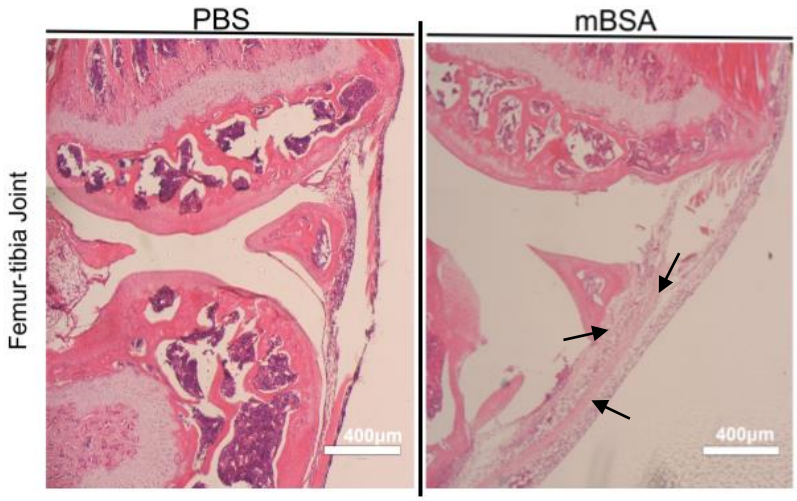

Supplementary Figure 5) Arthritis and cartilage damage in the knee joint 14 days post intra-articular mBSA injection. Representative histologic sections of knee joints from non-arthritic wild-type control mice (PBS) and from wild-type treated with mBSA (mBSA). Hematoxylin and eosin staining. Arrows show synovitis, joint space exudate and soft tissue inflammation.

Intravital microscopy (Pilot)

Animals. Wild-type male C57BL/6J mice aged 10–18 weeks were used for live microcirculation imaging of the cremaster and knee vasculature. Sample size will be increased in the future to ensure reproducibility and to allow for stringent statistical analysis.

Intravital preparation. Mice were anesthetized by intraperitoneal injection of 200 mg/kg of ketamine (Bayer Animal Health) and 10 mg/kg of xylazine (Bimeda-MTC). Anesthetic was maintained through timed intervals of intraperitoneal injections in a volume of 100 μL. After anesthesia, the left jugular vein was cannulated to permit the delivery of the fluorescence-labeled antibodies by intravenous administration: anti-mouse CD31 [PECAM1] Monoclonal Antibody PE-Cyanine7 (clone 390; identifies endothelial cells), Alexa-488– conjugated anti–mouse Ly-6G Antibody (identifies neutrophils). Both administered at a concentration of 0.5 mg/kg body weight. Neutrophil recruitment was induced by administration of CXCL1 directly to cremaster muscle (concentration in a volume of 100 μL).

The cremaster muscle was chosen as it is a thin muscular layer surrounding the testicles which is easily accessible with minor surgery. Due to its transparency, the blood vessels in the cremaster can be imaged using transmitted light(Secklehner, Lo Celso et al. 2017).. It can also be locally stimulated by exposure to fMLP or CXCL1 (KC) after exteriorization (Secklehner, Lo Celso et al. 2017). After cannulation, mice were placed on the cremaster imaging platform and firmly fixed with surgical tape. The upper skin of the scrotal sac was retracted with forceps and secured. After this procedure, the skin was prepared for exposure. The ventral surface of the pinned scrotal sac was incised, and the testicle placed back as to not cover the cremaster. Connective tissues between the scrotal skin and cremaster muscle were gently detached, and the separated scrotal skin was everted to avoid disturbing the cremaster muscle preparation. Finally, the cremaster muscle was gently spread on the silicone bed with thread. Before imaging, the prepared cremaster muscle was washed with 1x PBS in order to obtain a clear view and to keep it from drying. All intravital microscopy was performed using a Nikon A1R MP Confocal microscope equipped with a Plan Fluor X20 objective.

Reagents/Drugs. Ketamine (Bayer Animal Health) and 10 mg/kg of xylazine (Bimeda-MTC). Anti–mouse Ly-6G and anti-mouse CD31 [PECAM1] obtained from eBioscience.

Intravital Optimization

For intravital microscopy, the survival of mice had to be optimized. Initially the mouse survival rate was 1 hour, with just enough time for jugular vein cannulation surgery. We observed that when anesthesia was administered through the canula, the mice would rapidly fade. We also observed that the left jugular vein tends to be bigger, and that focusing from the start on cannulation of the left jugular vein made the cannulation procedure faster (~30min). Additionally, changing the anesthesia administration method to intraperitoneal (i. p.) injections of anesthesia at 40 minute intervals improved the survival rate, allowing for longer imaging times (the mice lasted, with no pain, under anesthesia for three to four hours). Initially, antibodies were administered before finding the desired field of view, but bleaching would rapidly occur. To decrease the bleaching of antibodies, we then first found the desired field of focus thorough bright-field and then administered the selected antibodies. We focused on areas with smaller vessels and slow flow, specifically where the venules-post-capillaries are located, since leukocytes leave vasculature only through these venules. For antibody selection, the cremaster muscle was used, as this was a faster surgical procedure to perform. Figure 12 is a representative image taken from the cremaster muscle after antibody and protocol optimization. In red, anti-mouse CD31 [PECAM1] was used to identify endothelial cells, and in green, anti–mouse Ly-6G was used to identify neutrophils. This pilot experiment was repeated on three male control-non-immunized mice, with neutrophil recruitment induced by CXCL-1 (KC) directly onto the cremaster. This procedure will allow the assessment of real-time neutrophil recruitment and will be used to investigate the effect of Hpb on cell recruitment in AIA mice.

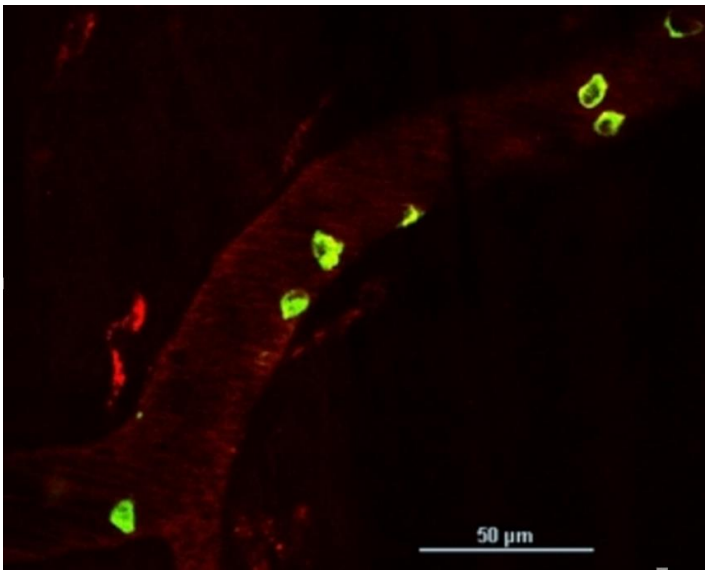

Supplementary Figure 6) CXCL-1-induced neutrophil recruitment in the cremaster muscle. Intravital microscopy was performed in the cremaster microcirculation of the mouse. Anti-mouse CD31 [PECAM1] Monoclonal Antibody (Red PE-Cyanine7; clone 390; identifies endothelial cells), Alexa-488– conjugated anti–mouse Ly-6G Antibody (Green; identifies neutrophils) were administered at a concentration of 0.5 mg/kg body weight.

Methods *in vitro:*

To assess how Hpb Excreted-secreted-products (ESP) affect neutrophil mechanisms in vitro, neutrophils were isolated from mouse bone marrow. To assess how UCA affects neutrophil mechanisms, neutrophils were isolated from mouse bone marrow (BM) and cultured in the presence or absence of UCA, and a UCA and LPS dose response was tested to optimized concentrations.

Helminth-Derived Metabolites. Helminth-derived excretory/secretory (HES) products were obtained as previously described (Valanparambil 2014). BALB/c mice were infected with 400-500 infective larvae (L3) of Heligmosomoides polygyrus bakeri (Hpb) for 21 days. Adult Hpb were collected from the small intestine and cultured in RPMI 1640 medium containing 2% w/v glucose, 80 mg/mL gentamicin, 100 U/mL penicillin/streptomycin and 20 mg/mL polymyxin B for 40 h at 37°C, 5% CO2. Supernatant was collected, centrifuged at 8000 ´ g for 10 min at 4°C and 0.2 mm filter sterilized.

Metabolites were isolated from proteins and exosomes using a 3 kDa MWCO centrifugation unit (UFC910024, Millipore) and centrifuged at 4000 ´ g for 40 min at 4°C. Helminth-derived metabolites were further fractionated using classical C18 column chromatography and nonpolar metabolites were eluted in acetonitrile at 100% v/v. The flow-through containing polar metabolites from the C18 column was further subjected to a universal polymeric reversed-phase sorbent containing column (WAT106202, Waters) and the polar metabolites were eluted using acetonitrile at 100% v/v. Polar and nonpolar metabolite stock fractions were concentrated using a speed vacuum concentrator and resuspended in ultrapure water and maintained at -20°C.

Preparation of neutrophils from bone marrow. To obtain BM, mice were necropsied and the femur and the tibia from both hind legs were removed and freed of soft tissue attachments, and the extreme distal tip of each extremity was cut off. Tibias and femurs were then placed in Mini tubes prepared with cut in bottom inside of collection tubes. Tubes were centrifuged (10 sec, 300 g, break 2, at 4°C). The cell suspension was resuspended in 52% Physiological Percoll and 1X PBS. The cells were then treated on a three-layer Percoll gradient of 72%, 64%, and 52% and centrifuged (2,600 rpm, 30 min, 6°C, acc 1, brk 0). The leucocytes from between the 64% and 72% interface and the upper part of the 72% layer were harvested, after carefully removing the cells from the upper phases. Cells were re-suspended in 14mL of 1X PBS and centrifuged

(15,000 rpm, 10 min, 6°C, acc 4, brk 4). Leucocytes were counted in a Neubauer chamber after staining with Turk's solution. Differential counts were obtained from cytospin preparations by evaluating the percentage of each leucocyte on a slide stained with May-Grünwald-Giemsa (Lopes, 2016).

TNF concentration and mechanisms. Neutrophils (1 X 10^6) were incubated in the presence or absence of LPS (1 μg/mL), UCA (200ug/mL, in DMSO) and DMSO. Neutrophils were divided into seven groups: (i) Neutrophils (ii) Neutrophils + DMSO, (iii) Neutrophils+ UCA, (iv) Neutrophils + UCA + DMSO, (v) Neutrophils + DMSO + LPS, (vi) Neutrophils + LPS and (vii) Neutrophils + UCA + LPS. To assess TNF concentration, the supernatants were collected after 24 hours, and protein levels were quantified using the Bradford method (Bio-Rad). TNF concentrations were measured by ELISA as per the manufacturer's instructions (R & D systems, Minneapolis, MN, USA).

Western Blot Analysis. For the western blot analysis, lysate preparations were prepared. A RIPA buffer was added to each sample based on sample protein concentrations. The Western blot was run through conventional methods. Samples were separated by electrophoresis on a denaturing 10–15% sodium dodecyl sulfate–polyacrylamide gel electrophoresis and transferred onto nitrocellulose membranes. Rainbow markers (Amersham Biosciences) were run in parallel to estimate molecular weights. Membranes were blocked for 1 h at room temperature with 5% BSA in TBS-T. After washing 3 X with TBS-T, 1° Ab solution [1:1000 dilution] was added and incubated at 4°C overnight. The next day, washing was repeated, and the membranes were incubated with horseradish peroxidase (HRP)-conjugated secondary antirabbit antibody [1:3,000]. Immunoreactive bands were visualized using an ECL detection system, according to the recommendations of the manufacturer (Amersham Biosciences). GAPDH was used as control, and Phospho TLR-4 was used for upstream analysis of TNF pathway.

ELISA Statistical analysis. Results are shown as the mean SEM. Difference among groups was evaluated by using ANOVA followed by Student-Newman-Keuls post hoc test. The level of significance was set at $P < 0.05$.

In-vitro Western Blot Statistical analysis. All results will be analyzed as the mean SEM. Normalized data analyzed by one-way analysis of variance, and differences between groups assessed using Student-Newman-Keuls posttest. P values less than 0.05 are considered significant.

10. Bibliography

Amu, S., S. P. Saunders, M. Kronenberg, N. E. Mangan, A. Atzberger and P. G. Fallon (2010). "Regulatory B cells prevent and reverse allergic airway inflammation via FoxP3-positive T regulatory cells in a murine model." J Allergy Clin Immunol **125**(5): 1114-1124.e1118.

Amulic, B., C. Cazalet, G. L. Hayes, K. D. Metzler and A. Zychlinsky (2012). "Neutrophil Function: From Mechanisms to Disease." Annual Review of Immunology **30**(1): 459-489.

Atkinson, S. M. and A. Nansen (2017). "Pharmacological Value of Murine Delayed-type Hypersensitivity Arthritis: A Robust Mouse Model of Rheumatoid Arthritis in C57BL/6 Mice." Basic Clin Pharmacol Toxicol **120**(2): 108-114.

Baddack, U., S. Hartmann, H. Bang, J. Grobe, C. Loddenkemper, M. Lipp and G. Muller (2013). "A chronic model of arthritis supported by a strain-specific periarticular lymph node in BALB/c mice." Nat Commun **4**: 1644.

Badolato, R. and J. J. Oppenheim (1996). "Role of cytokines, acute-phase proteins, and chemokines in the progression of rheumatoid arthritis." Semin Arthritis Rheum **26**(2): 526-538.

Barcelos, L. S., A. Talvani, A. S. Teixeira, G. D. Cassali, S. P. Andrade and M. M. Teixeira (2004). "Production and in vivo effects of chemokines CXCL1-3/KC and CCL2/JE in a model of inflammatory angiogenesis in mice." Inflamm Res **53**(10): 576-584.

Barlow, J. L., A. Bellosi, C. S. Hardman, L. F. Drynan, S. H. Wong, J. P. Cruickshank and A. N. McKenzie (2012). "Innate IL-13-producing nuocytes arise during allergic lung inflammation and contribute to airways hyperreactivity." J Allergy Clin Immunol **129**(1): 191-198.e191-194.

Barron, L. and T. A. Wynn (2011). "Macrophage activation governs schistosomiasis-induced inflammation and fibrosis." European Journal of Immunology **41**(9): 2509-2514.

Bas, D. B., J. Su, G. Wigerblad and C. I. Svensson (2016). "Pain in rheumatoid arthritis: models and mechanisms." Pain Manag **6**(3): 265-284.

Bashir, M. E., P. Andersen, I. J. Fuss, H. N. Shi and C. Nagler-Anderson (2002). "An enteric helminth infection protects against an allergic response to dietary antigen." J Immunol **169**(6): 3284-3292.

Becker, S., J. Quay, H. S. Koren and J. S. Haskill (1994). "Constitutive and stimulated MCP-1, GRO alpha, beta, and gamma expression in human airway epithelium and bronchoalveolar macrophages." American Journal of Physiology-Lung Cellular and Molecular Physiology **266**(3): L278-L286.

Behnke, J. M., D. M. Menge and H. Noyes (2009). "Heligmosomoides bakeri: a model for exploring the biology and genetics of resistance to chronic gastrointestinal nematode infections." Parasitology **136**(12): 1565-1580.

Bendele, A., J. McComb, T. Gould, T. McAbee, G. Sennello, E. Chlipala and M. Guy (1999). "Animal models of arthritis: relevance to human disease." Toxicol Pathol **27**(1): 134-142.

Bjorner, M. and L. Zhu (2019). "A minimally invasive, low-stress method for serial blood collection in aging mice." Pathobiol Aging Age Relat Dis **9**(1): 1647400.

Blum, A. M., L. Hang, T. Setiawan, J. P. Urban, Jr., K. M. Stoyanoff, J. Leung and J. V. Weinstock (2012). "Heligmosomoides polygyrus bakeri induces tolerogenic dendritic cells that block colitis and prevent antigen-specific gut T cell responses." J Immunol **189**(5): 2512-2520.

Brackertz, D., G. F. Mitchell and I. R. Mackay (1977). "Antigen-induced arthritis in mice. I. Induction of arthritis in various strains of mice." Arthritis Rheum **20**(3): 841-850.

Brüstle, A., S. Heink, M. Huber, C. Rosenplänter, C. Stadelmann, P. Yu, E. Arpaia, T. W. Mak, T. Kamradt and M. Lohoff (2007). "The development of inflammatory T(H)-17 cells requires interferon-regulatory factor 4." Nat Immunol **8**(9): 958-966.

Buck, A. H., G. Coakley, F. Simbari, H. J. McSorley, J. F. Quintana, T. Le Bihan, S. Kumar, C. Abreu-Goodger, M. Lear, Y. Harcus, A. Ceroni, S. A. Babayan, M. Blaxter, A. Ivens and R. M. Maizels (2014). "Exosomes secreted by nematode parasites transfer small RNAs to mammalian cells and modulate innate immunity." Nat Commun **5**: 5488.

Bueding, E. (1950). "Carbohydrate metabolism of schistosoma mansoni." J Gen Physiol **33**(5): 475-495.
Bullock, J., S. A. A. Rizvi, A. M. Saleh, S. S. Ahmed, D. P. Do, R. A. Ansari and J. Ahmed (2018). "Rheumatoid Arthritis: A Brief Overview of the Treatment." Med Princ Pract **27**(6): 501-507.
Cairns, E., S. Saunders, D. A. Bell, G. Blackler, P. Lac and L. Barra (2020). "The effect of sex on immune responses to a homocitrullinated peptide in the DR4-transgenic mouse model of Rheumatoid Arthritis." J Transl Autoimmun **3**: 100053.
Camberis, M., G. Le Gros and J. Urban, Jr. (2003). "Animal model of Nippostrongylus brasiliensis and Heligmosomoides polygyrus." Curr Protoc Immunol **Chapter 19**: Unit 19.12.
Camelo, A., J. L. Barlow, L. F. Drynan, D. R. Neill, S. J. Ballantyne, S. H. Wong, R. Pannell, W. Gao, K. Wrigley, J. Sprenkle and A. N. McKenzie (2012). "Blocking IL-25 signalling protects against gut inflammation in a type-2 model of colitis by suppressing nuocyte and NKT derived IL-13." J Gastroenterol **47**(11): 1198-1211.
Cascão, R., R. A. Moura, I. Perpétuo, H. Canhão, E. Vieira-Sousa, A. F. Mourão, A. M. Rodrigues, J. Polido-Pereira, M. V. Queiroz, H. S. Rosário, M. M. Souto-Carneiro, L. Graca and J. E. Fonseca (2010). "Identification of a cytokine network sustaining neutrophil and Th17 activation in untreated early rheumatoid arthritis." Arthritis Res Ther **12**(5): R196.
Castañeda-Lopez, M. E., I. Garza-Veloz, J. M. Ortiz-Rodriguez, R. Castañeda-Miranda, L. O. Solis-Sanchez, H. R. Vega-Carrillo, M. d. R. Martinez-Blanco, F. Trejo-Vazquez, G. Ornelas-Vargas, I. P. Rodriguez-Sanchez, H. A. Guerrero-Osuna, I. Delgado-Enciso, O. G. Meza-Zavala and M. d. l. L. Martinez-Fierro (2018). Animal Models of Rheumatoid Arthritis. Experimental Animal Models of Human Diseases - An Effective Therapeutic Strategy.
Catrina, A., A. Krishnamurthy and B. Rethi (2021). "Current view on the pathogenic role of anti-citrullinated protein antibodies in rheumatoid arthritis." RMD Open **7**(1).
Cecchi, I., I. Arias de la Rosa, E. Menegatti, D. Roccatello, E. Collantes-Estevez, C. Lopez-Pedrera and N. Barbarroja (2018). "Neutrophils: Novel key players in Rheumatoid Arthritis. Current and future therapeutic targets." Autoimmun Rev **17**(11): 1138-1149.
Chen, Z., D. Andreev, K. Oeser, B. Krljanac, A. Hueber, A. Kleyer, D. Voehringer, G. Schett and A. Bozec (2016). "Th2 and eosinophil responses suppress inflammatory arthritis." Nat Commun **7**: 11596.
Choi, S. and K. H. Lee (2018). "Clinical management of seronegative and seropositive rheumatoid arthritis: A comparative study." PLoS One **13**(4): e0195550.
Choi, S. and A. J. Snider (2015). "Sphingolipids in High Fat Diet and Obesity-Related Diseases." Mediators Inflamm **2015**: 520618.
Ciurtin, C., V. M. Cojocaru, I. M. Miron, F. Preda, M. Milicescu, M. Bojincă, O. Costan, A. Nicolescu, C. Deleanu, E. Kovàcs and V. Stoica (2006). "Correlation between different components of synovial fluid and pathogenesis of rheumatic diseases." Rom J Intern Med **44**(2): 171-181.
Clasquin, M. F., E. Melamud and J. D. Rabinowitz (2012). "LC-MS data processing with MAVEN: a metabolomic analysis and visualization engine." Curr Protoc Bioinformatics **Chapter 14**: Unit14.11.
Classon, C. H., M. Li, A. L. Clavero, J. Ma, X. Feng, C. A. Tibbitt, J. M. Stark, R. Cardoso, E. Ringqvist, L. Boon, E. J. Villablanca, A. G. Rothfuchs, L. Eidsmo, J. M. Coquet and S. Nylen (2022). "Intestinal helminth infection transforms the CD4(+) T cell composition of the skin." Mucosal Immunol **15**(2): 257-267.
Coakley, G., J. L. McCaskill, J. G. Borger, F. Simbari, E. Robertson, M. Millar, Y. Harcus, H. J. McSorley, R. M. Maizels and A. H. Buck (2017). "Extracellular Vesicles from a Helminth Parasite Suppress Macrophage Activation and Constitute an Effective Vaccine for Protective Immunity." Cell Rep **19**(8): 1545-1557.
Coelho, F. M., V. Pinho, F. A. Amaral, D. Sachs, V. V. Costa, D. H. Rodrigues, A. T. Vieira, T. A. Silva, D. G. Souza, R. Bertini, A. L. Teixeira and M. M. Teixeira (2008). "The chemokine receptors CXCR1/CXCR2 modulate antigen-induced arthritis by regulating adhesion of neutrophils to the synovial microvasculature." Arthritis Rheum **58**(8): 2329-2337.

Cooke, T. D., S. Richer, E. Hurd and H. E. Jasin (1975). "Localization of antigen-antibody complexes in intraarticular collagenous tissues." Ann N Y Acad Sci **256**: 10-24.
Cooper, P. J. (2009). "Interactions between helminth parasites and allergy." Curr Opin Allergy Clin Immunol **9**(1): 29-37.
Correale, J. and M. Farez (2007). "Association between parasite infection and immune responses in multiple sclerosis." Ann Neurol **61**(2): 97-108.
Cross, A., T. Barnes, R. C. Bucknall, S. W. Edwards and R. J. Moots (2006). "Neutrophil apoptosis in rheumatoid arthritis is regulated by local oxygen tensions within joints." J Leukoc Biol **80**(3): 521-528.
Cunha, T. M., M. M. Barsante, A. T. Guerrero, W. A. Verri, Jr., S. H. Ferreira, F. M. Coelho, R. Bertini, C. Di Giacinto, M. Allegretti, F. Q. Cunha and M. M. Teixeira (2008). "Treatment with DF 2162, a non-competitive allosteric inhibitor of CXCR1/2, diminishes neutrophil influx and inflammatory hypernociception in mice." Br J Pharmacol **154**(2): 460-470.
Cunha, T. M., W. A. Verri, Jr., G. G. Vivancos, I. F. Moreira, S. Reis, C. A. Parada, F. Q. Cunha and S. H. Ferreira (2004). "An electronic pressure-meter nociception paw test for mice." Braz J Med Biol Res **37**(3): 401-407.
DiNardo, A. R., T. Nishiguchi, E. M. Mace, K. Rajapakshe, G. Mtetwa, A. Kay, G. Maphalala, W. E. Secor, R. Mejia, J. S. Orange, C. Coarfa, K. N. Bhalla, E. A. Graviss, A. M. Mandalakas and G. Makedonas (2018). "Schistosomiasis Induces Persistent DNA Methylation and Tuberculosis-Specific Immune Changes." J Immunol **201**(1): 124-133.
Donskow-Łysoniewska, K., K. Krawczak and M. Doligalska (2012). "Heligmosomoides polygyrus: EAE remission is correlated with different systemic cytokine profiles provoked by L4 and adult nematodes." Experimental parasitology **132 2**: 243-248.
Donskow-Łysoniewska, K., P. Majewski, K. BRODACZEWSKA, K. JÓŹWICKA and M. DOLIGALSKA (2012). "Heligmosmoides polygyrus fourth stages induce protection against DSS-induced colitis and change opioid expression in the intestine." Parasite Immunology **34**(11): 536-546.
Doonan, J., F. E. Lumb, M. A. Pineda, A. Tarafdar, J. Crowe, A. M. Khan, C. J. Suckling, M. M. Harnett and W. Harnett (2018). "Protection Against Arthritis by the Parasitic Worm Product ES-62, and Its Drug-Like Small Molecule Analogues, Is Associated With Inhibition of Osteoclastogenesis." Front Immunol **9**: 1016.
Dunn, W. B., A. Erban, R. J. M. Weber, D. J. Creek, M. Brown, R. Breitling, T. Hankemeier, R. Goodacre, S. Neumann, J. Kopka and M. R. Viant (2013). "Mass appeal: metabolite identification in mass spectrometry-focused untargeted metabolomics." Metabolomics **9**(S1): 44-66.
Eiserich, J. P., S. Baldus, M.-L. Brennan, W. Ma, C. Zhang, A. Tousson, L. Castro, A. J. Lusis, W. M. Nauseef, C. R. White and B. A. Freeman (2002). "Myeloperoxidase, a Leukocyte-Derived Vascular NO Oxidase." Science **296**(5577): 2391-2394.
Elliott, D. E., T. Setiawan, A. Metwali, A. Blum, J. F. Urban, Jr. and J. V. Weinstock (2004). "Heligmosomoides polygyrus inhibits established colitis in IL-10-deficient mice." Eur J Immunol **34**(10): 2690-2698.
Feldmann, M., F. M. Brennan and R. N. Maini (1996). "Rheumatoid arthritis." Cell **85**(3): 307-310.
Filbey, K. J., J. R. Grainger, K. A. Smith, L. Boon, N. van Rooijen, Y. Harcus, S. Jenkins, J. P. Hewitson and R. M. Maizels (2014). "Innate and adaptive type 2 immune cell responses in genetically controlled resistance to intestinal helminth infection." Immunol Cell Biol **92**(5): 436-448.
Filbey, K. J., P. H. Mehta, K. J. Meijlink, C. Pellefigues, A. J. Schmidt and G. Le Gros (2020). "The Gastrointestinal Helminth Heligmosomoides bakeri Suppresses Inflammation in a Model of Contact Hypersensitivity." Front Immunol **11**: 950.
Finkelman, F. D., T. Shea-Donohue, J. Goldhill, C. A. Sullivan, S. C. Morris, K. B. Madden, W. C. Gause and J. F. Urban, Jr. (1997). "Cytokine regulation of host defense against parasitic

gastrointestinal nematodes: lessons from studies with rodent models." Annu Rev Immunol **15**: 505-533.
Fleming, J. O. (2013). "Helminth therapy and multiple sclerosis." Int J Parasitol **43**(3-4): 259-274.
Förger, F., N. Marcoli, S. Gadola, B. Möller, P. M. Villiger and M. Østensen (2008). "Pregnancy induces numerical and functional changes of CD4+CD25 high regulatory T cells in patients with rheumatoid arthritis." Ann Rheum Dis **67**(7): 984-990.
Fox, J. G., P. Beck, C. A. Dangler, M. T. Whary, T. C. Wang, H. N. Shi and C. Nagler-Anderson (2000). "Concurrent enteric helminth infection modulates inflammation and gastric immune responses and reduces helicobacter-induced gastric atrophy." Nat Med **6**(5): 536-542.
Frederique Ponchel, E. V., Sarah R Kingsbury & and Y. M. El-Sherbiny (2012). "CD4+ T-cell subsets in rheumatoid arthrit." International Journal of Clinical Rheumatology **7(1)**: 37–53
Gause, W. C., J. F. Urban, Jr. and M. J. Stadecker (2003). "The immune response to parasitic helminths: insights from murine models." Trends Immunol **24**(5): 269-277.
Goldenberg, M. M. (1999). "Leflunomide, a novel immunomodulator for the treatment of active rheumatoid arthritis." Clin Ther **21**(11): 1837-1852; discussion 1821.
Gonçalves, W. A., B. M. Rezende, M. P. E. d. Oliveira, L. S. Ribeiro, V. Fattori, W. N. d. Silva, P. H. D. M. Prazeres, C. M. Queiroz-Junior, K. T. d. O. Santana, W. C. Costa, V. A. Beltrami, V. V. Costa, A. Birbrair, W. A. Verri, F. Lopes, T. M. Cunha, M. M. Teixeira, F. A. Amaral and V. Pinho (2020). "Sensory Ganglia-Specific TNF Expression Is Associated With Persistent Nociception After Resolution of Inflammation." Frontiers in Immunology **10**: 3120.
Gorlino, C. V., M. N. Dave, R. Blas, M. I. Crespo, A. Lavanchy, H. Tamashiro, R. Pardo-Hildalgo, M. C. Pistoresi-Palencia and M. S. Di Genaro (2018). "Association between levels of synovial anti-citrullinated peptide antibodies and neutrophil response in patients with rheumatoid arthritis." Eur J Immunol **48**(9): 1563-1572.
Gosselt, H. R., I. B. Muller, G. Jansen, M. van Weeghel, F. M. Vaz, J. M. W. Hazes, S. G. Heil and R. de Jonge (2020). "Identification of Metabolic Biomarkers in Relation to Methotrexate Response in Early Rheumatoid Arthritis." Journal of Personalized Medicine **10**(4): 271.
Grainger, J. R., K. A. Smith, J. P. Hewitson, H. J. McSorley, Y. Harcus, K. J. Filbey, C. A. Finney, E. J. Greenwood, D. P. Knox, M. S. Wilson, Y. Belkaid, A. Y. Rudensky and R. M. Maizels (2010). "Helminth secretions induce de novo T cell Foxp3 expression and regulatory function through the TGF-β pathway." J Exp Med **207**(11): 2331-2341.
Hang, L., A. M. Blum, T. Setiawan, J. P. Urban, Jr., K. M. Stoyanoff and J. V. Weinstock (2013). "Heligmosomoides polygyrus bakeri infection activates colonic Foxp3+ T cells enhancing their capacity to prevent colitis." J Immunol **191**(4): 1927-1934.
Hang, L., S. Kumar, A. M. Blum, J. F. Urban, Jr., M. C. Fantini and J. V. Weinstock (2019). "Heligmosomoides polygyrus bakeri Infection Decreases Smad7 Expression in Intestinal CD4(+) T Cells, Which Allows TGF-beta to Induce IL-10-Producing Regulatory T Cells That Block Colitis." J Immunol **202**(8): 2473-2481.
Hang, L., T. Setiawan, A. M. Blum, J. Urban, K. Stoyanoff, S. Arihiro, H. C. Reinecker and J. V. Weinstock (2010). "Heligmosomoides polygyrus infection can inhibit colitis through direct interaction with innate immunity." J Immunol **185**(6): 3184-3189.
Hansen, T. V. A., M. Hansen, P. Nejsum, H. Mejer, M. Denwood and S. M. Thamsborg (2016). "Glucose Absorption by the Bacillary Band of Trichuris muris." PLOS Neglected Tropical Diseases **10**(9): e0004971.
Hayter, S. M. and M. C. Cook (2012). "Updated assessment of the prevalence, spectrum and case definition of autoimmune disease." Autoimmun Rev **11**(10): 754-765.
Heidari, B. (2011). "Rheumatoid Arthritis: Early diagnosis and treatment outcomes." Caspian J Intern Med **2**(1): 161-170.
Hensel, J. A., V. Khattar, R. Ashton and S. Ponnazhagan (2019). "Characterization of immune cell subtypes in three commonly used mouse strains reveals gender and strain-specific variations." Lab Invest **99**(1): 93-106.

Herrmann, M. L., R. Schleyerbach and B. J. Kirschbaum (2000). "Leflunomide: an immunomodulatory drug for the treatment of rheumatoid arthritis and other autoimmune diseases." Immunopharmacology **47**(2-3): 273-289.

Hewitson, J. P., Y. Harcus, J. Murray, M. van Agtmaal, K. J. Filbey, J. R. Grainger, S. Bridgett, M. L. Blaxter, P. D. Ashton, D. A. Ashford, R. S. Curwen, R. A. Wilson, A. A. Dowle and R. M. Maizels (2011). "Proteomic analysis of secretory products from the model gastrointestinal nematode Heligmosomoides polygyrus reveals dominance of Venom Allergen-Like (VAL) proteins." Journal of Proteomics **74**(9): 1573-1594.

Hiemstra, I. H., E. J. Klaver, K. Vrijland, H. Kringel, A. Andreasen, G. Bouma, G. Kraal, I. van Die and J. M. M. den Haan (2014). "Excreted/secreted Trichuris suis products reduce barrier function and suppress inflammatory cytokine production of intestinal epithelial cells." Molecular Immunology **60**(1): 1-7.

Houlden, A., K. S. Hayes, A. J. Bancroft, J. J. Worthington, P. Wang, R. K. Grencis and I. S. Roberts (2015). "Chronic Trichuris muris Infection in C57BL/6 Mice Causes Significant Changes in Host Microbiota and Metabolome: Effects Reversed by Pathogen Clearance." PLOS ONE **10**(5): e0125945.

Hübner, M. P., Y. Shi, M. N. Torrero, E. Mueller, D. Larson, K. Soloviova, F. Gondorf, A. Hoerauf, K. E. Killoran, J. T. Stocker, S. J. Davies, K. V. Tarbell and E. Mitre (2012). "Helminth protection against autoimmune diabetes in nonobese diabetic mice is independent of a type 2 immune shift and requires TGF-β." J Immunol **188**(2): 559-568.

Hur, B., V. K. Gupta, H. Huang, K. A. Wright, K. J. Warrington, V. Taneja, J. M. Davis, 3rd and J. Sung (2021). "Plasma metabolomic profiling in patients with rheumatoid arthritis identifies biochemical features predictive of quantitative disease activity." Arthritis Res Ther **23**(1): 164.

Irmler, I. M., M. Gajda and R. Brauer (2007). "Exacerbation of antigen-induced arthritis in IFN-gamma-deficient mice as a result of unrestricted IL-17 response." J Immunol **179**(9): 6228-6236.

Jacobsson, L. T., C. Turesson, J. A. Nilsson, I. F. Petersson, E. Lindqvist, T. Saxne and P. Geborek (2007). "Treatment with TNF blockers and mortality risk in patients with rheumatoid arthritis." Ann Rheum Dis **66**(5): 670-675.

Jang, S. W., M. K. Cho, M. K. Park, S. A. Kang, B. K. Na, S. C. Ahn, D. H. Kim and H. S. Yu (2011). "Parasitic helminth cystatin inhibits DSS-induced intestinal inflammation via IL-10(+)F4/80(+) macrophage recruitment." Korean J Parasitol **49**(3): 245-254.

Janneh, A. H. and B. Ogretmen (2022). "Targeting Sphingolipid Metabolism as a Therapeutic Strategy in Cancer Treatment." Cancers **14**(9): 2183.

Johnston, C. J., E. Robertson, Y. Harcus, J. R. Grainger, G. Coakley, D. J. Smyth, H. J. McSorley and R. Maizels (2015). "Cultivation of Heligmosomoides polygyrus: an immunomodulatory nematode parasite and its secreted products." J Vis Exp(98): e52412.

Johnston, C. J. C., D. J. Smyth, R. B. Kodali, M. P. J. White, Y. Harcus, K. J. Filbey, J. P. Hewitson, C. S. Hinck, A. Ivens, A. M. Kemter, A. O. Kildemoes, T. Le Bihan, D. C. Soares, S. M. Anderton, T. Brenn, S. J. Wigmore, H. V. Woodcock, R. C. Chambers, A. P. Hinck, H. J. McSorley and R. M. Maizels (2017). "A structurally distinct TGF-β mimic from an intestinal helminth parasite potently induces regulatory T cells." Nat Commun **8**(1): 1741.

Johnston, M. J., A. Wang, M. E. Catarino, L. Ball, V. C. Phan, J. A. MacDonald and D. M. McKay (2010). "Extracts of the rat tapeworm, Hymenolepis diminuta, suppress macrophage activation in vitro and alleviate chemically induced colitis in mice." Infect Immun **78**(3): 1364-1375.

Kagari, T., H. Doi and T. Shimozato (2002). "The Importance of IL-1β and TNF-α, and the Noninvolvement of IL-6, in the Development of Monoclonal Antibody-Induced Arthritis." The Journal of Immunology **169**(3): 1459-1466.

Kahnert, A., P. Seiler, M. Stein, S. Bandermann, K. Hahnke, H.-J. Mollenkopf and S. H. E. Kaufmann (2006). "Alternative activation deprives macrophages of a coordinated defense program to Mycobacterium tuberculosis." European Journal of Immunology **36**.

Kasman N, P. J., Mamdani M, Badley E. Badley E, Glazier R. (2004). "Arthritis and related conditions in Ontario ICES Atlas." Toronto, ON: Institute for Clinical Evaluative Sciences (ICES) **2 nd ed**.

Kidd, B. L., R. M. Langford and T. Wodehouse (2007). "Arthritis and pain. Current approaches in the treatment of arthritic pain." Arthritis Res Ther **9**(3): 214.

Kitagaki, K., T. R. Businga, D. Racila, D. E. Elliott, J. V. Weinstock and J. N. Kline (2006). "Intestinal helminths protect in a murine model of asthma." J Immunol **177**(3): 1628-1635.

Klinke, A., C. Nussbaum, L. Kubala, K. Friedrichs, T. K. Rudolph, V. Rudolph, H.-J. Paust, C. Schröder, D. Benten, D. Lau, K. Szocs, P. G. Furtmüller, P. Heeringa, K. Sydow, H.-J. Duchstein, H. Ehmke, U. Schumacher, T. Meinertz, M. Sperandio and S. Baldus (2011). "Myeloperoxidase attracts neutrophils by physical forces." Blood **117**(4): 1350-1358.

Kobayashi, S. D. and F. R. Deleo (2009). "Role of neutrophils in innate immunity: a systems biology-level approach." WIREs Systems Biology and Medicine **1**(3): 309-333.

Kokova, D. and O. A. Mayboroda (2019). "Twenty Years on: Metabolomics in Helminth Research." Trends Parasitol **35**(4): 282-288.

Krock, E., A. Jurczak and C. I. Svensson (2018). "Pain pathogenesis in rheumatoid arthritis-what have we learned from animal models?" Pain **159 Suppl 1**: S98-S109.

LaBeaud, A. D., I. Malhotra, M. King, C. L. King and C. H. King (2009). "Do Antenatal Parasite Infections Devalue Childhood Vaccination?" PLoS Neglected Tropical Diseases **3**.

Lai, W. Q., A. W. Irwan, H. H. Goh, H. S. Howe, D. T. Yu, R. Valle-Oñate, I. B. McInnes, A. J. Melendez and B. P. Leung (2008). "Anti-inflammatory effects of sphingosine kinase modulation in inflammatory arthritis." J Immunol **181**(11): 8010-8017.

Li, J., N. Che, L. Xu, Q. Zhang, Q. Wang, W. Tan and M. Zhang (2018). "LC-MS-based serum metabolomics reveals a distinctive signature in patients with rheumatoid arthritis." Clin Rheumatol **37**(6): 1493-1502.

Li, R., Y. Ma, J. Hong and Y. Ding (2022). "Nanoengineered therapy aiming at the etiology of rheumatoid arthritis." Nano Today **42**.

Liu, L., J. Jia, M. Jiang, X. Liu, C. Dai, B. L. Wise, N. E. Lane and W. Yao (2020). "High susceptibility to collagen-induced arthritis in mice with progesterone receptors selectively inhibited in osteoprogenitor cells." Arthritis Res Ther **22**(1): 165.

Liu, Q., K. Sundar, P. K. Mishra, G. Mousavi, Z. Liu, A. Gaydo, F. Alem, D. Lagunoff, D. Bleich and W. C. Gause (2009). "Helminth infection can reduce insulitis and type 1 diabetes through CD25- and IL-10-independent mechanisms." Infect Immun **77**(12): 5347-5358.

Logan, J., S. Navarro, A. Loukas and P. Giacomin (2018). "Helminth-induced regulatory T cells and suppression of allergic responses." Curr Opin Immunol **54**: 1-6.

Lopes, F., F. M. Coelho, V. V. Costa, E. L. Vieira, L. P. Sousa, T. A. Silva, L. Q. Vieira, M. M. Teixeira and V. Pinho (2011). "Resolution of neutrophilic inflammation by H2O2 in antigen-induced arthritis." Arthritis Rheum **63**(9): 2651-2660.

Lopes, F., R. Graepel, J. L. Reyes, A. Wang, B. Petri, J. J. McDougall, K. A. Sharkey and D. M. McKay (2016). "Involvement of Mast Cells in alpha7 Nicotinic Receptor Agonist Exacerbation of Freund's Complete Adjuvant-Induced Monoarthritis in Mice." Arthritis Rheumatol **68**(2): 542-552.

Lopes, F., C. Matisz, J. L. Reyes, H. Jijon, A. Al-Darmaki, G. G. Kaplan and D. M. McKay (2016). "Helminth Regulation of Immunity: A Three-pronged Approach to Treat Colitis." Inflamm Bowel Dis **22**(10): 2499-2512.

Lopes, F., F. A. Vicentini, N. L. Cluny, A. J. Mathews, B. H. Lee, W. A. Almishri, L. Griffin, W. Goncalves, V. Pinho, D. M. McKay, S. A. Hirota, M. G. Swain, Q. J. Pittman and K. A. Sharkey (2020). "Brain TNF drives post-inflammation depression-like behavior and persistent pain in experimental arthritis." Brain Behav Immun **89**: 224-232.

Luckheeram, R. V., R. Zhou, A. D. Verma and B. Xia (2012). "CD4⁺T Cells: Differentiation and Functions." Clinical and Developmental Immunology **2012**: 1-12.

Ma, K., L. Yang, R. Shen, B. Kong, W. Chen, J. Liang, G. Tang and B. Zhang (2018). "Th17 cells regulate the production of CXCL1 in breast cancer." International Immunopharmacology **56**: 320-329.
Machado-Vieira, R., G. Salvadore, N. DiazGranados, L. Ibrahim, D. Latov, C. Wheeler-Castillo, J. Baumann, I. D. Henter and C. A. Zarate, Jr. (2010). "New therapeutic targets for mood disorders." ScientificWorldJournal **10**: 713-726.
Maizels, R. M. (2020). "Regulation of immunity and allergy by helminth parasites." Allergy **75**(3): 524-534.
Maizels, R. M., J. P. Hewitson, J. Murray, Y. M. Harcus, B. Dayer, K. J. Filbey, J. R. Grainger, H. J. McSorley, L. A. Reynolds and K. A. Smith (2012). "Immune modulation and modulators in Heligmosomoides polygyrus infection." Exp Parasitol **132**(1): 76-89.
Maizels, R. M., H. H. Smits and H. J. McSorley (2018). "Modulation of Host Immunity by Helminths: The Expanding Repertoire of Parasite Effector Molecules." Immunity **49**(5): 801-818.
Malmström, V., A. I. Catrina and L. Klareskog (2017). "The immunopathogenesis of seropositive rheumatoid arthritis: from triggering to targeting." Nat Rev Immunol **17**(1): 60-75.
Mangan, N. E., N. van Rooijen, A. N. McKenzie and P. G. Fallon (2006). "Helminth-modified pulmonary immune response protects mice from allergen-induced airway hyperresponsiveness." J Immunol **176**(1): 138-147.
Mark Ritchie and Mainak Mal (2012). "UPLC BEH HILIC: The Preferred Separation

Chemistry for Targeted Analysis of

Phospholipids."
Maruszewska-Cheruiyot, M., K. Donskow-Lysoniewska, K. Piechna, K. Krawczak and M. Doligalska (2019). "L4 stage Heligmosomoides polygyrus prevents the maturation of dendritic JAWS II cells." Exp Parasitol **196**: 12-21.
Maruszewska-Cheruiyot, M., L. Szewczak, K. Krawczak-Wojcik, M. Glaczynska and K. Donskow-Lysoniewska (2021). "The production of excretory-secretory molecules from Heligmosomoides polygyrus bakeri fourth stage larvae varies between mixed and single sex cultures." Parasit Vectors **14**(1): 106.
Mauri, C., R. O. Williams, M. Walmsley and M. Feldmann (1996). "Relationship between Th1/Th2 cytokine patterns and the arthritogenic response in collagen-induced arthritis." Eur J Immunol **26**(7): 1511-1518.
McSorley, H. J. and R. M. Maizels (2012). "Helminth infections and host immune regulation." Clin Microbiol Rev **25**(4): 585-608.
Metwali, A., T. Setiawan, A. M. Blum, J. Urban, D. E. Elliott, L. Hang and J. V. Weinstock (2006). "Induction of CD8+ regulatory T cells in the intestine by Heligmosomoides polygyrus infection." Am J Physiol Gastrointest Liver Physiol **291**(2): G253-259.
Michla, M. and C. Wilhelm (2022). "Food for thought – ILC metabolism in the context of helminth infections." Mucosal Immunology.
Mittal, M., M. R. Siddiqui, K. Tran, S. P. Reddy and A. B. Malik (2014). "Reactive Oxygen Species in Inflammation and Tissue Injury." Antioxidants & Redox Signaling **20**(7): 1126-1167.
Monroy, F. G. and F. J. Enriquez (1992). "Heligmosomoides polygyrus: a model for chronic gastrointestinal helminthiasis." Parasitol Today **8**(2): 49-54.
Moreno, Y., P. P. Gros, M. Tam, M. Segura, R. Valanparambil, T. G. Geary and M. M. Stevenson (2011). "Proteomic analysis of excretory-secretory products of Heligmosomoides polygyrus assessed with next-generation sequencing transcriptomic information." PLoS Negl Trop Dis **5**(10): e1370.
Morimoto, M., N. Azuma, H. Kadowaki, T. Abe and Y. Suto (2017). "Regulation of type 2 diabetes by helminth-induced Th2 immune response." J Vet Med Sci **78**(12): 1855-1864.

Moura, R. A., R. Cascão, I. Perpétuo, H. Canhão, E. Vieira-Sousa, A. F. Mourão, A. M. Rodrigues, J. Polido-Pereira, M. V. Queiroz, H. S. Rosário, M. M. Souto-Carneiro, L. Graca and J. E. Fonseca (2011). "Cytokine pattern in very early rheumatoid arthritis favours B-cell activation and survival." Rheumatology (Oxford) **50**(2): 278-282.

Muralidharan, S., F. Torta, M. K. Lin, A. Olona, M. Bagnati, A. Moreno-Moral, J.-H. Ko, S. Ji, B. Burla, M. R. Wenk, H. G. Rodrigues, E. Petretto and J. Behmoaras (2022). "Immunolipidomics Reveals a Globoside Network During the Resolution of Pro-Inflammatory Response in Human Macrophages." Frontiers in Immunology **13**.

Murphy, G. and H. Nagase (2008). "Reappraising metalloproteinases in rheumatoid arthritis and osteoarthritis: destruction or repair?" Nat Clin Pract Rheumatol **4**(3): 128-135.

Nandakumar, K. S. and R. Holmdahl (2006). "Antibody-induced arthritis: disease mechanisms and genes involved at the effector phase of arthritis." Arthritis Res Ther **8**(6): 223.

Narasimhan, R., R. Coras, S. B. Rosenthal, S. R. Sweeney, A. Lodi, S. Tiziani, D. Boyle, A. Kavanaugh and M. Guma (2018). "Serum metabolomic profiling predicts synovial gene expression in rheumatoid arthritis." Arthritis Research & Therapy **20**(1): 164.

Nehring Sara, M. S. (2022). "C Reactive Protein."

Neill, D. R., S. H. Wong, A. Bellosi, R. J. Flynn, M. Daly, T. K. Langford, C. Bucks, C. M. Kane, P. G. Fallon, R. Pannell, H. E. Jolin and A. N. McKenzie (2010). "Nuocytes represent a new innate effector leukocyte that mediates type-2 immunity." Nature **464**(7293): 1367-1370.

Nicholson, J. K. and J. C. Lindon (2008). "Systems biology: Metabonomics." Nature **455**(7216): 1054-1056.

Noviello Mde, L., N. V. Batista, L. P. Dourado, R. V. Pereira, A. G. Oliveira, G. B. Menezes and D. C. Cara (2013). "Prolonged ingestion of ovalbumin diet by Ova sensitized mice suppresses mBSA-induced arthritis." Cell Immunol **284**(1-2): 20-28.

Nunes, P., N. Demaurex and M. C. Dinauer (2013). "Regulation of the NADPH oxidase and associated ion fluxes during phagocytosis." Traffic **14**(11): 1118-1131.

O'Neil, L. J. and M. J. Kaplan (2019). "Neutrophils in Rheumatoid Arthritis: Breaking Immune Tolerance and Fueling Disease." Trends Mol Med **25**(3): 215-227.

Odobasic, D., A. R. Kitching, Y. Yang, K. M. O'Sullivan, R. C. Muljadi, K. L. Edgtton, D. S. Tan, S. A. Summers, E. F. Morand and S. R. Holdsworth (2013). "Neutrophil myeloperoxidase regulates T-cell-driven tissue inflammation in mice by inhibiting dendritic cell function." Blood **121**(20): 4195-4204.

Odobasic, D., Y. Yang, R. C. Muljadi, K. M. O'Sullivan, W. Kao, M. Smith, E. F. Morand and S. R. Holdsworth (2014). "Endogenous myeloperoxidase is a mediator of joint inflammation and damage in experimental arthritis." Arthritis Rheumatol **66**(4): 907-917.

Osbourn, M., D. C. Soares, F. Vacca, E. S. Cohen, I. C. Scott, W. F. Gregory, D. J. Smyth, M. Toivakka, A. M. Kemter, T. le Bihan, M. Wear, D. Hoving, K. J. Filbey, J. P. Hewitson, H. Henderson, A. Gonzàlez-Cìscar, C. Errington, S. Vermeren, A. L. Astier, W. A. Wallace, J. Schwarze, A. C. Ivens, R. M. Maizels and H. J. McSorley (2017). "HpARI Protein Secreted by a Helminth Parasite Suppresses Interleukin-33." Immunity **47**(4): 739-751.e735.

Ostensen, M. and P. M. Villiger (2007). "The remission of rheumatoid arthritis during pregnancy." Semin Immunopathol **29**(2): 185-191.

Palmer, D. G., N. Hogg and P. A. Revell (1986). "Lymphocytes, polymorphonuclear leukocytes, macrophages and platelets in synovium involved by rheumatoid arthritis. A study with monoclonal antibodies." Pathology **18**(4): 431-437.

Palsson, B. (2009). "Metabolic systems biology." FEBS Letters **583**(24): 3900-3904.

Pelly, V. S., Y. Kannan, S. M. Coomes, L. J. Entwistle, D. Ruckerl, B. Seddon, A. S. MacDonald, A. McKenzie and M. S. Wilson (2016). "IL-4-producing ILC2s are required for the differentiation of TH2 cells following Heligmosomoides polygyrus infection." Mucosal Immunol **9**(6): 1407-1417.

Peres, R. S., G. B. Santos, N. T. Cecilio, V. A. Jabor, M. Niehues, B. G. Torres, G. Buqui, C. H. Silva, T. D. Costa, N. P. Lopes, M. C. Nonato, F. S. Ramalho, P. Louzada-Junior, T. M. Cunha, F. Q. Cunha, F. S. Emery and J. C. Alves-Filho (2017). "Lapachol, a compound targeting pyrimidine metabolism, ameliorates experimental autoimmune arthritis." Arthritis Res Ther **19**(1): 47.

Progatzky, F., M. Shapiro, S. H. Chng, B. Garcia-Cassani, C. H. Classon, S. Sevgi, A. Laddach, A. C. Bon-Frauches, R. Lasrado, M. Rahim, E. M. Amaniti, S. Boeing, K. Shah, L. J. Entwistle, A. Suarez-Bonnet, M. S. Wilson, B. Stockinger and V. Pachnis (2021). "Regulation of intestinal immunity and tissue repair by enteric glia." Nature **599**(7883): 125-130.

Qiu, J., B. Wu, S. B. Goodman, G. J. Berry, J. J. Goronzy and C. M. Weyand (2021). "Metabolic Control of Autoimmunity and Tissue Inflammation in Rheumatoid Arthritis." Front Immunol **12**: 652771.

Qiu, S., X. Fan, Y. Yang, P. Dong, W. Zhou, Y. Xu, Y. Zhou, F. Guo, Y. Zheng and J. Q. Yang (2017). "Schistosoma japonicum infection downregulates house dust mite-induced allergic airway inflammation in mice." PLoS One **12**(6): e0179565.

Rajamanickam, A., S. Munisankar, C. Dolla, P. A. Menon, K. Thiruvengadam, T. B. Nutman and S. Babu (2020). "Helminth infection modulates systemic pro-inflammatory cytokines and chemokines implicated in type 2 diabetes mellitus pathogenesis." PLoS Negl Trop Dis **14**(3): e0008101.

Rausch, S., J. Huehn, D. Kirchhoff, J. Rzepecka, C. Schnoeller, S. Pillai, C. Loddenkemper, A. Scheffold, A. Hamann, R. Lucius and S. Hartmann (2008). "Functional analysis of effector and regulatory T cells in a parasitic nematode infection." Infect Immun **76**(5): 1908-1919.

Reynolds, L. A., K. J. Filbey and R. M. Maizels (2012). "Immunity to the model intestinal helminth parasite Heligmosomoides polygyrus." Semin Immunopathol **34**(6): 829-846.

Rosas, E. C., L. B. Correa and M. d. G. Henriques (2017). Neutrophils in Rheumatoid Arthritis: A Target for Discovering New Therapies Based on Natural Products. Role of Neutrophils in Disease Pathogenesis.

Rzepecka, J., M. L. Coates, M. Saggar, L. Al-Riyami, J. Coltherd, H. K. Tay, J. K. Huggan, L. Janicova, A. I. Khalaf, I. Siebeke, C. J. Suckling, M. M. Harnett and W. Harnett (2014). "Small molecule analogues of the immunomodulatory parasitic helminth product ES-62 have anti-allergy properties." Int J Parasitol **44**(9): 669-674.

Salgame, P., G. S. Yap and W. C. Gause (2013). "Effect of helminth-induced immunity on infections with microbial pathogens." Nat Immunol **14**(11): 1118-1126.

Sanchez-Lopez, E., A. Cheng and M. Guma (2019). "Can Metabolic Pathways Be Therapeutic Targets in Rheumatoid Arthritis?" Journal of Clinical Medicine **8**(5): 753.

Sandilands, G. P., J. McCrae, K. Hill, M. Perry and D. Baxter (2006). "Major histocompatibility complex class II (DR) antigen and costimulatory molecules on in vitro and in vivo activated human polymorphonuclear neutrophils." Immunology **119**(4): 562-571.

Sarter, K., M. Kulagin, G. Schett, N. L. Harris and M. M. Zaiss (2017). "Inflammatory arthritis and systemic bone loss are attenuated by gastrointestinal helminth parasites." Autoimmunity **50**(3): 151-157.

Sasaki, C., T. Hiraishi, T. Oku, K. Okuma, K. Suzumura, M. Hashimoto, H. Ito, I. Aramori and Y. Hirayama (2019). "Metabolomic approach to the exploration of biomarkers associated with disease activity in rheumatoid arthritis." PLoS One **14**(7): e0219400.

Saunders, K. A., T. Raine, A. Cooke and C. E. Lawrence (2007). "Inhibition of autoimmune type 1 diabetes by gastrointestinal helminth infection." Infect Immun **75**(1): 397-407.

Schumacher, C., I. Clark-Lewis, M. Baggiolini and B. Moser (1992). "High- and low-affinity binding of GRO alpha and neutrophil-activating peptide 2 to interleukin 8 receptors on human neutrophils." Proc Natl Acad Sci U S A **89**(21): 10542-10546.

Secklehner, J., C. Lo Celso and L. M. Carlin (2017). "Intravital microscopy in historic and contemporary immunology." Immunol Cell Biol **95**(6): 506-513.

Segura, M., Z. Su, C. Piccirillo and M. M. Stevenson (2007). "Impairment of dendritic cell function by excretory-secretory products: a potential mechanism for nematode-induced immunosuppression." Eur J Immunol **37**(7): 1887-1904.
Setiawan, T., A. Metwali, A. M. Blum, M. N. Ince, J. F. Urban, Jr., D. E. Elliott and J. V. Weinstock (2007). "Heligmosomoides polygyrus promotes regulatory T-cell cytokine production in the murine normal distal intestine." Infect Immun **75**(9): 4655-4663.
Shaw, M., B. F. Collins, L. A. Ho and G. Raghu (2015). "Rheumatoid arthritis-associated lung disease." Eur Respir Rev **24**(135): 1-16.
Shiozawa, S., K. Tsumiyama, K. Yoshida and A. Hashiramoto (2011). "Pathogenesis of Joint Destruction in Rheumatoid Arthritis." Archivum Immunologiae et Therapiae Experimentalis **59**(2): 89-95.
Silva, R. L., A. H. Lopes, R. M. Guimarães and T. M. Cunha (2017). "CXCL1/CXCR2 signaling in pathological pain: Role in peripheral and central sensitization." Neurobiology of Disease **105**: 109-116.
Smith, K. A., K. Hochweller, G. J. Hämmerling, L. Boon, A. S. MacDonald and R. M. Maizels (2011). "Chronic helminth infection promotes immune regulation in vivo through dominance of CD11cloCD103- dendritic cells." J Immunol **186**(12): 7098-7109.
Smolen, J. S., D. Aletaha, A. Barton, G. R. Burmester, P. Emery, G. S. Firestein, A. Kavanaugh, I. B. McInnes, D. H. Solomon, V. Strand and K. Yamamoto (2018). "Rheumatoid arthritis." Nature Reviews Disease Primers **4**(1): 18001.
Sokka, T., S. Toloza, M. Cutolo, H. Kautiainen, H. Makinen, F. Gogus, V. Skakic, H. Badsha, T. Peets, A. Baranauskaite, P. Geher, I. Ujfalussy, F. N. Skopouli, M. Mavrommati, R. Alten, C. Pohl, J. Sibilia, A. Stancati, F. Salaffi, W. Romanowski, D. Zarowny-Wierzbinska, D. Henrohn, B. Bresnihan, P. Minnock, L. S. Knudsen, J. W. Jacobs, J. Calvo-Alen, J. Lazovskis, R. Pinheiro Gda, D. Karateev, D. Andersone, S. Rexhepi, Y. Yazici, T. Pincus and Q.-R. Group (2009). "Women, men, and rheumatoid arthritis: analyses of disease activity, disease characteristics, and treatments in the QUEST-RA study." Arthritis Res Ther **11**(1): R7.
Steinfelder, S., N. L. O'Regan and S. Hartmann (2016). "Diplomatic Assistance: Can Helminth-Modulated Macrophages Act as Treatment for Inflammatory Disease?" PLoS Pathog **12**(4): e1005480.
Strzepa, A., K. A. Pritchard and B. N. Dittel (2017). "Myeloperoxidase: A new player in autoimmunity." Cell Immunol **317**: 1-8.
Su, Z., M. Segura, K. Morgan, J. C. Loredo-Osti and M. M. Stevenson (2005). "Impairment of protective immunity to blood-stage malaria by concurrent nematode infection." Infect Immun **73**(6): 3531-3539.
Sun, Y., G. Liu, Z. Li, Y. Chen, Y. Liu, B. Liu and Z. Su (2013). "Modulation of dendritic cell function and immune response by cysteine protease inhibitor from murine nematode parasite Heligmosomoides polygyrus." Immunology **138**(4): 370-381.
Tak, P. P., T. J. M. Smeets, M. R. Daha, P. M. Kluin, K. A. E. Meijers, R. Brand, A. E. Meinders and F. C. Breedveld (1997). "Analysis of the synovial cell infiltrate in early rheumatoid synovial tissue in relation to local disease activity." Arthritis & Rheumatism **40**(2): 217-225.
Tanaka, D., T. Kagari, H. Doi and T. Shimozato (2006). "Essential role of neutrophils in anti-type II collagen antibody and lipopolysaccharide-induced arthritis." Immunology **119**(2): 195-202.
Tarnowski, M., A. Paradowska-Gorycka, E. Dąbrowska-Zamojcin, M. Czerewaty, S. Słuczanowska-Głąbowska and A. Pawlik (2016). "The effect of gene polymorphisms on patient responses to rheumatoid arthritis therapy." Expert Opin Drug Metab Toxicol **12**(1): 41-55.
Tecchio, C. and M. A. Cassatella (2016). "Neutrophil-derived chemokines on the road to immunity." Seminars in Immunology **28**(2): 119-128.
Teitsma, X. M., W. Yang, J. W. G. Jacobs, A. Pethö-Schramm, M. E. A. Borm, A. C. Harms, T. Hankemeier, J. M. van Laar, J. W. J. Bijlsma and F. Lafeber (2018). "Baseline metabolic profiles of early rheumatoid arthritis patients achieving sustained drug-free remission after

initiating treat-to-target tocilizumab, methotrexate, or the combination: insights from systems biology." Arthritis Res Ther **20**(1): 230.
Turunen, S., J. Huhtakangas, T. Nousiainen, M. Valkealahti, J. Melkko, J. Risteli and P. Lehenkari (2016). "Rheumatoid arthritis antigens homocitrulline and citrulline are generated by local myeloperoxidase and peptidyl arginine deiminases 2, 3 and 4 in rheumatoid nodule and synovial tissue." Arthritis Res Ther **18**(1): 239.
Valanparambil, R. M., M. Segura, M. Tam, A. Jardim, T. G. Geary and M. M. Stevenson (2014). "Production and analysis of immunomodulatory excretory-secretory products from the mouse gastrointestinal nematode Heligmosomoides polygyrus bakeri." Nat Protoc **9**(12): 2740-2754.
Valanparambil, R. M., M. Tam, A. Jardim, T. G. Geary and M. M. Stevenson (2017). "Primary Heligmosomoides polygyrus bakeri infection induces myeloid-derived suppressor cells that suppress CD4(+) Th2 responses and promote chronic infection." Mucosal Immunol **10**(1): 238-249.
van Beuningen, H. M., W. B. van den Berg, J. Schalkwijk, O. J. Arntz and L. B. van de Putte (1989). "Age- and sex-related differences in antigen-induced arthritis in C57Bl/10 mice." Arthritis Rheum **32**(6): 789-794.
van den Berg, W. B., L. A. Joosten and P. L. van Lent (2007). "Murine antigen-induced arthritis." Methods Mol Med **136**: 243-253.
van den Berg, W. B. and L. B. van de Putte (1985). "Electrical charge of the antigen determines its localization in the mouse knee joint. Deep penetration of cationic BSA in hyaline articular cartilage." Am J Pathol **121**(2): 224-234.
Vonkeman, H. E. and M. A. van de Laar (2010). "Nonsteroidal anti-inflammatory drugs: adverse effects and their prevention." Semin Arthritis Rheum **39**(4): 294-312.
Walk, S. T., A. M. Blum, S. A. Ewing, J. V. Weinstock and V. B. Young (2010). "Alteration of the murine gut microbiota during infection with the parasitic helminth Heligmosomoides polygyrus." Inflamm Bowel Dis **16**(11): 1841-1849.
Walmsley, S. R., C. Print, N. Farahi, C. Peyssonnaux, R. S. Johnson, T. Cramer, A. Sobolewski, A. M. Condliffe, A. S. Cowburn, N. Johnson and E. R. Chilvers (2005). "Hypoxia-induced neutrophil survival is mediated by HIF-1alpha-dependent NF-kappaB activity." J Exp Med **201**(1): 105-115.
Wang, W., J. Cui, H. Ma, W. Lu and J. Huang (2021). "Targeting Pyrimidine Metabolism in the Era of Precision Cancer Medicine." Front Oncol **11**: 684961.
Wei, J., G. Xie, Z. Zhou, P. Shi, Y. Qiu, X. Zheng, T. Chen, M. Su, A. Zhao and W. Jia (2011). "Salivary metabolite signatures of oral cancer and leukoplakia." Int J Cancer **129**(9): 2207-2217.
Weinstock, J. V. and D. E. Elliott (2009). "Helminths and the IBD hygiene hypothesis." Inflamm Bowel Dis **15**(1): 128-133.
Wen, Z., K. Jin, Y. Shen, Z. Yang, Y. Li, B. Wu, L. Tian, S. Shoor, N. E. Roche, J. J. Goronzy and C. M. Weyand (2019). "N-myristoyltransferase deficiency impairs activation of kinase AMPK and promotes synovial tissue inflammation." Nat Immunol **20**(3): 313-325.
Weng, M., D. Huntley, I. F. Huang, O. Foye-Jackson, L. Wang, A. Sarkissian, Q. Zhou, W. A. Walker, B. J. Cherayil and H. N. Shi (2007). "Alternatively activated macrophages in intestinal helminth infection: effects on concurrent bacterial colitis." J Immunol **179**(7): 4721-4731.
Weyand, C. M., B. Wu and J. J. Goronzy (2020). "The metabolic signature of T cells in rheumatoid arthritis." Current Opinion in Rheumatology **32**(2).
White, M. P. J., C. J. C. Johnston, J. R. Grainger, J. E. Konkel, R. A. O'Connor, S. M. Anderton and R. M. Maizels (2020). "The Helminth Parasite Heligmosomoides polygyrus Attenuates EAE in an IL-4Ralpha-Dependent Manner." Front Immunol **11**: 1830.
White, M. P. J., C. J. C. Johnston, J. R. Grainger, J. E. Konkel, R. A. O'Connor, S. M. Anderton and R. M. Maizels (2020). "The Helminth Parasite Heligmosomoides polygyrus Attenuates EAE in an IL-4Rα-Dependent Manner." Front Immunol **11**: 1830.

Widdifield, J., J. M. Paterson, S. Bernatsky, K. Tu, G. Tomlinson, B. Kuriya, J. C. Thorne and C. Bombardier (2014). "The epidemiology of rheumatoid arthritis in Ontario, Canada." Arthritis Rheumatol **66**(4): 786-793.

Wilson, M. S., M. D. Taylor, A. Balic, C. A. Finney, J. R. Lamb and R. M. Maizels (2005). "Suppression of allergic airway inflammation by helminth-induced regulatory T cells." J Exp Med **202**(9): 1199-1212.

Wilson, M. S., M. D. Taylor, M. T. O'Gorman, A. Balic, T. A. Barr, K. Filbey, S. M. Anderton and R. M. Maizels (2010). "Helminth-induced CD19+CD23hi B cells modulate experimental allergic and autoimmune inflammation." Eur J Immunol **40**(6): 1682-1696.

Wipke, B. T. and P. M. Allen (2001). "Essential role of neutrophils in the initiation and progression of a murine model of rheumatoid arthritis." J Immunol **167**(3): 1601-1608.

Wiria, A. E., Y. Djuardi, T. Supali, E. Sartono and M. Yazdanbakhsh (2012). "Helminth infection in populations undergoing epidemiological transition: a friend or foe?" Semin Immunopathol **34**(6): 889-901.

Wittkowski, H., D. Foell, E. af Klint, L. De Rycke, F. De Keyser, M. Frosch, A. K. Ulfgren and J. Roth (2007). "Effects of intra-articular corticosteroids and anti-TNF therapy on neutrophil activation in rheumatoid arthritis." Ann Rheum Dis **66**(8): 1020-1025.

Wright, H. L., M. Lyon, E. A. Chapman, R. J. Moots and S. W. Edwards (2020). "Rheumatoid Arthritis Synovial Fluid Neutrophils Drive Inflammation Through Production of Chemokines, Reactive Oxygen Species, and Neutrophil Extracellular Traps." Front Immunol **11**: 584116.

Wright, H. L., R. J. Moots and S. W. Edwards (2014). "The multifactorial role of neutrophils in rheumatoid arthritis." Nat Rev Rheumatol **10**(10): 593-601.

Xu, L., C. Chang, P. Jiang, K. Wei, R. Zhang, Y. Jin, J. Zhao, L. Xu, Y. Shi, S. Guo and D. He (2022). "Metabolomics in rheumatoid arthritis: Advances and review." Front Immunol **13**: 961708.

Yoon, N., A. K. Jang, Y. Seo and B. H. Jung (2021). "Metabolomics in Autoimmune Diseases: Focus on Rheumatoid Arthritis, Systemic Lupus Erythematous, and Multiple Sclerosis." Metabolites **11**(12).

Zhang, Z. and C. Zhao (2013). Sphingosine-1-Phosphate and Rheumatoid Arthritis: Pathological Implications and Potential Therapeutic Targets. Innovative Rheumatology.

CV

Ana Gabriela Madrigal; M.SC.

Email: agmadrigal2@gmail.com

Education

Dec 2022 **MASTERS OF SCIENCE (M.SC.)**
Institute of Parasitology
McGill University
Master's Thesis: Helminth infection modulation of AIA: Characterizing the effects of H*eligmosomoides polygyrus bakeri* infection on knee joint inflammation
Related coursework: Parasitology, Cell Biology

May 2019 **MASTERS OF SCIENCE (M.SC.)**
Department of Molecular Microbiology and Immunology;
Johns Hopkins Bloomberg School of Public Health
Master's Thesis: Chagas Disease, a Diagnostic Enigma
Related coursework: Immunology, Parasitology, Vector Biology, Virology, Statistical Computing, Drug Development

August 2015 **Bachelor of Science (BS)**
Major: Biological Sciences: Emphasis Microbiology and Immunology
Minor: Chemistry, Cognitive Science
University of California Merced
Related coursework: Biochemistry, Parasitology, Neuroscience, Neurobiology, Virology, Cancer Genetics & Tumor Biology, Inorganic Chemistry, Organic Chemistry, Scientific Computation for Chemistry

Publications

1. Madrigal, Ana G, et al. "Detection of Parasite-Derived Transrenal DNA for the Diagnosis of Chronic Trypanosoma Cruzi Infection." MedRxiv, Cold Spring Harbor Laboratory Press, 1 Jan. 2019, www.medrxiv.org/content/10.1101/19010934v1.

Awards

2021 **Nikon Small World in Motion (Honorable mention)**
https://www.nikonsmallworld.com/galleries/2021-small-world-in-motion-competition/neutrophils-rolling-through-mouse-blood-vessel

2020 **Graduate Mobility Award**
Encourages graduate students to study and conduct research abroad as part of their McGill degree program by deferring part of the cost of the international experience.

2020 **Lister Family Engaged Science 3MT Competition (2nd place winner)**
3 Minute Thesis Competition

Talks

2021 **Lister Science Chats**
Lister Science Chats connect members of the community through live science talks with. These chats feature graduate students giving an engaging 10-minute talk on their research and conclude with a Q&A period.

2021 **Lister Family Engaged Science 3MT Competition (Judge)**

2022 **Canadian Arthritis Research Conference**
Research Presentation Day (10 min. oral presentation)

Research Experience

Aug 2019- Current **Lab Graduate Researcher**
Fernando Lopes Lab, Parasitology Department, McGill

With emphasis in small molecules extracted from Heligmosomoides polygyrus bakeri as a novel treatment for Rheumatoid Arthritis. Developing and analyzing methods for extracting and analyzing parasitic excreted secreted products.

- Characterizing and standardizing Antigen Induced Arthritis model in our group
- Maintaining C57BL/6 wild type (WT) mice colony, and *Heligmosomoides polygyrus bakeri* life cycle
- Live-microscopy standardization and confocal microscope visualization
- Lab activities included but not restricted to: Knee histology preparation, Metabolomic analysis, Neutrophil isolation, Cell culture, Seahorse XF Cell Mito Stress Test assay, ELISA's, Western blots. As well as training of undergraduate and graduate students on assays and lab equipment use.

Nov 2017- June 2019 **Lab Graduate Researcher**,
Laboratory of Clive Shiff, PhD
Department of Molecular Microbiology and Immunology
Johns Hopkins Bloomberg School of Public Health, Baltimore, MD.
T. cruzi detection through Tr-DNA in human urine samples collected on filter paper from the field.

- Develop and optimize primers and their PCR protocols
- Optimize extraction techniques for filtered urine, as well as perform extractions from blood and unfiltered urine using kits
- Perform data analysis and generate tables and figures
- Utilize Nanodrop, FluorChem imagers, and sequencing programs
- Collaborate on drafting IRBs and building consent forms for human sample collection
- Train new lab members in PCR and gel electrophoresis techniques and oversee lab management
- Developed a project and new lab protocols for lab high school trainee

Feb 2016- Aug 2017 **Lab Graduate Researcher,**

Saier lab, Section of Molecular Biology, University of California San Diego

- Characterized a putative transporter protein family called the YeeE/YedE family through several bioinformatic analyses, such as: PSI-BLAST and CD-HIT (for homologue identification), multiple sequence alignments (for protein classification), MEME (to identify functional motifs), and HMMTOP (for topology)
- Performed Phylogenetic analysis using an in-house program called SuperFamilyTree

Oct 2016-Aug 2017 **Lab Graduate Researcher,**

Caffrey lab, Skaggs School of Pharmacy and Pharmaceutical Sciences, University of California San Diego

- Screened *T. brucei* through high throughput analysis: running assays cultures, passaging, screening, plate reading, and data analysis
- Culturing and handling of C. elegans

Aug 2013-Aug 2015 **Lab Undergraduate Researcher,**

Hirst lab, Soft Matter and biophysics, University of California Merced

- Focused on the structure and phase behavior of lipid membranes
- Developed lipid bilayers utilizing DOPC, DPPC, and other lipid types
- Studied the mechanical properties of lipid vesicles using a dual beam optical laser trap and fluorescent microscope

---

Teaching Experience

Feb 2021 – Apr 2021 **Teaching Assistant,** Department Parasitology, McGill University, Montreal, QC

Course Title: (BTEC 619) Winter 2021

- 1 term (Dr. Thavy Long)

Jan 2021 – Feb 2021 **Teaching Assistant,** Department Parasitology, McGill University, Montreal, QC

Course Title: (BTEC 620) Winter 2021

- 1 term (Dr. Igor Cestari)

Sep 2020 – Dec 2020 **Teaching Assistant,** Department Parasitology, McGill University, Montreal, QC

Course Title: Immunology (PARA 438) Fall 2020

- Graded exams, papers and group assignments as well as held online office hours for students. 1 term (Dr. Fernando Lopes)

Jan 2020 – April 2020 **Teaching Assistant,** Department Parasitology, McGill University, Montreal, QC

Course Title: Biochemistry I (LSCI-211) Winter 2020

- Held office hours once weekly. Prepared and held review session for students, and graded exams. 1 term (Dr. Reza Salavati & Dr. Igor Cestari)

Oct 2018 - Dec 2018 **Teaching Assistant,** Department of Molecular Microbiology and Immunology,

Johns Hopkins Bloomberg School of Public Health, Baltimore, MD

Course Title: Biology of Parasitism

- Maintained Lab Notebook Guide, organized microscope slides for lab sections, communicated with students, held office hours, and graded exams and assignments. 1 term (Dr. Clive J. Shiff & Dr. David A. Sullivan)

Nov 2017- Dec 2018 **Lab Mentor**, Shiff lab, Department of Molecular Microbiology and Immunology,

Johns Hopkins Bloomberg School of Public Health, Baltimore, MD.

- Oversee training and supervision of High School student for the Ingenuity Science programs at the Baltimore Polytechnic Institute
- Instruct student on the scientific technique, PCR and extraction protocols

Skills and Additional Training

Professional Training

Aug. 2019 Certificate in Tropical Medicine, Johns Hopkins Bloomberg School of Public Health, Baltimore, MD

Recent Hazards Trainings

Sep. 2019 Safe Use of Biological Safety Cabinets/ Introduction to Biosafety/ Workplace Hazardous Materials Information System (W.H.M.I.S.), Environmental Health and Safety, McGill University

Oct. 2019 Hazardous Waste Management & Disposal for Laboratory, Environmental Health and Safety, McGill University

Oct. 2017 Biosafety: Bloodborne Pathogens Training, Skaggs School of Pharmacy and Pharmaceutical Sciences, University of California San Diego

Software

- Proficient with Excel, Word, PowerPoint, and other Microsoft Office Software
- GraphPad Prism
- Bioinformatic tools: BioV Suite, Fig Tree, MEME
- Alpha View
- PSI-BLAST, Primer-BLAST (NCBI)
- MetaboAnalyst

Programming

- Basic scripting knowledge in R, BASH Shell, Linux, Python, C, and C++

Technical Skills

- Mouse handling/breeding
- Parasite Culturing (*T. brucei, H. polygyrus*)
- *C. elegans* cultures
- Intra-vital microscopy
- Metabolomic analysis
- High Throughput analysis
- DNA Extractions
- Sequence Analysis
- FluorChem imagers
- Confocal image acquisition
- Electrophoresis
- PCR
- ELISA
- Western Blots
- Cell culture

Languages

- Fluent in English and Spanish

Co-Curricular Record

Sep 14 2020 **AGSEM TA Training:** Info Session for Teaching Assistants

Hosted by: SKILLSETS Graduate Workshops

Sep 14 2020 **AGSEM TA Training:** Engaging with Zoom as a TA

Hosted by: SKILLSETS Graduate Workshops

Oct 01 2020 **Getting Started With Supervision**

Hosted by: SKILLSETS Graduate Workshops

Nov 03 2020 **Rise and Write** – Online

Hosted by: Graphos - McGill Writing Centre, Graduate Communication Program

Mar 16 2021 **Making your work open access**

Hosted by: McGill Library

Jan 26 2022 **3MT | MT180 Competition 2022**

Hosted by: SKILLSETS Graduate Workshops